DENSITIES OF STATES FOR DISORDERED HAMILTONIANS

NAHEED ZAMAN, MATHEMATICS DEPARTMENT

A thesis submitted for the degree of Doctor of Philosophy of the University of London and the Diploma of Imperial College.

ABSTRACT

The densities of states of disordered materials are calculated by the use of the continued fraction method. Transition metal alloys are the main topic of discussion, but the continued fraction method is applied to other systems also to show its efficiency and simplicity. Chapter 1 presents the assumptions and the concepts employed in this theses and gives arguments for the use of the continued fraction method. Chapter 2 gives the modification of the density of states expression due to LLoyd(1967). It has wide applications in many fields but for the present it is used to discuss only the density of states of transition metals and their alloys. Chapter 3 presents the calculation of the density of states for the face-centred cubic transition metal alloys in a single site approximation. Chapter 4 gives the cluster theory for the alloys with a d band only. These calculations do not make use of chapter 2, but are prerequisite for chapter 5 and are interesting in themselves. In chapter 5 the formulation of chapter2, the cluster theory for the tight binding d bands of chapter 4 together with the sp band and its hybridization effects with the d bands are used to calculate the density of states of real transition metal alloys. In chapter 6 two applications of this theory are given. One is to experiment in calculating the low temperature specific heat coefficient of Ni-Pt alloys; and the other is to disordered Heisenberg ferromagnet to show the power and versatility of the present method. Finally at the end of the thesis a published work dealing with the application of the continued fraction method to one-dimensional binary alloy is attached.

ACKNOWLEDGEMENTS

Iwould like to thank Dr.R.L.Jacobs for his patient and constant supervision of my work. I would also to thank all members of the Mathematical Physics staff and fellow students for their encouragement. I am indebted to my father and to my husband for their ceaseless support and encouragement.

Table of Contents

CHAPTER 1

INTRODUCTION

In this thesis we shall discuss a wide range of problems concerning disordered materials. The disorder considered will be lattice disorder only. Such disorder is exhibited by substitutional binary alloys, in which the different constituent atoms occupy the same lattice position. The general requirement for the formation of an alloy of this type is that the radii of the constituent atoms should be nearly equal.

There has been considerable interest over the last years in the electronic properties of substitutional disordered alloys and in the development of theoretical techniques for their description. One method for finding the densities of states of simple materials is the continued fraction method of Haydock(1972). This method which depends on developing the Green function as an infinite continued fraction does not depend on the use of the Bloch theorem or the band structure E(k) in any way. Instead the electronic structure at one atomic site is related to the local environment of near neighbouring atoms. This method has been succesfully applied to deal with disorder in simple systems (such as simple cubic materials) by Cubiotti et al (1975, Jacobs 1974). In this thesis we will try to apply it to more complicated systems such as transition metals alloys. The method gives a Green function which is an analytic function(in the complex variable sense) of the complex energy E and thus avoids many of the

difficulties which have plagued previous theories (Nickel et al 1973).

The main aim of this chapter is to present the concepts, techniques and assumptions used in this thesis. In section 1.2 we will give a description of Haydocks technique. Its mathematical basis is the same as that of the Lanczos alogrithm, which is now a standard method of numerical analysis for tridiagonalizing any matrix (Householder 1964). Haydock et al (1972) have applied this technique to a calculation of the diagonal elements of the inverse of a tight binding matrix, which they then used to calculate the density of states for ordered crystals. In section 1.3 we will give a review of the extension of this technique to calculating the diagonal elements of the inverse of a tight binding matrix for a disordered crystals. In this section only the density of states of simple models such as the simple cubic s band will be discussed. In section 1.4 we will briefly describe the principles of the Korringa, Kohn and Rostoker method(KKR), which is sufficiently powerful to deal with the electronic structure of a transition metal, and we will show how the secular equation of the KKR theory can be used to derive a model Hamiltonian secular equation such as that of Mueller (1967). In section 1.5 we will give the principles of the derivation of Lloyds formula (1967) for the density of states in site representation, because this is the formula which we will use to calculate the dos of transition metal alloys. In the last section of this chapter we will give a plan of the rest of the thesis.

1.2 CONTINUED FRACTION METHOD

If we are given the Hamiltonian of a system of electrons, the specification of the Green function, $G=(E-H)^{-1}$, or particular

matrix elements(e.g $\langle 0|G|0\rangle$), is a major step in solving for the details of the electronic structure. In the tight binding model, the Hamiltonian is given as a matrix, whose elements are the self-energies and near neighbour hopping integrals. Haydock's method sets up a new basis in which the Hamiltonian has a tridiagonal representation, from which the diagonal matrix elements of the Green function are very simply derived. A tridiagonal matrix is one whose non-zero elements appear only on the main diagonal and the two adjacent diagonals.

Here we will discuss the simple cases only, where there is only one orbital per atomic site, but it can be extended to deal with cases where there are many orbitals per atomic site(tight binding d bands). First we will show how we can set up a new basis set which will give us a tridiagonal representation for a tight binding Hamiltonian for ordered crystals. Then we will show how we can express the diagonal element of the inverse matrix as a continued fraction.

The tight binding Hamiltonian for ordered crystals is given by

$$H = \sum_{i \neq j}' t\, c_i^{+} c_j \qquad (1.1)$$

where c_i^{+} is the creation operator for electrons on site i, and the summation is confined to nearest neighbour pairs. The new basis set is defined as follows:

$$\begin{aligned} |0) &= |0\rangle \\ |1) &= N_1[H|0) - |0)(0|H|0)] \\ |2) &= N_2[H|1) - |1)(1|H|1) - |0)(0|H|1)] \\ &\text{- - - - - - - - - - - - - - - - - -} \end{aligned} \qquad (1.2)$$

In this set of basis functions each ket is orthogalized to the previous ket(in the ordinary Schmidt fashion) and each ket is normalized by the factor N_i to unity. This basis set though not complete is sufficient for our purposes, because expanding the 0-0 diagonal element of the Green function in the form

$$\langle 0|\frac{1}{E-H}|0\rangle = \langle 0|\left[\frac{1}{E}+\frac{H}{E^2}+\frac{H^2}{E^3}+\frac{H^3}{E^4}+\ldots\ldots\right]|0\rangle \qquad (1.3)$$

we see that we need only those kets which are generated by the operation of various powers of H on $|0\rangle$.

The secular equation in this basis set can be easily seen to be tridiagonal. That is we have a secular equation of the form

$$\begin{bmatrix} \langle 0|H|0\rangle - E & \langle 0|H|1\rangle & 0 & 0 & 0 & \ldots \\ \langle 1|H|0\rangle & \langle 1|H|1\rangle - E & \langle 1|H|2\rangle & & & \\ 0 & \langle 2|H|1\rangle & \langle 2|H|2\rangle - E & \langle 2|H|3\rangle & 0 & \\ 0 & 0 & & & & \\ 0 & 0 & & & & \\ \ldots\ldots\ldots\ldots\ldots\ldots\ldots & & & & & \end{bmatrix} \qquad (1.4)$$

with $\langle i|H|j\rangle = 0$ unless $|i-j| \leq 1$ (1.4a)

We can understand equation (1.4a) by examining one matrix element such as $\langle 2|H|0\rangle$. From equation (1.2) we have

$$H|0\rangle = N_1^{-1}|1\rangle + |0\rangle\langle 0|H|0\rangle$$

$$\therefore \langle 2|H|0\rangle = N_1^{-1}\langle 2|1\rangle + \langle 2|0\rangle\langle 0|H|0\rangle = 0$$

because the basis set is orthonormal.

The density of states of any electron system is defined as

$$n(E) = +\frac{Im}{\pi}\langle 0|G|0\rangle = \frac{Im}{\pi}\left[\langle 0|\frac{1}{H-E}|0\rangle\right] \qquad (1.5)$$

which suggests that we must find the diagonal element of the inverse of the matrix given by equation (1.4). Using the Theorem which says that inverse of any matrix can be written as

$$\begin{bmatrix} A & B \\ C & D \end{bmatrix}^{-1} = \begin{bmatrix} (A-BD^{-1}C)^{-1} & -(D-CA^{-1}B)^{-1}BA^{-1} \\ -D^{-1}C(A-BD^{-1}C)^{-1} & (D-CA^{-1}B)^{-1} \end{bmatrix} \qquad (1.6)$$

we can write the inverse of the matrix of equation (1.4). If we denote the diagonal elements of the matrix in equation (1.4) by a_i $(i = 0,1,\ldots n)$ and the off-diagonal elements by $b_i (i = 0,1,\ldots n)$ then the 0–0 diagonal element of the inverse of matrix given by equation (1.4) is

$$\langle 0|G|0\rangle = \frac{1}{a_0 - E - b_0 d_0^{-1} b_0} \qquad (1.7)$$

where

$$d_i^{-1} = \frac{1}{a_{i+1} - E - b_{i+1} d_{i+1}^{-1} b_{i+1}} \qquad (1.8)$$

Thus $\langle 0|G|0\rangle$ is given by a continued fraction expansion from the repeated application of equation (1.8).(a_i, b_i) are called Haydock's coefficient in the rest of the thesis, here i refers to the level of the continued fraction. The termination of the continued fraction is the next problem. There are many kinds of terminations discussed by Haydock et al (1975), but the one we use in the thesis is the square root termination. The form and properties of which are discussed in the next section.

1.3 ALLOY THEORY

The continued fraction method of Haydock et al (1972) has been extended and adapted by Cubiotti et al (1973, 1975) and Jacobs(1973,1974) to study the disordered materials. A review of the alloy theory for simple systems is given here.

The disordered tight binding Hamiltonian used in these papers is

$$H = \sum_i \epsilon_i c_i^+ c_i + \sum_{i \neq j} t_{ij} c_i^+ c_j \qquad (1,9)$$

where i and j are site indices, c_i is an annihilation operator for electrons, $\epsilon_i = \pm \frac{1}{2} \delta$ (the sign depending on whether the site is occupied by an A type or a B type atom), the second summation is taken over the nearest neighbour only and t_{ij} is the hopping matrix between the sites i and j . The disorder in ϵ_i is called the diagonal disorder and the disorder in t_{ij} off-diagonal disorder.

The continued fraction method enables us to write the diagonal elements of the unaveraged Green function(for a particular configuration

in the alloy) in the form

$$F = 1/(a_0 - E - b_0 | (a_1 - E - b_1 / (a_2 - E - \cdots)))$$

The averaged Green function is then obtained by multiplying the Green function for a given configuration by the probability of occurence of that configuration and summing the result over all configurations.

The new basis set (as required by the Haydock method) for the above Hamiltonian is set up as follows:

We first split the Hamiltonian into two parts

$$H = H_1 + H_2 \tag{1.10}$$

where

$$H_1 = \sum_{ij}{}' t_{ij} c_i^+ c_j$$

and

$$H_2 = \sum_i \epsilon_i n_i$$

The new set of basis function is then chosen to be

$$\begin{aligned}
|0\rangle &= |0\rangle \\
|1,0\rangle &= N_{10}\left[H_1|0\rangle - |0\rangle\langle 0|H_1|0\rangle\right] \\
|0,1\rangle &= N_{01}\left[H_2|0\rangle - |0\rangle\langle 0|H_2|0\rangle - |1,0\rangle\langle 1,0|H_2|0\rangle\right] \\
|2,0\rangle &= N_{20}\left[H_1|1,0\rangle - 0T\right] \\
|1,1\rangle &= N_{11}\left[H_2|1,0\rangle - 0T\right] \\
|3,0\rangle &= N_{30}\left[H_1|2,0\rangle - 0T\right] \\
|2,1\rangle &= N_{21}\left[H_2|2,0\rangle - 0T\right] \\
&\cdots\cdots\cdots \\
&\cdots\cdots\cdots
\end{aligned} \tag{1.11}$$

where OT represents the orthogonalizing terms which serves to orthogonalize each ket to all previous kets. The notation $|i,j\rangle$ for the elements of the basis set (1.11) serves to indicate that the element $|i,j\rangle$ is constructed from the ket $|0\rangle$ by i operations of H_1 and j of H_2 . (This notation is ambiguous beyond a certain level). Our new basis is larger than that of Haydock et al (discussed in the previous section) and is thus sufficient for the problem. It is, however more convenient because the matrix elements of H in the new basis set show a strong tendency to depend on the parameters referring to a single shell only.

The proper termination of the continued fraction is very important (Haydock et al 1975), because if the fraction is merely cut short then the density of states is the sum of a collection of δ functions. One way of avoiding this undesirable result is to continue the fraction with an average of the continuations appropriate to the two pure components. This continuation ensures that the Lifshitz condition is satisfied(i.e the density of states is non-zero over the whole range in which either of the two pure components has a nOn-zero density of states).

An alternative approadh to the alloy problem is offered by the coherent potential approximation(CPA)(Velicky et al 1968). A formulation of this method appropriate to a tree or a Bethe lattice which starts from the continued fraction method is given by Jacobs(1973). The principle of CPA is that the central atom is treated exactly but

the environment is treated in the average and is chosen self-consistently. The average Green function for the substitutional binary alloy AB with a fraction c of atoms of type A and (1-c) of type B(c and (1-c) are also the probabilities of occurence of the configurations with an A atom or a B atom on the central site in CPA respectively) is given by

$$\overline{\langle 0|G|0\rangle} = \frac{c}{\frac{1}{2}\delta - \varepsilon - Zt^2\bar{F}} + \frac{1-c}{\frac{1}{2}\delta - \varepsilon - Zt^2\bar{F}} . \qquad (1.12)$$

where Z is the coordination number of the tree lattice and $\bar{F}$ is the termination to the continued fraction and is given by

$$\bar{F} = c F_A + (1-c) F_B \qquad (1.13)$$

where

$$F_A = \frac{1}{\frac{1}{2}\delta - \varepsilon - (z-1) t^2 \bar{F}} \qquad (1.14)$$

$$F_B = \frac{1}{-\frac{1}{2}\delta - \varepsilon - (z-1) t^2 \bar{F}} \qquad (1.15)$$

After substituting equations(1.14) and (1.15) into equation (1.13) and letting $Z \to \infty$ and $t \to t/\sqrt{z}$ a cubic is obtained which is the same as the cubic of Velicky et al (1968).

A more literal application of the continued fraction method is made by Jacobs(1974) and Cubiotti et al(1975). They used the

the continued fraction method with a non-selfconsistent termination to calculate the density of states of a single s band tight binding Hamiltonian in a cluster approximation. At the level of approximation to which they proceeded the average Green function depends on the number of atoms of each type on the central site and in the first three nearest neighbour shells. The diagonal matrix element of the Green function is expressed as a continued fraction in the following way:

$$\langle 0|G|0\rangle = \left[E_X - E - G_1\right]^{-1}$$

$$G_1 = (6t^2)\left[E_Z - E - G_2' - G_2\right]^{-1}$$

$$G_2' = \frac{(6-Z)Z}{36}\,\delta^2\left[-E + \frac{3-Z}{6}\delta\right]^{-1}$$

$$G_2 = 9t^2\left[E_W - E - G_3' - G_3\right]^{-1}$$

$$G_3' = \frac{(54-W)}{(54)^2}\,W\delta^2\left[-E + \frac{27-W}{54}\delta\right]^{-1}$$

$$G_3 = \frac{85}{9}\,t^2\,\bar{F}(E)$$

$$\bar{F}(E) = cF\left(\tfrac{1}{2}\delta - E\right) + (1-c)\,F\left(-\tfrac{1}{2}\delta - E\right)$$

$$F(E) = \frac{E \pm (E^2 - 4b^2t^2)^{\frac{1}{2}}}{2bt^2} \qquad (1.16)$$

where

$$E_X = -X\tfrac{1}{2}\delta + (1-X)\tfrac{1}{2}\delta$$

$$E_Z = \frac{-Z\tfrac{1}{2}\delta + (6-Z)\tfrac{1}{2}\delta}{6}$$

$$E_W = \frac{-W\tfrac{1}{2}\delta + (54-W)\tfrac{1}{2}\delta}{54}$$

$$W = N + 4M \qquad (1.17)$$

and X and Z are the numbers of atoms of type B on the central site (X=0 or 1) and in the nearest neighbour shell respectively(i.e Z ranges from 0to 6), and M and N are the numbers of atoms of type B in the 2nd and 3rd nearest neighbour shells, c is the concentration of atoms of type A, $\bar{F}(E)$ is the termination of the continued fraction (and this is the type of termination which is used throughout this thesis), $2bt$ gives the bandwidth of the material. If M_n is the probability of occurence of a particular configuration n in the nearest neighbour shells, then the average Green function is given by

$$\overline{\langle 0|G|0\rangle} = \sum_X \sum_n M_n \langle 0|G^{X,n}|0\rangle \qquad (1.18)$$

The result obtained for a pure simple cubic material are close to the exact result. For an alloy, the minority band shows a central peak, with humped shoulders on either side(bonding and antibonding effect). This result is very similar to Alben et al (1975). The position and height of the central peak is approximately maintained throughout the concentration range.

Another application of the continued fraction technique to

calculating the density of states of binary alloys is given by Zaman and Jacobs(1975, bound with the thesis at the end). This calculation is for one dimensional linear chain of atoms.

The great advantage of the continued fraction method is that it takes very little computer time as compared to other methods (Alben et al 1975).

1.4 KKR THEORY

In this section we will give a brief account of the KKR theory and its use to derive the model Hamiltonian in mixed tight binding-nearly plane wave basis functions.

The lattice potential $V(\underline{r})$ is taken to be of the muffin-tin form, that is spherically symmetrical within a sphere of radius r_c centred on each lattice site, and zero elsewhere. The wave function within each sphere is expanded in spherical harmonics: i.e for brevity

$$Y_L = Y_{lm}(\theta,\phi) \tag{1.19}$$

where $L=\{lm\}$, and θ and ϕ are polar angles of the vector $\underline{r}$. Then

$$\Psi(\underline{r}) = \sum_L i^l C_L R_l(r) Y_L(\underline{r}) \tag{1.20}$$

within a sphere, provided that $R_l(r)$ is the radial function satisfying the Schrodinger equation there in. The coefficient C_L are determined, for each value of the Bloch wave vector $\underline{k}$, by the set of homogeneous

linear equations

$$\sum_{LL'} \Lambda_{LL'} C_{L'} = 0 \qquad (1.21)$$

derived from a variational form of Schrodinger equation for the system. The matrix $\Lambda_{LL'}$ has components which depends, in a complicated way on the crystal structure and on the radial wave functions that appear in equation (1.20). The components are not, for example, the same for different values of the quantum number m, so that the sum over L' in (1.21) implies a double summation over l' and m' ; if we go as far as d waves the matrix $\Lambda_{LL'}$ is 9x9. These components are all functions of the energy, and the condition that a non-vanishing set of coefficients C_L can be found is that the determinant of this matrix be zero.This implies that the energy eigenvalues are solutions of the equation

$$\det |\Lambda_{LL'}| = 0$$

The practical utility of the scheme for determining the eigenvalues, then depends on the form of the equation. Following Kohn and Rostoker (1954), but using real spherical harmonics as suggested by Ham and Segall(1961), we can express the determinantal condition as follows:

$$\det \| A_{LL'} + k \cot \eta_l \delta_{LL'} \| = 0 \qquad (1.22)$$

where

$$k = \sqrt{E}$$

and

$$A_{LL'} = -(4\pi)^2 N \sum_{g} \frac{j_\ell(|\underline{k}-\underline{g}|R)\, j_{\ell'}(|\underline{k}-\underline{g}|R')\, Y_L(\underline{k}-\underline{g})\, Y_{L'}(\underline{k}-\underline{g})}{j_\ell(kR)\, j_{\ell'}(kR')\quad |\underline{k}-\underline{g}|^2 - E}$$

$$- k\,\delta_{LL'}\,\frac{n_\ell(kR)}{j_\ell(kR)} \qquad (1.23)$$

where N^{-1} is the volume of unit cell.

The main disadwantage in the use of KKR equations in practical calculations is that the eigenvalues take a long time to calculate because the matrix elements are energy dependent. The interpolation scheme of Hodges et al (1966) and Mueller(1967) were motivated primarily by a desire to remove the energy dependence from the off-diagonal matrix elements and this was achieved by writting the secular equation for the eigenvalue E as follows:

$$\det |H_m - EI| = 0 \qquad (1.24)$$

where I is the unit matrix and H_m is an energy-independent model Hamiltonian of the hybrid nearly-free-electron-tightbinding form: that is

$$H_m = \left(\begin{array}{c|c} C_{gg'} & H_{gL} \\ \hline H^*_{gL'} & R_{LL'} \end{array} \right) \qquad (1.25)$$

where $C_{gg'}$ represents the conduction block, $R_{LL'}$ represents the resonance block written in the tight binding form between the localized resonant states

(i.e d states for the transition metals) and H_{gL} represents the hybridization of the localized states wth the plane waves. H^{*}_{gL} is the hermitian conjugate of H.The sucess of this interpolation scheme led Heine (1967), Hubbard(1967), Jacobs(1968) and Pettifor(1969) to derive the model Hamiltonian from first principles.A brief account of the algebra of this derivation is given below.

Equation (1.23) can be written as follows:

$$A_{LL'} = -\sum_{g} \frac{\gamma_L(\underline{k}-\underline{g})\gamma_{L'}(\underline{k}-\underline{g})}{|\underline{k}-\underline{g}|^2-E} - K\frac{\eta_\ell(KR)}{\dot{\jmath}_\ell(KR)}\delta_{LL'} \qquad (1.26)$$

where

$$\gamma_L = 4\pi\sqrt{N}\ \frac{\dot{\jmath}_\ell(|\underline{k}-\underline{g}|R)\,Y_L(\underline{k}-\underline{g})}{\dot{\jmath}_\ell(KR)}$$

The term $K\cot\eta_\ell$ of equation (1.22) for the transition metals can be written in the resonance form (Heine 1967)

$$K\cot\eta_\ell = \frac{E_d - E}{\Gamma} \qquad \text{for } \ell=2 \qquad (1.27)$$

For ℓ=0,1 and $\ell > 2$, the phaseshift η_ℓ is small. The secular equation(1.22) can now be written as

$$\det\left|\left| -\sum_{g}\frac{\gamma_L(\underline{k}-\underline{g})\gamma_{L'}(\underline{k}-\underline{g})}{|\underline{k}-\underline{g}|^2-E} + \frac{E_d'-E}{\Gamma}\,\delta_{LL'}\right|\right| = 0 \qquad (1.28)$$

where

$$E_d' = E_d - \Gamma K \frac{\eta_2(KR)}{j_2(KR)} \tag{1.29}$$

Following Hubbard(1967) the above equation can be written as(a similar proceedure has been presented by Jacobs 1968)

$$\det \Big\| -\sum_{g} \frac{\gamma_L(k-g)\, S^2(k,g,E)\, \gamma_{L'}(k-g)}{|k-g|^2 - E}\,\Gamma + \sum_{g} \frac{\gamma_L(k-g)\left[1 - S^2(k,g,E)\right]\gamma_{L'}(k-g)}{|k-g|^2 - E}\,\Gamma + (E_d' - E)\,\delta_{LL'} \Big\| = 0 \tag{1.30}$$

where

$$S(k,g,E) = \mathrm{Exp}\left[(E - (k-g)^2)/\alpha\right]$$

The secular equation (1.30) is rewritten as follows with its second term in direct lattice space(taking its Fourier transform, Slater and Koster 1954)

$$\det \Big\| -\sum_{g} \frac{\gamma_L(k-g)\, S^2(k,g,E)\, \gamma_{L'}(k-g)\,\Gamma}{|k-g|^2 - E} + \sum_{s\neq 0} e^{ik\cdot r_s} I_{LL'}^{(s)}(k) + (E_d' - E)\,\delta_{LL'} \Big\| = 0 \tag{1.31}$$

Unfolding this we get

$$\begin{vmatrix} (|k-g|^2 - E)\,\delta_{gg'} & \sqrt{\Gamma}\, S(k,g,E)\, \gamma_L(k-g) \\ \sqrt{\Gamma}\, S(k,g,E)\, \gamma_L(k-g) & \sum_{s\neq 0} e^{ik\cdot r_s} I_{LL'}^{(s)} + (E_d' - E)\,\delta_{LL'} \end{vmatrix} = 0 \tag{1.32}$$

The hybridization submatrix is made energy independent by putting $E=E_d$. This is accurate in the low energy region. We have thus arrived at model Hamiltonian (1.25) with its block matrices

$$C_{gg'} = \left[|\underline{k}-\underline{g}|^2 - E \right] \delta_{gg'}$$

$$H_{gL} = \sqrt{\Gamma}\, S(k,g,E)\, \gamma_L(\underline{k}-\underline{g})$$

$$R_{LL'} = \sum_s e^{i\underline{k}\cdot\underline{r}_s} I_{LL'}^{(s)} + (E_d' - E)\delta_{LL'} \qquad (1.33)$$

(l and l' are both equal to 2)

1.5 LLOYD's FORMULA

Here we will give a brief derivation of Lloyd's formula(1967) for the density of states of a muffin-tin Hamiltonian.

In quantum mechanics it is generally true that if an eigen value problem is such that its eigenvalues are the solutions of an equation of the form

$$\det | A(E) | = 0 \qquad (1.34)$$

then the density of eigen states may be written as

$$g(E) = -\frac{1}{\pi} \mathrm{Im}\, \mathrm{Tr} \left\{ \left[\frac{d}{dE} A(E+i\epsilon) \right] \left[A(E+i\epsilon) \right]^{-1} \right\} \qquad (1.35)$$

Now we know that the energy eigen values are the solutions of the KKR secular equation (1.31) which is of a similar form to equation(1.34) But the KKR secular equation (1.31) is in k representation, which is suitable for ordered materials when the Bloch theorem holds. For the disordered materials it is better to use site representation (where no use of Bloch theorem is made). In this representation the KKR secular equation can be written as (Lloyd 1967)

$$\det \left| G^{+}_{LL'}(\underline{r}_s - \underline{r}'_s) + t^{-1}_{Ls}\, \delta^{\underline{r}_s \underline{r}'_s}_{LL'} \right| = 0 \qquad (1.36)$$

where

$$t^{-1}_{Ls} = k \cot \eta_{ls} - i k$$

and

$$G^{+}_{LL'}(\underline{r}_s - \underline{r}'_s) = -4\pi k \sum_{L''} i^{l''} h^{+}_{l''}(k|\underline{r}_s - \underline{r}'_s|)\, Y_{L''}(\underline{r}_s - \underline{r}'_s)\, C_{L'LL''} \qquad |\underline{r}_s - \underline{r}'_s| \neq 0$$

$$= 0 \qquad |\underline{r}_s - \underline{r}'_s| = 0$$

Using the general principle quoted above the formula for the density of states for the secular equation (1.36) is

$$\rho(E) = -\frac{1}{\pi} \mathrm{Im}\, \mathrm{Tr} \left[\frac{d}{dE} \left\{ G^{+}_{LL'}(\underline{r}_s - \underline{r}'_s) + t^{-1}_{Ls} \delta^{\underline{r}_s \underline{r}'_s}_{LL'} \right\} \left\{ G^{+}_{LL'}(\underline{r}_s - \underline{r}'_s) + t^{-1}_{Ls} \delta^{\underline{r}'_s \underline{r}_s}_{LL'} \right\}^{-1} \right] \qquad (1.37)$$

This formula will be the basis of the alloy theory developed later for transition metals and their alloys.

1.6 PLAN OF THE REST OF THE THESIS

We conclude this chapter by giving the plan of the rest of the thesis. In chapter 2 we modify Lloyd's expression for the density of states of a muffin-tin Hamiltonian(1967) to a form more suitable for numerical calculations. In chapter 3 this modified formula is used to calculate the density of states of transition metal alloys in a single site approximation. In chapter 4, the density of states of a tight binding d band alloys are calculated in cluster theory by the use of continued fraction technique. Chapter 5 calculates the electronic spectrum of the real transition metal alloys in the cluster approximation. In chapter 6 we apply the methods of chapter 3 and chapter 4 to evaluate the low temperature specific heat coefficient for Ni-Pt alloys, and we compare the results with the experiment. Also in chapter 6 we apply the continued fraction method to the disordered Heisenberg ferromagnet.

CHAPTER 2

THEORY FOR THE DENSITY OF STATES

2.1 INTRODUCTION

In this chapter we will develop a theory for the density of states for the transition metals and transition metal alloys. The development of theory means the manipulation of the expression for the density of states of a muffin-tin Hamiltonian presented by Lloyd (1967, Lloyd and Smith 1971). The main aim of the manipulation is to transform the Lloyds expression into a form more transparent physically and more suitable for numerical calculations.

The solution of the Schrodinger equation

$$\left[-\nabla^2 + V(r) - E\right]\psi(r) = 0 \qquad (2.1)$$

means finding the energy eigenvalues. These energy eigenvalues are related to the density of states. One of the central problems in the band theory of solids is to find the propagating solutions of the above Schrodinger equation, in which the potential has the periodicity of the lattice under consideration. Exact solutions of this problem are in general not possible, so a number of approximate methods are applied. The best and the most commonly used one is that which approximates the effective potential $V(r)$ by a muffin-tin

potential. The muffin-tin potential is a potential which is symmetrical inside a sphere constructed within an atomic polyhedra and is constant outside. Lloyd (1967) used this muffin-tin potential in his Hamiltonian

$$H = -\nabla^2 + V(\underline{r}) \tag{2.2}$$

where $V(\underline{r})$ is the sum of spherically symmetric contributions from sites $\{\underline{r}_s\}$ at which atoms of various types are situated i.e

$$\left.\begin{aligned} V(\underline{r}) &= \sum_{\underline{r}_s} v_{r_s}(|\underline{r}-\underline{r}_s|) \qquad |\underline{r}-\underline{r}_s| \leq r_i \\ &= 0 \qquad\qquad\qquad\quad |\underline{r}-\underline{r}_s| > r_i \end{aligned}\right\} \tag{2.3}$$

where r_i is the radius of the inscribed sphere. Using the Hamiltonian given by equation(2.2) in Schrodinger equation (2.1) Lloyd obtained an expression for the integrated density of states

$$N(E) = N_0(E) - \frac{1}{\pi} \mathrm{Im}\, \mathrm{Tr} \ln \left\{ t^{-1}_{L r_s} \delta_{LL'} \delta_{r_s r_{s'}} + G^{+}_{LL'}(\underline{r}_s - \underline{r}_{s'}) \right\} \tag{2.4}$$

where $N_0(E)$ is the integrated density of states for the empty lattice or the free electrans. The t-matrix is given in terms of the phase shifts $\eta_{L r_s}$

$$\left.\begin{aligned} t^{-1}_{L r_s} &= K \cot \eta_{L r_s} - iK \\ K &= \sqrt{E} \end{aligned}\right\} \tag{2.5}$$

and

$$G^{+}_{LL'}(r_s - r_s') = 4\pi K \sum_{L''} i^{l'+l-l'} C_{LL'L''} Y_{L''}(r_s - r_s')\, h^{+}_{\ell''}(K|r_s - r_s'|) \quad r_s - r_s' \neq 0$$
$$= 0 \quad r_s - r_s' = 0 \qquad (2.6)$$

where

$$C_{LL'L''} = \int Y^{*}_{L}(\theta,\phi)\, Y_{L'}(\theta,\phi)\, Y_{L''}(\theta,\phi)\, d\Omega \qquad (2.7)$$

and $h^{+}_{\ell''}$ is the spherical Hankel function defined by Messiah(1964; it should be noted here that our $h^{+}_{L} = -h^{+}_{L}$ of Messiah's).; and $Y_L(\theta,\phi)$ is a spherical harmonic.

It follows immediately from equation (2.4) that ordinary density of states is given (in symbolic notation) by

$$n(E) = n_0(E) - \frac{1}{\pi} \mathrm{Im}\, \mathrm{Tr} \left\{ \left(\frac{\partial}{\partial E} t^{-1} + \frac{\partial}{\partial E} G^{+} \right) \left(t^{-1} + G^{+} \right)^{-1} \right\} \qquad (2.8)$$

where $n_0(E)$ is the density of states of the free electrons. The matrix $(t^{-1} + G^{+})$ in the denominator of equation (2.8) is the Korringa-Kohn-Rostoker matrix(Kohn and Rostoker 1954) in site representation.

The density of states equations(2.4 and 2.8) have been little used for actual calculations. The reason for this is that there are three main difficulties in the use of expression (2.8).

The first is that for an infinite material the $(t^{-1}+G^{+})$ is infinite and this feature of equation (2.8) must be treated properly to avoid obtaining a density of states which is just a collection of δ functions. In many other cases the matrix is very large and is also very difficult to handle. The second difficulty is that where as in equation (2.8) $\frac{\partial}{\partial E}t^{-1}$ is diagonal in site indeci, $\frac{\partial}{\partial E}G^{+}$ is not and therefore, unless we think of some other solution, we will have to perform the difficult and tedious task of calculating <u>all</u> the elements of the inverse matrix $(t^{-1}+G^{+})^{-1}$. The final difficulty is that matrix $G^{+}_{LL'}(r_s-r_s')$ does not drop off rapidly as $|r_s-r_s'|$ increases if the energy is positive (the situation of greatest intrest).

The first difficulty which is equivalent to inverting an in-finite matrix has been fully discussed by Haydock <u>et al</u> (1972) for ordered crystals. In Haydock's paper the Lanczos alogrithm (Householder 1964) is applied to the calculation of the diagonal elements of the inverse of a tight-binding matrix. The same method has been adapted to the calculations of the diagonal elements of the inverse of a tight-binding matrix for the disordered crystals (alloys) by Jacobs (1973,1974, Cubiotti et al 1975). The second difficulty of calculating the off-diagonal elements of the inverse matrix can be overcome by manipulating equation (2.8) so that only diagonal elements of the inverse matrix appear.

The final difficulty can be handled in certain cases such as those of transition metals where the long range behaviour

of G^+ can be attributed to the plane waves hybridizing with the d bands (Jacobs 1968, Hubbard 1969). In this case the plane-wave contributions can be unfolded from the matrix leaving a tight-binding d matrix with short range ramnants replacing G^+ . Thus a partial solution to this difficulty is available. This will then offer us a new technique for practical calculations of the density of states of a muffin-tin Hamiltonian for an infinite crystal in a situation where the long range behaviour of the matrix elements $G^+_{LL'}(\underline{r}_s - \underline{r}_{s'})$ can be handled.

Hence in order to make use of equation (2.8) we must find a solution to the second problem. In this chapter we will present a solution to this difficulty and this will be done in two stages. The first discussed in section 2.2 is to show that the derivative $\frac{\partial}{\partial E} G^+$ can be written as a quadratic function of the matrix G^+ . The second stage, discussed in section 2.3, is to use the expression for the derivative $\frac{\partial}{\partial E} G^+$ in equation (2.8) and make the simplification to arrive at an expression for the density of states where the inverse $(t^{-1} + G^+)^{-1}$ is multiplied by diagonal matrices only.

This then provides a technique which depends on calculating only the diagonal elements of $(t^{-1} + G^+)^{-1}$.

The results of this chapter will be used to calculate the density of states of the transition metals and transition metal alloys in chapter 3 in a single site approximation and in chapter 5 in a cluster approximation.

2.2 DERIVATIVE OF G^+ WITH RESPECT TO ENERGY

The terms $G^+_{LL'}(r_s - r_s')$ occuring in the Lloyds formula (equation(2.8)) and defined explicitly by equation (2.6) are coefficients in the expansion of the Green function

$$G^0(r, r') = -\frac{1}{4\pi} \frac{\exp(ik|r - r'|)}{|r - r'|} \tag{2.9}$$

in terms of spherical harmonics and spherical Bessel functions. i.e.

$$G^0(r - r_s, r' - r') = \sum_{LL'} j_\ell(kr) Y_L(r) G^+_{LL'}(r_s - r_s') j_{L'}(kr') Y^*_{L'}(r') \tag{2.10}$$

provided

$$r_s \neq r_s' \quad \text{and} \quad |r - r'| < |r_s - r_s'|$$

and if $r_s = r_s'$

$$G^0(r - r_s, r' - r_s) = k \sum_L j_L(kr) h^+_\ell(kr') Y_L(r) Y^*_L(r') \tag{2.11}$$

for $r < r'$, and a expression with r and r' interchanged when $r' < r$

Now we want to find an expression for the derivative with respect to energy of G^+ thus defined by equation (2.10). The procedure for finding the formula for $\frac{\partial}{\partial E} G^+$ is split into following three parts.

(i) FINDING TWO DIFFERENT EQUATIONS FOR $\frac{\partial}{\partial E} G^0$

Differentiating equation (2.10) with respect to energy E we get

$$\frac{\partial}{\partial E} G^{\circ}(\underline{r}-\underline{r}_s, \underline{r}'-\underline{r}_s') = \sum_{LL'} \Big[j_L'(kr) \frac{\underline{r}}{2k} Y_L(\underline{r})\, G^{+}_{LL'}(\underline{r}_s-\underline{r}_s')\, j_{L'}(kr')\, Y^{*}_{L'}(\underline{r}')$$

$$+ j_L(kr)\, Y_L(\underline{r}) \frac{\partial}{\partial E} G^{+}_{LL'}(\underline{r}_s-\underline{r}_s')\, j_{L'}(kr')\, Y^{*}_{L'}(\underline{r}') \qquad (2.12)$$

$$+ j_L(kr)\, Y_L(\underline{r})\, G^{+}_{LL'}(\underline{r}_s-\underline{r}_s')\, j_{L'}'(kr') \frac{\underline{r}'}{k}\, Y^{*}_{L'}(\underline{r}') \Big]$$

This expression contains $\frac{\partial}{\partial E} G^{+}$, therefore in order to get a formula for this we need an alternative expression for $\frac{\partial}{\partial E} G^{\circ}(\underline{r}-\underline{r}_s, \underline{r}'-\underline{r}_s)$ To get this alternative expression we note that the Green function defined by equation (2.9) satisfy the following equation

$$(\nabla^2 + E)\, G^{\circ}(\underline{r}, \underline{r}') = \delta(\underline{r}-\underline{r}') \qquad (2.13)$$

From this it follows

$$\frac{\partial}{\partial E} G^{\circ}(\underline{r}-\underline{r}_s, \underline{r}'-\underline{r}_s') = -\int_{\text{all space}} G^{\circ}(\underline{r}-\underline{r}_s, \underline{r}'')\, G^{\circ}(\underline{r}'', \underline{r}'-\underline{r}_s')\, d^3\underline{r}'' \qquad (2.14)$$

or

$$\left.\begin{aligned} \frac{\partial}{\partial E} G^{\circ}(\underline{r}-\underline{r}_s, \underline{r}'-\underline{r}_s') &= -\sum_{\underline{r}_s''} \int_{\text{cell}} G^{\circ}(\underline{r}-\underline{r}_s, \underline{r}''-\underline{r}_s'')\, G^{\circ}(\underline{r}''-\underline{r}_s'', \underline{r}'-\underline{r}_s')\, d^3\underline{r}'' \\ &= \Big[\sum_{\underline{r}_s'' \neq \underline{r}_s', \underline{r}_s} \int_{\text{cell}} G^{\circ}(\underline{r}-\underline{r}_s, \underline{r}''-\underline{r}_s'')\, G^{\circ}(\underline{r}''-\underline{r}_s'', \underline{r}'-\underline{r}_s')\, d^3\underline{r}'' \\ &+ \sum_{\underline{r}_s''=\underline{r}_s'} \int_{\text{cell}} G^{\circ}(\underline{r}-\underline{r}_s, \underline{r}''-\underline{r}_s')\, G^{\circ}(\underline{r}''-\underline{r}_s', \underline{r}'-\underline{r}_s')\, d^3\underline{r}'' \\ &+ \sum_{\underline{r}_s''=\underline{r}_s} \int_{\text{cell}} G^{\circ}(\underline{r}-\underline{r}_s, \underline{r}''-\underline{r}_s)\, G^{\circ}(\underline{r}''-\underline{r}_s, \underline{r}'-\underline{r}_s')\, d^3\underline{r}'' \Big] \end{aligned}\right\} \qquad (2.15)$$

Substitute equations (2.10) or (2.11) as appropriate { equation (2.10) is valid for $\underline{r}_s \neq \underline{r}_s'$ and $|\underline{r}-\underline{r}'| < |\underline{r}_s-\underline{r}_s'|$ and (2.11) is valid for $\underline{r}_s = \underline{r}_s'$ } into the right hand side of equation (2.15). It is also

convenient to make the approximation of replacing the integral over unit cells in the lattice by integrals over spheres of the same volume centred at the same site. This approximation, while not necessary, enables us to write down simple explicit expressions, it does no violence to the structure of the result and can be expected to give reasonable numerical answers. The result of this procedure gives the following equation

$$\frac{\partial}{\partial E} G^{0}(\underline{r}-\underline{r}_s, \underline{r}'-\underline{r}_s')$$

$$= -\sum_{LL'} \Big\{ \sum_{L''} \sum_{\underline{r}_s'' \neq \underline{r}_s', \underline{r}_s} j_\ell(kr) Y_L(\underline{r}) G^{+}_{LL''}(\underline{r}_s-\underline{r}_s'') \alpha_{\ell''} G^{+}_{L''L'}(\underline{r}_s''-\underline{r}_s') j_{\ell'}(kr') Y^{*}_{L'}(\underline{r}')$$

$$+ K j_L(kr) Y_L(\underline{r}) G^{+}_{LL'}(\underline{r}_s-\underline{r}_s') \Big[h^{+}_{\ell'}(kr') \int_0^r r''^2 j_{\ell''}(kr'') j_{\ell'}(kr'')\, dr''$$

$$+ j_{\ell'}(kr') \int_r^{r_A} r''^2 h^{+}_{\ell'}(kr'') j_{\ell'}(kr'')\, dr'' \Big] Y^{*}_{L'}(\underline{r}')$$

$$+ K Y_L(\underline{r}) \Big[h^{+}_{\ell}(kr) \int_0^r r''^2 j_{\ell}(kr'') j_{\ell}(kr'')\, dr''$$

$$+ j_{\ell}(kr) \int_r^{r_A} r''^2 h^{+}_{\ell}(kr'') j_{\ell}(kr'')\, dr'' \Big] G^{+}_{LL'}(\underline{r}_s-\underline{r}_s') j_{\ell'}(kr') Y^{*}_{L'}(\underline{r}') \Big\} \qquad (2.16)$$

where

$$\alpha_{\ell''} = \int_0^{r_A} j_{\ell''}(kr'')\, j_{\ell''}(kr'')\, r''^2\, dr'' \qquad (2.17)$$

and r_A is the radius of a sphere of the same volume as the unit cell. (It should be noted that the above approximation is not

valid for all r and r'. We can consider, for example, terms in the sum over $\underset{\sim}{r}_s''$ where $|\underset{\sim}{r}_s - \underset{\sim}{r}_s''|$ is equal to the nearest neighbour distance d_{nn}. It is then easy to choose $\underset{\sim}{r}$ and $\underset{\sim}{r}'$ both within a unit cell such that $|\underset{\sim}{r}-\underset{\sim}{r}''| > |\underset{\sim}{r}_s-\underset{\sim}{r}_s''|$ which invalidates the use of equation (2.10). Similar arguments apply to terms in this sum where $|\underset{\sim}{r}_s''-\underset{\sim}{r}_s'|$ is equal to the nearest neighbour distance and to the remaining two terms in the curly bracket when $|\underset{\sim}{r}_s-\underset{\sim}{r}_s'|$ is equal to the nearest neighbour distance. The above equation is however certainly true for r and r' small enough since then the condition $|\underset{\sim}{r}-\underset{\sim}{r}''|<d_{nn}$ and $|\underset{\sim}{r}'-\underset{\sim}{r}''|<d_{nn}$ for r'' within a unit cell is satisfied. Subject to this restriction on the magnitudes of r and r' the result is always true. This weak result is sufficient for our purposes since we are interested only in obtaining an expression for the coefficient $\frac{\partial}{\partial E}\zeta^+$). To proceed further we must simplify the expression in the square brackets in equation (2.16). This is done in the second part of this section.

(ii) SIMPLIFICATION

Let

$$S(k,r) = h_\ell^+(kr)\int_0^r j_\ell^2(kr'')\,r''^2\,dr'' + j_\ell(kr)\int_r^{r_A} h_\ell^+(kr'')\,j_\ell(kr'')\,r''^2\,dr''$$

$$= \left\{ h_\ell^+(kr)\int_0^r j_\ell^2(kr'')\,r''^2\,dr'' - j_\ell(kr)\int_0^r h_\ell^+(kr'')\,j_\ell(kr'')\,r''^2\,dr'' \right\}$$

$$+ j_\ell(kr)\int_0^{r_A} h_\ell^+(kr'')\,j_\ell(kr'')\,r''^2\,dr''$$

$$= R(k,r) + T(k,r) \qquad (2.18)$$

where

$$R(k,r) = h_\ell^+(kr)\int_0^r j_\ell^2(kr'')\,r''^2\,dr'' - j_\ell(kr)\int_0^r h_\ell^+(kr'')\,j_\ell(kr'')\,r''^2\,dr'' \qquad (2.19)$$

$$T(k,r) = j_\ell(kr)\int_0^{r_A} h_\ell^+(kr'')\,j_\ell(kr'')\,r''^2\,dr'' \qquad (2.20)$$

Using equation (B1) from appendix B and $x''=kr''$, omitting the limits for the present $T(k,r)$ can be written as:

$$T(k,r) = j_\ell(kr)\,k^{-3}\int h_\ell^+(x'')\,j_\ell(x'')\,x''^2\,dx''$$

$$= j_\ell(kr)\,k^{-3}\left\{\tfrac{1}{2}x''^3\left[\left(j_{\ell-1}(x'')\,h_{\ell-1}^+(x'')\right.\right.\right.$$

$$\left.\left.\left. - \frac{\ell+1}{x''}\,j_\ell(x'')\,h_{\ell-1}^+(x'') + j_\ell(x'') - \frac{\ell}{x''}\,j_{\ell-1}(x'')\,h_\ell^+(x'')\right] - \tfrac{\ell}{2}\right\}\right.$$

$$= j_\ell(kr)\,k^{-3}\left\{\tfrac{1}{2}k^3r''^3\left[\left(j_{\ell-1}(kr'')\,h_{\ell-1}^+(kr'')\right.\right.\right.$$

$$\left.\left. - \frac{\ell+1}{kr''}\,j_\ell(kr'')\,h_{\ell-1}^+(kr'') + j_\ell(kr'')\,h_\ell^+(kr'')\right.\right.$$

$$\left.\left.\left. - \frac{\ell}{kr''}\,j_{\ell-1}(kr'')\,h_\ell^+(kr'')\right] - \tfrac{\ell}{2}\right\}\right.$$

Now putting in the limits

$$T(k,r) = j_\ell(kr)\left\{\tfrac{1}{2}r_A^3\left[\left(j_{\ell-1}(kr_A)\,h_{\ell-1}^+(kr_A) - \frac{\ell+1}{kr_A}\,j_\ell(kr_A)\,h_\ell^+(kr_A)\right.\right.\right.$$

$$\left.\left.\left. + j_\ell(kr_A)\,h_\ell^+(kr_A) - \frac{\ell}{kr_A}\,j_{\ell-1}(kr_A)\,h_\ell^+(kr_A)\right] - \tfrac{\ell}{2}k^{-3}\right\}\right. \qquad (2.21)$$

The same treatment is applied to $R(k,r)$ using equations (B1), (B2) and $x'' = kr''$

$$R(k,r) = k^{-3}\left[h_\ell^+(kr)\int_0^r j_\ell^2(x'')\,x''^2\,dx''\right.$$

$$\left. - j_\ell(kr)\int_0^r h_\ell^+(x'')\,j_\ell(x'')\,x''^2\,dx''\right]$$

$$= k^{-3}\left[h_\ell^+(kr)\left\{\tfrac{1}{2}x''^3\left[j_\ell^2(x'') - j_{\ell-1}(x'')\,j_{\ell+1}(x'')\right]\right\}\right.$$

$$- j_\ell(kr)\left\{\tfrac{1}{2}x''^3\left[j_{\ell-1}(x'')\,h_{\ell-1}^+(x'') - \frac{\ell+1}{x''}\,j_\ell(x'')\,h_{\ell-1}^+(x'')\right.\right.$$

$$\left.\left. + j_\ell(x'')\,h_\ell^+(x'') - \frac{\ell}{x''}\,j_{\ell-1}(x'')\,h_\ell^+(x'')\right] - \frac{\ell}{2}\right\}\Big]_0^r$$

$$= k^{-3}\left[h_\ell^+(kr)\left\{\tfrac{1}{2}k^3r''^3\left[j_\ell^2(kr'') - j_{\ell-1}(kr'')\,j_{\ell+1}(kr'')\right]\right\}\right.$$

$$- j_\ell(kr)\left\{\tfrac{1}{2}k^3r''^3\left[j_{\ell-1}(kr'')\,h_{\ell-1}^+(kr'') - \frac{\ell+1}{kr''}\,j_\ell(kr'') + h_\ell^+(kr'')\right.\right.$$

$$\left.\left. + j_\ell(kr)\,h_\ell^+(kr'') - \frac{\ell}{kr''}\,j_{\ell-1}(kr'')\,h_\ell^+(kr'')\right] - \frac{\ell}{2}\right\}\Big]_0^r$$

$$R(k,r) = \tfrac{1}{2}r^3\left[h_\ell^+(kr)\left[j_\ell^2(kr) - j_{\ell-1}(kr)\,j_{\ell+1}(kr)\right]\right.$$

$$- j_\ell(kr)\left[j_{\ell-1}(kr)\,h_{\ell-1}^+(kr) - \frac{\ell+1}{kr}\,j_\ell(kr)\,h_\ell^+(kr)\right.$$

$$\left.\left. + j_\ell(kr)\,h_\ell^+(kr) - \frac{\ell}{kr}\,j_{\ell-1}(kr)\,h_\ell^+(kr)\right]\right\} + \tfrac{\ell}{2}k^{-3}j_\ell(kr) \qquad (2.22)$$

This can be further simplified by the use of some standard results

for spherical Bessel functions set out in appendix B.

$$R(k,r) = \tfrac{1}{2} r^3 \Big[h_\ell^+(kr)\, j_\ell^{\,2}(kr) - h_\ell^+(kr)\, j_{\ell-1}(kr)\, j_{\ell+1}(kr)$$

$$- j_\ell(kr)\, j_{\ell-1}(kr)\, h_\ell^+(kr) + \frac{\ell+1}{kr}\, j_\ell^{\,2}(kr)\, h_\ell^+(kr)$$

$$- j_\ell^{\,2}(kr)\, h_\ell^+(kr) + \frac{\ell}{kr}\, j_{\ell-1}(kr)\, h_\ell^+(kr)\, j_\ell(kr) \Big] + \frac{\ell}{2} k^{-3} j_\ell(kr)$$

$$= \tfrac{1}{2} r^3 \Big[- h_\ell^+(kr)\, j_{\ell-1}(kr) \Big[j_{\ell+1}(kr) - \frac{\ell}{kr}\, j_\ell(kr) \Big]$$

$$- j_\ell(kr)\, h_{\ell-1}^+(kr) \Big[j_{\ell+1}(kr) - \frac{\ell+1}{kr}\, j_\ell(kr) \Big] \Big] + \frac{\ell}{2} k^{-3} j_\ell(kr)$$

$$= \tfrac{1}{2} r^3 \Big[- h_\ell^+(kr)\, j_{\ell-1}(kr)\, \frac{(\ell+1) j_{\ell+1}(kr) - \ell\, j_{\ell-1}(kr)}{2\ell+1}$$

$$- j_\ell(kr)\, h_{\ell-1}^+(kr)\, \frac{\ell\, j_{\ell-1}(kr) - (\ell+1) j_{\ell+1}(kr)}{2\ell+1} \Big] + \frac{\ell}{2} k^{-3} j_\ell(kr)$$

from (B3)

$$= \tfrac{1}{2} r^3 \Big[\frac{(\ell+1) j_{\ell+1}(kr) - \ell\, j_{\ell-1}(kr)}{2\ell+1} \Big] \Big[- h_\ell^+(kr) j_{\ell-1}(kr) + j_\ell(kr)\, h_{\ell-1}^+(kr) \Big]$$

$$+ \tfrac{1}{2} k^{-3} j_\ell(kr)$$

$$= \tfrac{1}{2} k^{-2} r \Big[\frac{(\ell+1) j_{\ell+1}(kr) - \ell\, j_{\ell-1}(kr)}{2\ell+1} \Big] + \frac{\ell}{2} k^{-3} j_\ell(kr)$$

from (B4)

$$= \tfrac{1}{2} k^{-2} r \Big[- j_\ell'(kr) \Big] + \frac{\ell}{2} k^{-3} j_\ell(kr) \qquad (2.23)$$

The results of equations (2.21) and (2.23) can now be used to write $S(k,r)$ as a linear combination of $j_\ell(kr)$ and $j_\ell'(kr)$ viz.

$$S(k,r) = -\tfrac{1}{2} k^{-2} r j_\ell'(kr) + k^{-2} \beta_\ell(k,r_A) j_\ell(kr) \qquad (2.24)$$

where

$$\beta_\ell(k,r_A) = \tfrac{1}{2} k^3 r_A^3 \Big[j_{\ell-1}(kr_A)\, h^+_{\ell-1}(kr_A) - \frac{\ell+1}{kr_A} j_\ell(kr_A)\, h^+_{\ell-1}(kr_A) + j_\ell(kr_A)\, h^+_\ell(kr_A) - \frac{\ell}{kr_A} j_\ell(kr_A)\, h^+_\ell(kr_A) \Big] \qquad (2.25)$$

(iii) A NEW FORMULA FOR $\frac{\partial}{\partial E} G^+$

In this part we use the results of equation (2.24) to simplify equation (2.16) of part (i). The right hand side of simplified equation (2.16) is then equated to the right hand side of equation (2.12); we note that the terms involving derivatives of $j_\ell(kr)$ cancel leaving us with a result depending on terms quadratic in $j_\ell(kr)$ only viz.

$$\sum_{LL'} j_\ell(kr)\, Y_L(\hat{r}) \frac{\partial}{\partial E} G^+_{LL'}(r_S - r_S')\, j_{L'}(kr')\, Y^*_{L'}(\hat{r}')$$

$$= -\sum_{LL'} \Big\{ \sum_{L''} \sum_{r_S'' \neq r_S', r_S} j_\ell(kr)\, Y_L(\hat{r})\, G^+_{LL''}(r_S - r_S'')\, \alpha_{\ell''}\, G^+_{L''L'}(r_S'' - r_S')\, j_{\ell'}(kr')\, Y^*_{L'}(\hat{r}')$$

$$+ j_\ell(kr)\, Y_L(\hat{r})\, G^+_{LL'}(r_S - r_S')\, \beta_{\ell'}(k,r_A)\, Y^*_{L'}(\hat{r}')$$

$$+ Y_L(\hat{r})\, \beta_\ell(k,r_A)\, G^+_{LL'}(r_S - r_S')\, j_{\ell'}(kr')\, Y^*_{L'}(\hat{r}') \qquad (2.26)$$

Equation (2.26), as we stated in part (i) is only valid for sufficiently small r and r', but the formula we get for $\frac{\partial}{\partial E} G^+$

after equating the coefficients of $j_\ell(kr)Y_L(\underline{r})$ and $j_{\ell'}(kr)Y^*_{L'}(\underline{r})$ on both sides of the above equation, is true for all values of the parameters.

$$\frac{\partial}{\partial E} G^+_{LL'}(\underline{r}_s - \underline{r}_s') = -\sum_{L''} \sum_{r_s'' \neq r_s', r_s} G^+_{LL''}(\underline{r}_s - \underline{r}_s'')\, \alpha_{\ell''}\, G^+_{L''L'}(\underline{r}_s'' - \underline{r}_s')$$

$$- G^+_{LL'}(\underline{r}_s - \underline{r}_s')\beta_{\ell'}(k, r_A) - \beta_\ell(k, r_A)\, G^+_{LL'}(\underline{r}_s - \underline{r}_s') \qquad (2.27)$$

This shows that $\frac{\partial}{\partial E} G^+$ is a quadratic function of G^+. This result is closely related to the classical result for the Greens function defined by

$$g = (E - H)^{-1} \quad \text{viz}$$

$$\frac{\partial}{\partial E} g = -g\,g \qquad (2.28)$$

The difference is due to the fact that G^+, itself, is not a Greens function but is, instead, a coefficient in the expansion of a Greens function in an energy dependent basis. We should emphasise here again that the derivative of G^+ satisfy an approximate equation (2.27) only, because we have used the sphere approximation for the unit cell in deriving it. The exact result will differ from this in that α and β will be non-diagonal matrices with two angular momentum indices. They will not however depend on site indices or be matrices between site indices.

2.3 A NEW FORMULA FOR THE DENSITY OF STATES.

The formula for $\frac{\partial}{\partial E} G^+_{LL'}(\underline{r}_s - \underline{r}_s')$ thus derived in section 2.2 and given precisely by equation (2.27) can now be used in expression (2.8) to deduce a new formula for the density of states:

$$n(E) = n_0(E) - \frac{1}{\pi} \mathrm{Im\,Tr}\left[\left(\frac{d}{dE} t^{-1}\right)\left(t^{-1}+G^{+}\right)^{-1} - G^{+}\alpha G^{+}\left(t^{-1}+G^{+}\right)^{-1}\right.$$

$$\left. - G^{+}\beta\left(t^{-1}+G^{+}\right)^{-1} - \beta G^{+}\left(t^{-1}+G^{+}\right)^{-1}\right] \qquad (2.29)$$

In each of the last three terms of this we add and subtract t^{-1} from one factor of G^{+}. Using the properties of the trace and cancelling $(t^{-1}+G^{+})^{-1}$ where possible we get

$$n(E) = n_0(E) - \frac{1}{\pi} \mathrm{Im\,Tr}\left[\left(\frac{d}{dE} t^{-1}\right)\left(t^{-1}+G^{+}\right)^{-1} - G^{+}\alpha\right.$$

$$\left. + G^{+}\alpha t^{-1}\left(G^{+}+t^{-1}\right)^{-1} - 2\beta + 2\beta t^{-1}\left(t^{-1}+G^{+}\right)^{-1}\right] \qquad (2.30)$$

Repeating the same manipulation once more we have

$$n(E) = n_0(E) - \frac{1}{\pi} \mathrm{Im\,Tr}\left[\left(\frac{d}{dE} t^{-1}\right)\left(t^{-1}+G^{+}\right)^{-1} - G^{+}\alpha\right.$$

$$+ \alpha t^{-1} - t^{-1}\alpha t^{-1}\left(t^{-1}+G^{+}\right)^{-1} - 2\beta$$

$$\left. + 2\beta t^{-1}\left(t^{-1}+G^{+}\right)^{-1}\right] \qquad (2.31)$$

We can drop the term $G^{+}\alpha$ because it has a zero trace. It can be easily checked that the imaginary part of the trace of $-\frac{2\beta}{\pi}$ is equal to $2n_0(E)$. The term $-\frac{1}{\pi}\mathrm{Im\,Tr}(\alpha t^{-1}) = \frac{1}{\pi}\mathrm{Tr}(\alpha K)$ is nearly equal to the density of states of free electrons, $n_0(E)$ in this sphere approximation and is exactly $n_0(E)$ if we do not make this approximation. The final expression for the density of states is therefore

$$n(E) = -\frac{1}{\pi} \mathrm{Im\,Tr}\left[\left(\frac{d}{dE} t_L^{-1} - t_L^{-1}\alpha_\ell t_L^{-1} + 2\beta_\ell t_L^{-1}\right]\left[t^{-1}+G^{+}\right]^{-1}\right.$$

(2.32)

This shows that for a muffin-tin Hamiltonian $n(E)$ depends on the diagonal matrix elements between site indices of the inverse, $(t^{-1}+G^{+})^{-1}$ only. (The numerator $(\frac{d}{dE}t^{-1}-t^{-1}\alpha t^{-1}+2\beta t^{-1})$ is diagonal between site indices).

We must note that for transition metals the trace is over l=0, l=1 and l=2 angular momenta only for $l > 2$ the imaginary part of the trace of the above expression is very small so that it can be ignored. For l=0 and l=1 it can be proved (proof given in appendix A) that

$$-\frac{1}{\pi}\,\mathrm{Im}\,\mathrm{Tr}\left[\left(\frac{d}{dE}t_l^{-1}-t_l^{-1}\alpha_l t_l^{-1}+2\beta_l t_l^{-1}\right)\left(t_l^{-1}+G^{+}_{LL'}\right)^{-1}\right] \simeq n_0(E)$$

and we will be left with the following expression with the trace over the l=2 angular momentum only

$$n(E)=n_0(E)-\frac{1}{\pi}\,\mathrm{Im}\,\mathrm{Tr}\left[\frac{d}{dE}t_2^{-1}-t_2^{-1}\alpha_2 t_2^{-1}+2\beta_2 t_2^{-1}\right]\left[t_2^{-1}+G^{+}_{2m,2m'}\right]^{-1} \qquad (2.33)$$

This is the expression which will be used in numerical calculations in the following chapters.

In the next section we shall examine equation(2.32) in detail.

2.4 DISCUSSION

We shall now examine equation (2.32) in three different cases. In the first case we shall use a form for t^{-1} which is appropriate to a nearly free electron metal; in the second case a form appropriate to a metal with d-band lying entirely below the

conduction band and the muffin-tin zero (an example of such a metal is Zn); and in the third case we shall use a form appropriate to an ordinary transition or noble metal such as Ni or Cu with the d-band crossing and hybridizing the conducton band.

(i) For a nearly-free-electron like metal (Na, K etc.) the pseudo-potential is weak and weakly energy-dependent which implies that t_o^{-1} is large and weakly energy-dependent where

$$t^{-1} = t_o^{-1} - ik$$
$$t_o^{-1} = k \cot \eta_l \qquad (2.34)$$

With the above statements we shall see that the first term in the trace of equation (2.32) will give a small contribution to the density of states. Because the first term then becomes

$$I_m Tr\left[\frac{d}{dE} t^{-1}(t^{-1}+G^+)^{-1}\right]$$
$$= Tr\left[\left\{\frac{d}{dE} t_o^{-1} - \frac{d}{dE}(ik)\right\} t (1+G^+t)^{-1}\right]$$
$$\to 0 \quad \text{because } t \to 0$$

and the last term gives

$$I_m Tr\left[2\beta t^{-1}(t^{-1}+G^+)^{-1}\right]$$
$$= I_m Tr\left[2\beta (1+G^+t)^{-1}\right]$$
$$= I_m Tr\left[2\beta - 2\beta G^+ t\right]$$

The trace of $2\beta G^+ t$ is zero and the imaginary part of the trace of the term 2β is $-2n_o(E)$.

The second term reduces to $-n_o(E)$ by the following argument

$$\mathrm{Im\,Tr}\left[t^{-1}\alpha t^{-1}(t^{-1}+G^{+})^{-1}\right]$$

$$= \mathrm{Im\,Tr}\left[t^{-1}\alpha - t^{-1}\alpha G^{+}t + \cdots\right]$$

$$= \mathrm{Im\,Tr}\left[(t_{0}^{-1}-ik)\alpha - \alpha G^{+}\cdots\right]$$

$$\simeq -n_{0}(E)$$

The net result to the density of states to lowest order is $n_0(E)$, the density of states for free electrons. There are three points to notice in this elementry calculation. The first is that equation (2.32) gives the correct result very easily. The second is that it is the first term outside the trace and the last and the second terms within the trace of the equation (2.32) which make up the important nearly-free-electron term. The third is that in the trace it is necessary to sum over all low angular momentum even when a restricted Korringa-Kohn-Rostoker matrix (Kohn and Rostoker 1954) including only a few angular momenta is sufficient to give the correct energy bands. This last point is important in transition metals where a secular equation involving an l=2 KKR matrix gives a reasonable approximation to the energy bands. The suppresed l=0 and l=1 parts of the matrix nevertheless give the major nearly-free-electron terms in equation (2.32).

(ii) We now examine metals like Zn, where there is a d-band lying below the conduction band and the muffin-tin zero. At energies in the region of the d-band the l=2 element of the inverse t-matrix is given by

$$t_{2}^{-1} = (E_d - E)/\Gamma - ik \qquad (2.35)$$

where E_d is negative, Γ is nearly constant and ik is real. All other matrix elements of t^{-1} are large and weakly energy dependent. At these energies $G^+_{LL'}(r_s - r_s')$ is given by;

$$G^+_{LL'}(r_s - r_s') = 4\pi i k' \sum_{L''} i^{l''-l-l'} C_{LL'L''} Y_{L''}(r_s - r_s')\, h^+_{l''}(ik'|r_s - r_s'|)$$

where

$$h^+_{l''}(ik'|r_s - r_s'|) \underset{|r_s - r_s'| \to \infty}{\longrightarrow} (-i)^{l+1} \frac{e^{-k'(|r_s - r_s'|)}}{k'(|r_s - r_s'|)} \qquad k' \text{ is real}$$

which shows that $G^+_{LL'}(r_s - r_s')$ is Hermitian and drops off rapidly as $(r_s - r_s')$ increases and the denominator in the trace of equation (2.32) takes on the form of d–d tight-binding block in site representation. The zero of the denominator lie in a region whose width is of the order of Γ centred about the real energy $E_d' = E_d - ik\Gamma$. It is clear from this that the term ik which is due to hybridization of the d-band with the free electron bands at higher energies gives rise to a net downward shift of the d band. The first term in the numerator of equation (2.32) gives rise to a constant which when multiplied by the inverse tight binding matrix gives the d band density of states completely. The remaining terms are quadratic or linear in $E - E_d'$, and thus vanish in the centre of the d band; they give rise to small hybridization corrections. The free-electron bands occur at much higher energies and the major contributions to the density of states comes as before from the first term and l=0 and l=1 parts of the second term in the trace.

(iii) Finally we examine the case of the transition metals (Cu, Ni, ...etc) where the d bands cross the conduction band. The inverse t-matrix is given by equation(2.35) E_d is now positive, consequently

at d band energies E is positive and $i\kappa$ is imaginary and the hybridization due to this term in the denominator of equation (2.32) no longer gives rise to a uniform downward shift of the d band. Instead it gives an additional broadening to the d band consistent with the idea that part of the d band is hybridized downwards and part upwards. The imaginary part $-\frac{d}{d\epsilon}(i\kappa)$ in the first term of the numerator when multiplied by the real part of $(t^{-1}+G^{+})^{-1}$ nevertheless produces a net downward shift of the d band since it contains a factor $(E_d-\epsilon)$ which changes sign at the centre of the d band. We may interpret this shift as due to the fact that there are always more conduction bands above the d bands than below. The remaining terms in the numerator disappear either quadratically or linearly in the d band region and consequently give at the most small hybridization or broadening.

CHAPTER 3

SINGLE SITE THEORY FOR TRANSITION METAL ALLOYS

3.1 INTRODUCTION

In this chapter we will present a continued fraction method for calculating the electronic spectrum of the transition metal alloys. This method has been used in the multiple site theory for a single s band Hamiltonian (Jacobs 1974, Cubiotti et al 1975). It is much harder to do the multiple site theory for a degenerate d band transition metal Hamiltonian (see next chapter). Therefore in this chapter we will restrict ourselves to a single theory. In a single site approximation, the central atom is treated exactly and electron hops from the central atom to the average environment. There are two kinds of single site theories commonly used, the coherent potential approximation (CPA) and the average t-matrix approximation (ATA); we shall however use a single site theory which is different from these and nevertheless, in common with the CPA, preserves the lowest six moments of the density of states correctly.

We begin in section 3.2 by investigating the accuracy of our single site theory for a tight binding s band Hamiltonian. In § 3.3 we will apply this single site theory for calculating

the electronic spectrum of the transition metal alloys. In the above calculations we use a model in which the l=2 component of the binary alloy in the pure-material limits have identical shapes, the only difference being the absolute position of the bands in energy. In section 3.4 we discuss the numerical results and conclude.

3.2 ACCURACY OF SINGLE-SITE THEORY

In this section we calculate the density of states for a single tight binding s band by the continued fraction method in our single site approximation. The results obtained are compared with the density of states curves calculated in the coherent potential approximation and in the multiple site theory (Cubiotti et al, 1975). We will also calculate numerically and analytically the moments of the s band density of states in our approximation and compare them with the exact results and show that we have the same accuracy as those obtained in CPA by Velicky et al (1968).

In a very simplified single site approximation for an AB alloy, the average Green function (for a semi-elliptical band of bandwidth 4 units) can be written as (equation(1.12) of chapter I)

$$\langle G \rangle = \frac{c}{E_A - E - F} + \frac{(1-c)}{E_B - E - F} \qquad (3.1)$$

where c is the concentration of atoms of type A

$$E_A = \tfrac{1}{2}\delta \quad ; \quad E_B = -\tfrac{1}{2}\delta \qquad (3.2)$$

δ is the bandwidth or separation between the atomic levels.

and

$$\overline{F} = cF_A + (1-c)F_B \tag{3.3}$$

where F_A and F_B are given by the equations

$$F_A = \frac{(E_A-E) \pm \sqrt{(E_A-E)^2 - 4}}{2} \tag{3.4}$$

$$F_B = \frac{(E_B-E) \pm \sqrt{(E_B-E)^2 - 4}}{2} \tag{3.5}$$

Therefore we now know the average Green function defined by equation (3.1). Hence we can calculate the average density of states by the formula

$$n(E) = \frac{1}{\pi} \operatorname{Im} \langle G \rangle \tag{3.6}$$

In figure (3.1) and (3.1b) we compare the numerical results of our single site theory and that of the coherent potential approximation for a semi-elliptical tight binding s band. Figure (3.1) is for c=.4 and figure (3.1b)is for c=.2. In both the figures the dotted line curve represents the CPA and the full line curve our single site theory. The CPA curves are flat and broad, and their width and height decrease with the decrease in concentration. But the single site curves are narrow and peaked at the centre. The height at the centre of the band is maintained with the decrease in concentration.

Now we will do the calculations for a simple cubic material using our single site theory in order to compare the results with

the multiple site theory for simple cubic (Cubiotti et al 1976).

The average Green function for a simple cubic (with six nearest neighbours) in our single site approximation is

$$\langle G \rangle = \frac{c}{E_A - E - \bar{F}} + \frac{(1-c)}{E_B - E - \bar{F}} \qquad (3.7)$$

where E_A, E_B, $\bar{F}$ and c are the same as defined before, but now

$$F_A = \left[9/(E_A - E - \frac{85}{9} FD(E_A - E)) \right]^{-1} \qquad (3.8)$$

and

$$F_B = \left[9/(E_B - E - \frac{85}{9} FD(E_B - E)) \right]^{-1} \qquad (3.9)$$

where

$$FD(E) = \frac{E \pm \sqrt{E^2 - 36}}{18} \qquad (3.10)$$

The sign in the last equation is selected so as to have correct analytic behaviour for FD(E).

Figure (3.1c) and figure (3.1d) compare the results for a simple cubic s band in our single site theory and the multiple site theory. The full line curves are for single site theory and the dotted line ones for multiple site theory. The similarity of the curves obtained from our single site theory and from the cluster

theory (Cubiotti et al 1975; 25 sites) demonstrate the likely convergence of our method. The CPA does not seem to be close to the likely converged result of our method.

Now we will examine, mathematically and numerically, the moments of the density of states function obtained in the single site theory for a semi-elliptical band. Mathematically the moments of the density of states are defined as the coefficients of the terms in the expansion of the average Green function in powers of energy i.e

$$\langle G \rangle = \sum_{p=0}^{\infty} \frac{M_p}{E^{p+1}} \qquad (3.11)$$

To get these coefficients we proceed as follows:

Expanding equation (3.4) in powers of energy in the limit $E \to \infty$ and keeping the first four terms only we have

$$F_A = -\frac{1}{E} - \frac{\delta/2}{E^2} - \frac{\delta^2/4 + 1}{E^3} - \frac{\delta^3/8 + 3\delta/2}{E^4} \qquad (3.12)$$

Similarly expanding equation (3.5) we get

$$F_B = -\frac{1}{E} + \frac{\delta/2}{E^2} - \frac{\delta^2/4 + 1}{E^3} + \frac{\delta^3/8 + 3\delta/2}{E^4} \qquad (3.13)$$

Substituting equations (3.11) and (3.12) into equation (3.3) we have

$$\bar{\bar{F}} = -\frac{1}{E} + \frac{(1-2c)\,\delta/2}{E^2} - \frac{\delta^2/4+1}{E^3} + \frac{(1-2c)(\delta^3/8+\delta/2)}{E^4} \qquad (3.14)$$

Using this expression of $\bar{\bar{F}}$ in equation(3.1) we get

$$\langle G\rangle = -\frac{1}{E} + \frac{(1-2c)\,\delta/2}{E^2} - \frac{\delta^2/4+1}{E^3} + \frac{(1-2c)(\delta/2+\delta^3/8)}{E^4}$$

$$- \frac{1}{E^5}\left[\frac{\delta^4}{16} + \delta^2 + (1-2c)^2\frac{\delta^2}{2} + 2\right]$$

$$+\frac{1}{E^6}\left[(1-2c)\frac{\delta^5}{32} + (1-2c)\frac{5}{4}\delta^3 + 5(1-2c)\delta\right] \qquad (3.15)$$

which gives

$$M_0 = 1$$

$$M_1 = -(1-2c)\frac{\delta}{2}$$

$$M_2 = \frac{\delta^2}{4} + 1$$

$$M_3 = -(1-2c)\left(\frac{3}{2}\delta + \frac{\delta^3}{8}\right)$$

$$M_4 = \left(\frac{\delta^4}{16} + \delta^2 + (1-2c)^2\frac{\delta^2}{2} + 2\right)$$

$$M_5 = -\left[(1-2c)\frac{\delta^5}{32} + (1-2c)\frac{5}{4}\delta^3 + (1-2c)5\delta\right] \qquad (3.16)$$

Comparing these moments with those given in equation (3.30) of Velicky et al (1968), we see that they are the same as the exact results and those of the CPA.

Numerically as a check on the arithematic we calculated the density of states moments by the defination

$$\mu_p = \int dE\ E^p n(E) \qquad (3.17)$$

where the numerical value of n(E) is the same as given by equation (3.6). We find that these computed results for μ_p (given in Table 3.1) agree very well with those evaluated from the mathematical formula of equation (3.16). This proves that our single site theory is of comparable accuracy to CPA as far as the moments of the density of states are concerned.

Having thus established the accuracy of the single site theory for a simple Hamiltonian, we will apply it to the complicated transition metal Hamiltonian in the next section.

3.3 TRANSITION METAL ALLOY

(i) Plan of calculations

The density of states function for transition metals is characterised by a narrow and high d electron density of states superimposed on a broad low sp density of states. Three ingredients are used to calculate density of states of transition metal alloy. These are:

(a) The density of states of the two pure components.

(b) The modification of Lloyd's formula discussed in chapter 2,

which gives us the density of states of a transition metal in terms of the diagonal elements of an inverse matrix.

(c) The single site theory of section 3.2, which enables us to calculate the diagonal elements of the inverse matrix in an alloy approxi mation.

The first ingredient is discussed in detail in section 3.2(i), while the details of the second and third ingredients are discussed below.

We restate the Lloyd's modified formula here as;

$$n(E) = n_c(E) + \frac{Im}{\pi} Tr\left\{ D\left[t_2^{-1} + G^{+}_{LL'} \right]^{-1} \right\} \tag{3.18}$$

where

$$n_c(E) = \frac{1}{\pi}\left[\alpha_0 k + 3\alpha_1 k \right] \tag{3.19}$$

$$D = t_2^{-1} \alpha_\ell t_2^{-1} - 2\beta_\ell t_2^{-1} - \frac{d}{dE} t_2^{-1} \tag{3.20}$$

$$\alpha_\ell = \tfrac{1}{2} x^3 \left[j_\ell^2(xk) - j_{\ell-1}(xk)\, j_{\ell+1}(xk) \right] \tag{3.21}$$

$$\left.\begin{aligned} \beta_\ell = \tfrac{1}{2} x^3 k \Big[& j_{\ell-1}(xk)\, n_{\ell-1}(xk) - \frac{\ell+1}{xk} j_\ell(xk)\, n_{\ell-1}(xk) \\ & + j_\ell(xk)\, n_\ell(xk) - \frac{\ell}{xk} j_{\ell-1}(xk)\, n_\ell(xk) \Big] \\ & - ik\alpha_\ell \end{aligned}\right\} \tag{3.22}$$

$$
\left.
\begin{aligned}
t_2^{-1} &= \kappa \cot \eta_2 - i\kappa \\
&= t_0^{-1} - i\kappa \\
\kappa &= \sqrt{E} \\
\tan \eta_2 &= W(E)/(E_d - E)
\end{aligned}
\right\} \qquad (3.23)
$$

In these equations $G^{+}_{LL'}$ is the coefficient in an expansion of the free electron Green function, which is discussed later; κ is the radius of the sphere of the same volume as the unit cell; E_d is the position of the d resonance; j_l and n_l are the spherical Bessel function and Neuman function respec-tively; η_2 is the phase shift for the d electron orbitals, i.e l=2. The phase shift can be accurately represented over the entire width of the d band if the energy dependence of $W(E)$ is approximated in the following form (Pettifor, 1969)

$$
W(E) = \frac{\omega}{2} \kappa j_2^2(\kappa r_i) / \kappa_d j_2^2(\kappa_d r_i) \qquad (3.24)
$$

$$
\kappa_d = \sqrt{E_d} \qquad (3;25)
$$

where r_i is the radius of the inscribed sphere; ω is the width of the d resonance at $E=E_d$ and is fully discussed by Hubbard (1969).

To formulate the single site theory we consider a random

substitutional alloy AB. The fractional concentration of the two constituents are c and (1-c) respectively, and their distribution throughout the lattice is assumed to be random. For this alloy the density of states equation (3.6) in a single site approximation discussed in section 3.2 can be written as:

$$n(E) = n_0(E) + \frac{I_m}{\pi} \mathrm{Tr} \left\{ c D_A \left[\hat{t}_2^{A\,-1} + G^{+}_{2m2m'} + \bar{F}_{2m2m'} \right]^{-1} + (1-c) D_B \left[t_2^{B\,-1} + G^{+}_{2m2m'} + \bar{F}_{2m2m'} \right]^{-1} \right\} \qquad (3.26)$$

where

$$\left.\begin{aligned} D_A &= t_2^{A\,-1} \alpha_\ell \, t_2^{A\,-1} - 2\beta_\ell t_2^{A\,-1} - \frac{d}{dE} t_2^{A\,-1} \\ D_B &= t_2^{B\,-1} \alpha_\ell \, t_2^{B\,-1} - 2\beta_\ell t_2^{B\,-1} - \frac{d}{dE} t_2^{B\,-1} \end{aligned}\right\} \qquad (3.27)$$

$\bar{F}$ is the termination to the continued fraction in a single site approximation i.e

$$\bar{F}_{2m2m'} = c F^{A}_{2m2m'} + (1-c) F^{B}_{2m2m'} \qquad (3.28)$$

where $F^{A}_{2m2m'}$ and $F^{B}_{2m2m'}$ are the terminators to the continued fraction corresponding to pure A and pure B materials respectively, these are evaluated in the next sub-section.

3.3(ii) Band structure

We know that the shape of the d band electronic spectrum of all the transition metals is the same, therefore we

will calculate the density of states for an arbitrary transition metal and make it to behave as the density of states for A and B materials by shifting the centre of the d band to E_d^A and E_d^B respectively. The density of states of e_g and t_{2g} symmetry, denoted by ρ_e and ρ_t respectively in the d band region of a transition metal is calculated using the Model Hamiltonian (Jacobs 1968) derived from the KKR method. The explicit expression used in the calculation is:

$$D_{mm'}(E) = \left(\frac{\pi}{aN}\right)^3 \sum_K \left\{ \left[T_{mm'}(K) - E S_{mm'} - \sum_n \frac{\Gamma_m(K+K_n)\,\Gamma_{m'}^*(K+K_n)}{|K+K_n|^2 - E} \right]^{-1} \right\} \quad (3\cdot29)$$

where

$$\Gamma_m(K+K_n) = A_l\, j_2(|K+K_n| R_n)\, Y_L(K+K_n)\, f_c(|K+K_n|) \quad (3\cdot30)$$

$$\begin{aligned} f_c(x) &= 1 && \text{when} \quad x \leq 4\cdot25 \\ &= 1\cdot176(5\cdot1-x) && \text{when} \quad 4\cdot25 < x \leq 5\cdot1 \\ &= 0 && \text{when} \quad x > 5\cdot1 \end{aligned} \quad (3;31)$$

K_n is the reciprocal lattice vector and only the following four values are used

$$\begin{aligned} k_0 &= \frac{2\pi}{a}(0,0,0) \\ k_1 &= \frac{2\pi}{a}(\bar{1},\bar{1},\bar{1}) \\ k_2 &= \frac{2\pi}{a}(0,\bar{2},0) \\ k_3 &= \frac{2\pi}{a}(\bar{1},\bar{1},1) \end{aligned} \quad (3.32)$$

where a is the lattice constant, R_H and A_H are constants. The integeration in the k space is done in the $\frac{1}{48}^{th}$ of the Brillouin zone.* N is the number of points at which the integration is done. The three components of the k vector k_x, k_y and k_z satisfy the following condition:

$$k_x \leq k_y \leq k_z \tag{3.33}$$

The values of the parameters, the spherical harmonics and the tight binding $T(k)_{mm'}$, Slater and Koster (1954) matrix elements used in this part of the computer programme are given in Table 3.2. $D_{mm'}$ turns out to be a diagonal matrix with three components equal and the other two equal to each other. The e_g and t_{2g} components of the density of states can now be calculated by taking the imaginary part of the trace over the corresponding equal diagonal matrix elements. These are then made to behave as ρ_e^A, ρ_t^A and ρ_e^B, ρ_t^B components of the density of states of the A and B materials by shifting their centres to E_d^A and E_d^B respectively.

It is necessary in order to write down expression for $F_{mm'}^A$ and $F_{mm'}^B$ of equation(3.28) to define intermediate quantities for pure materials K_1^A, K_2^A and K_1^B, K_2^B which have their imaginary parts given by the equations:

$$\begin{aligned} I_m K_1^A &= \frac{\pi}{5D_A}\, \rho_e^A \\ I_m K_2^A &= \frac{\pi}{5D_A}\, \rho_t^A \end{aligned} \tag{3.34}$$

---

* We are grateful to Prof Callaway for providing us with the weighting factors at corners and edges of the Brillouin zone.

$$\mathrm{Im}\ k_1^B = \frac{\pi}{5D_B}\rho_e^B$$

$$\mathrm{Im}\ k_2^B = \frac{\pi}{5D_B}\rho_t^B \qquad (3.35)$$

The real parts of K_1^A, K_2^A and K_1^B, K_2^B are the Hilbert transforms of the above quantities. These quantities are roughly analogous to the quantities in the denominator of equation (3.1) for the single site theory.

As K_1^A and K_2^A, K_1^B and K_2^B are the two separate groups of the elements of the diagonal matrices, therefore the matrices $F^A_{mm'}$ and $F^B_{mm'}$ of equation (3.28) which are defined in terms of these quantities also fall into two groups F_1^A, F_2^A, F_1^B and F_2^B. The precise equations are:

$$\left.\begin{aligned}\left[{}^At_2^{-1} + G^+_{2m2m'} + F_1^A\right]^{-1} &= k_1^A \\ \left[{}^At_2^{-1} + G^+_{2m2m'} + F_2^A\right]^{-1} &= K_2^A\end{aligned}\right\} \qquad (3.36)$$

$$\left.\begin{aligned}\left[{}^Bt_2^{-1} + G^+_{2m2m'} + F_1^B\right]^{-1} &= k_1^B \\ \left[{}^Bt_2^{-1} + G^+_{2m2m'} + F_2^B\right]^{-1} &= K_2^B\end{aligned}\right\} \qquad (3.37)$$

Therefore

$$\left.\begin{aligned}F_1^A &= \left[(k_1^A)^{-1} - G^+_{2m2m'} - {}^At_2^{-1}\right] \\ F_2^A &= \left[(k_2^A)^{-1} - G^+_{2m2m'} - {}^At_2^{-1}\right]\end{aligned}\right\} \qquad (3.38)$$

$$F_1^B = \left[(K_1^B)^{-1} - G^+_{2m2m'} - {}^B t_2^{-1} \right]$$

$$F_2^B = \left[(K_2^B)^{-1} - G^+_{2m2m'} - {}^B t_2^{-1} \right] \qquad (3.39)$$

(As K_1^A , K_2^A , K_1^B and K_2^B are just numbers, there is no difficulty in taking their inverse).

After substituting the value of $\bar{F}$ into the equation (3.26) we see that $G^+_{2m2m'}$ cancels, therefore in this single site calculations we need not bother about the value of $G^+_{2m2m'}$. The trace in equation (3.26) is now over two terms only.

To do the numerical calculations for the density of states we must clearly define the quantities occuring in equation(3.27). α_ℓ and β_ℓ are the same as defined by equations (3.22) and (3.23), and the other quantities are defined by the following set of equations:

$$ {}^A t_2^{-1} = k \cot \eta_2^A - ik$$

$$ {}^B t_2^{-1} = k \cot \eta_2^B - ik \qquad (3.40)$$

$$\tan \eta_2^A = c_A k j_2^2 (kR_i) / (E_d^A - E) \qquad (3.41)$$

$$\tan \eta_2^B = c_B k j_2^2 (kR_i) / (E_d^B - E) \qquad (3.42)$$

$$C_A = \frac{\omega_A}{2} \; 1./ k_d^A \, j_2^2 (k_d^A r_i) \tag{3.43}$$

$$C_B = \frac{\omega_B}{2} \; 1./ k_d^B \, j_2^2 (k_d^B r_i) \tag{3.44}$$

$$\left.\begin{aligned} k_d^A &= \sqrt{E_d^A} \\ k_d^B &= \sqrt{E_d^B} \end{aligned}\right\} \tag{3.45}$$

$$\left.\begin{aligned} \frac{d}{dE}\,{}^A t_2^{-1} = &- \frac{1}{C_A j_2^2(k r_i)} - \frac{j_1(k r_i)}{j_2(k r_i)} \frac{r_i}{k} \, k \cot \eta_2^A \\ &+ \frac{3}{E} \, k \cot \eta_2^A - \frac{i}{2k} \end{aligned}\right\} \tag{3.46}$$

$$\left.\begin{aligned} \frac{d}{dE}\,{}^B t_2^{-1} = &- \frac{1}{C_B j_2^2(k r_i)} - \frac{j_1(k r_i)}{j_2(k r_i)} \frac{r_i}{k} \, k \cot \eta_2^B \\ &+ \frac{3}{E} \, k \cot \eta_2^B - \frac{i}{2k} \end{aligned}\right\} \tag{3.47}$$

where ω_A and ω_B are the resonance widths for the d bands of A and B type materials respectively. E_d^A and E_d^B are the centres of the two d bands. r_i is the radius of the Wigner Sietz sphere. The values of the parameters used in the calculations are given in Table 3.3.

3.3(iii) Conclusion

Our strategy has been to use the density of states of the pure materials(obtained by a different method) to calculate

the terminators F^{A}_{nm} and F^{B}_{mm} for the pure materials. Thus avoiding the direct calculations of F^{A}_{mm} and F^{B}_{mm} by the continued fraction method, a much more difficult proceedure.

The numerical results are presented and discussed in the next section.

3.4 DISCUSSION AND CONCLUSION

Figure (3.2) gives ρ_e and ρ_t, the e_g and t_{2g} components of the density of states of an arbitrary transition metal calculated from the interpolation scheme of the Model Hamiltonian. The total density of states is then obtained by adding to the s density of states an appropriately weighted combination of the two components ρ_e and ρ_t. These components of the density of states of the transition metal are used as data in all subsiquent calculations.

Figure (3.3) gives the density of states of the two components of the alloy in the pure limit. The d component having the same shape but different band centres. The area under the curve for E less than .8 is roughly equal to the number of d electrons and the s electrons.

In figure (3.4) the electronic spectrum for two symmetrical concentrations c=.2 and c=.8 is presented. We see that an addition of a small amount of impurity results in the appearance

of a high density of states around its d band centre at the expense of the density of states at the upper edge of the d band of the host metal. The total area upto E=.8 for the curves of each concentration remains the same as before.

Figure (3.5) gives the results for c=.4 and c=.6, and we see that with the increase of the concentration the minority band grows at the expense of the majority band.

Figure (3.6) is the picture of a 50-50 alloy. There are two smooth roughly symmetrical peaks around the centres of the two bands with area under the curve renaining the same.

From the various figures it is clear that the effect of alloying is that the height of the bands remain almost unchanged and the half width is multiplied by a factor c, but the centre of gravity of the bands roughly maintain their position. These are the special features of this type of approximation as compared to CPA, in which the width of the band , however defined and height of each sub-band go as $\sqrt{c}$, and the centre of gravity is shifted by amount proportional to (1-c).

The calculations in this single site theory take very little computer time, because there are no self-consistent equations to be solved.

TABLE 3.1

THE MOMENTS $\mu_n \times 10^{n-2}$ FOR FULL LINE CURVES IN FIGURES 3.1 AND 3.1b AND THOSE CALCULATED FROM EQUATUION(3.16)

c= .4

n	$\mu_n \times 10^{n-2}$	
	NUMERICAL	ANALYTIC
0	99.8986	10.0000
1	-99.7512	-100.0000
2	2498.4631	2501.0000
3	-2496.7733	-2503.0000
4	62538.1249	62601.0200
5	-62593.2612	-62750.1000

c= .2

n	$\mu_n \times 10^{n-2}$	
	NUMERICAL	ANALYTIC
0	99.8125	10.0000
1	-299.1139	-300.0000
2	2496.3129	2501.0000
3	-7486.7841	-7509.0000
4	62500.1002	62609.0200
5	-187689.7650	-188230.3000

TABLE 3.2

REAL SPHERICAL HARMONICS

$$Y_1 = \sqrt{15/4\pi}\, xy/r^2$$

$$Y_2 = \sqrt{15/4\pi}\, yz/r^2$$

$$Y_3 = \sqrt{15/4\pi}\, zx/r^2$$

$$Y_4 = \sqrt{15/4\pi}\, (x^2-y^2)/2r^2$$

$$Y_5 = \sqrt{15/4\pi}\, (3z^2-r^2)/2r^2$$

TABLE 3.2 CONTINUED

THE TIGHT BINDING MATRIX ELEMENTS

$$T_{xy,xy} = E_d + 3dd\sigma \cos x \cos y + 2dd\pi(\cos x + \cos y)\cos z + dd\delta(\cos x \cos y + 2\cos x \cos z + 2\cos y \cos z)$$

$$T_{xy,yz} = 2(-dd\pi + dd\delta)\sin z \sin x$$

$$T_{xy,zx} = 2(-dd\pi + dd\delta)\sin y \sin z$$

$$T_{xy,x^2-y^2} = 0$$

$$T_{xy,3z^2-r^2} = \sqrt{3}(dd\sigma - dd\delta)\sin x \sin y$$

$$T_{yz,yz} = E_d + 3dd\sigma \cos y \cos z + 2dd\pi(\cos y + \cos z)\cos x + dd\delta(\cos y \cos z + 2\cos x \cos y + 2\cos z \cos x)$$

$$T_{yz,zx} = 2(-dd\pi + dd\delta)\sin x \sin y$$

$$T_{yz,x^2-y^2} = \frac{3}{2}(dd\sigma - dd\delta)\sin y \sin z$$

$$T_{yz,3z^2-r^2} = \frac{\sqrt{3}}{2}(-dd\sigma + dd\delta)\sin y \sin z$$

$$T_{zx,zx} = E_d + 3dd\sigma \cos z \cos x + 2dd\pi(\cos z + \cos x)\cos y + dd\delta(\cos z \cos x + 2\cos y \cos z + 2\cos x \cos y)$$

TABLE 3.2 CONTINUED

$$T_{zx,x^2-y^2} = -\frac{3}{2}(dd\sigma - dd\delta)\sin x \sin z$$

$$T_{zx,3z^2-r^2} = \frac{\sqrt{3}}{2}(-dd\sigma + dd\delta)\sin x \sin z$$

$$T_{x^2-y^2,x^2-y^2} = E_d + 4dd\pi\cos x \cos y + (\tfrac{3}{4}dd\sigma + dd\pi + \tfrac{9}{4}dd\delta)(\cos x \cos z + \cos y \cos z)$$

$$T_{x^2-y^2,3z^2-r^2} = \sqrt{\tfrac{3}{4}}(dd\sigma - 4dd\pi + 3dd\delta)(\cos x \cos z - \cos y \cos z)$$

$$T_{3z^2-r^2,3z^2-r^2} = E_d + \tfrac{1}{4}dd\sigma(4\cos x \cos y + \cos x \cos z + \cos y \cos z) + 3dd\pi(\cos x \cos z + \cos y \cos z) + \tfrac{3}{4}dd\delta(4\cos x \cos y + \cos x \cos z + \cos y \cos z)$$

$$x = \frac{\bar{\lambda}}{N}k_x \quad , \quad y = \frac{\bar{\lambda}}{N}k_y \quad , \quad z = \frac{\bar{\lambda}}{N}k_z$$

E_d = .5 Ryd

A_H = .8826 Ryd

R_H = 3.592 a_B

$dd\sigma$ = -0.0296 Ryd

$dd\pi$ = 0.0147 Ryd

$dd\delta$ = -0.0024 Ryd

a = 6.8088 a_B

TABLE 3.3

$E_d^A = .4$ Ryd

$E_d^B = .6$ Ryd

$a = 6.8088$

$r_i = .620 \times .629\ a \quad a_B$

$w_A = .0338$ ryd

$w_B = .0402$ ryd

FIGURE 3.1

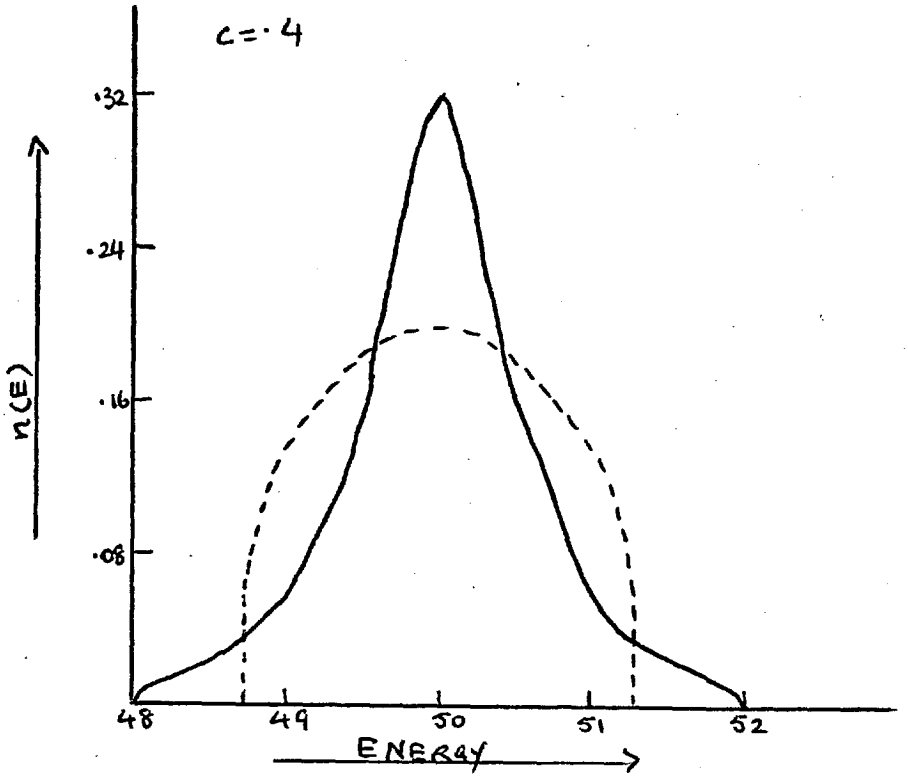

The density of states for semi-elliptical band alloy. The full line curve is for single site theory and the dotted line for CPA.

FIGURE 3.1b

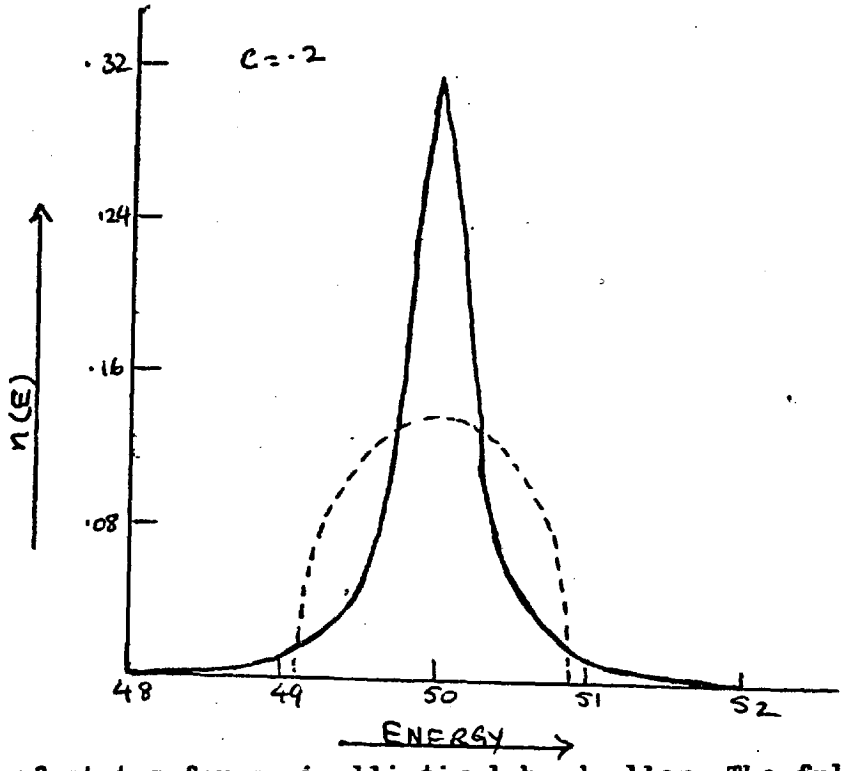

The density of states for semi-elliptival band alloy. The full line curve is for single site theory and the dotted line for CPA.

FIGURE 3.1c

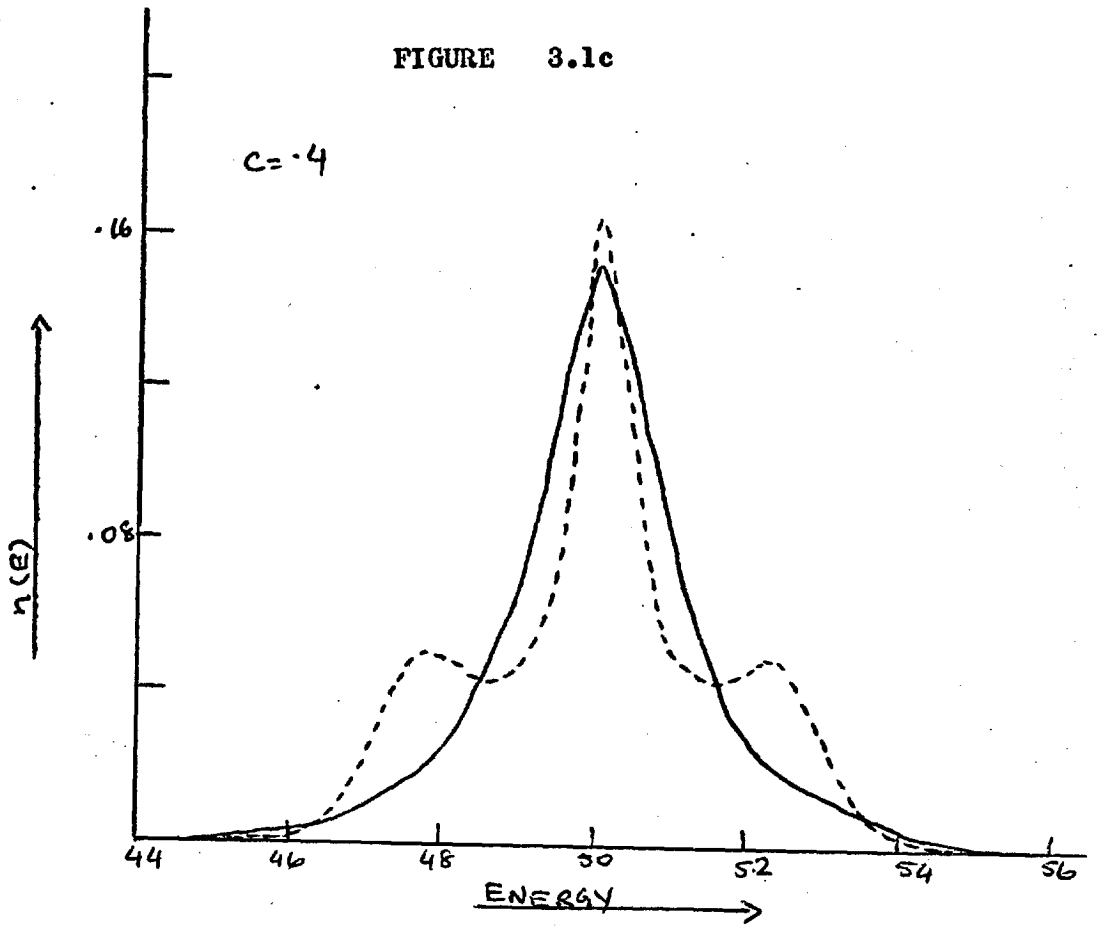

The density of states for c=.4. The dotted line curve is for multiple site and the full line curve is for single site theory.

FIGURE 3.1d

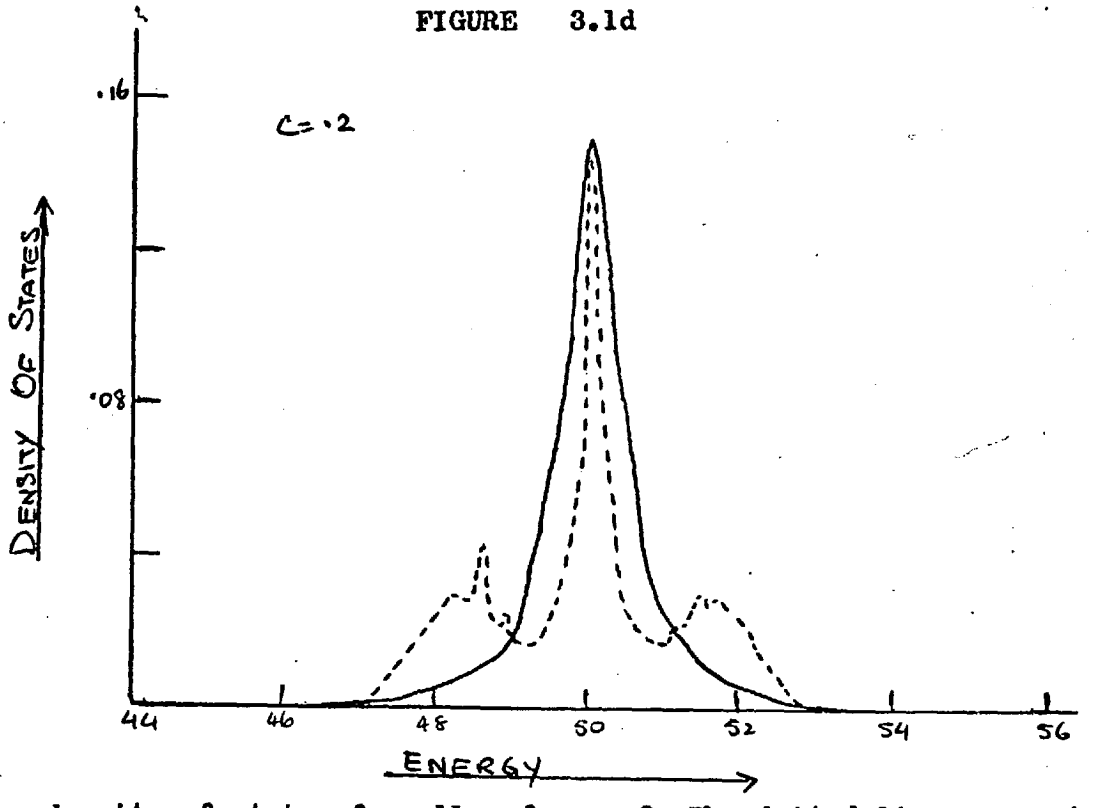

The density of states for alloy for c=.2. The dotted line curve is for cluster theory and full line curve is for single site theory.

FIGURE 3.2

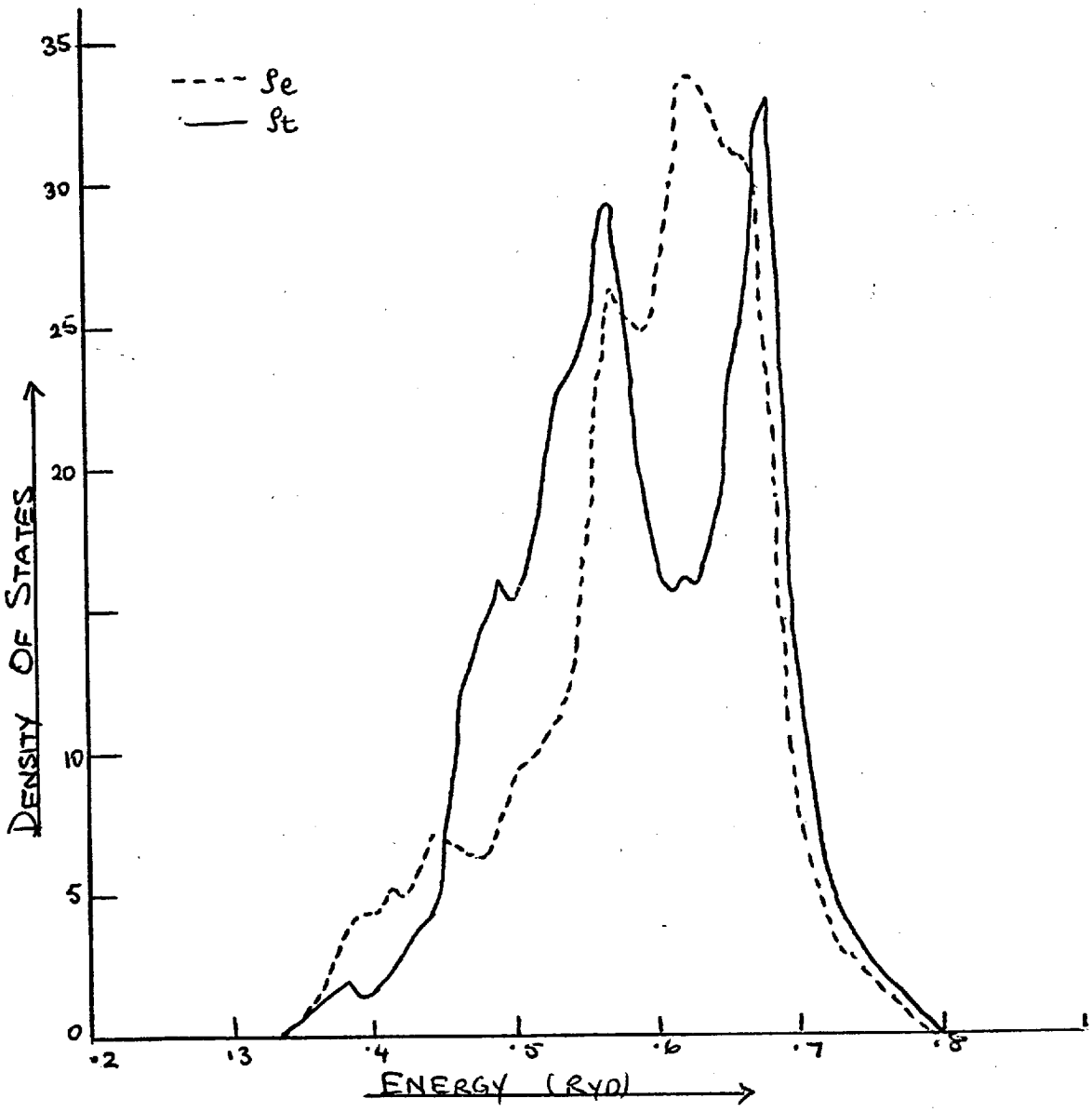

Plot of E and T component of the d band density of states of transition metal.

FIGURE 3.3

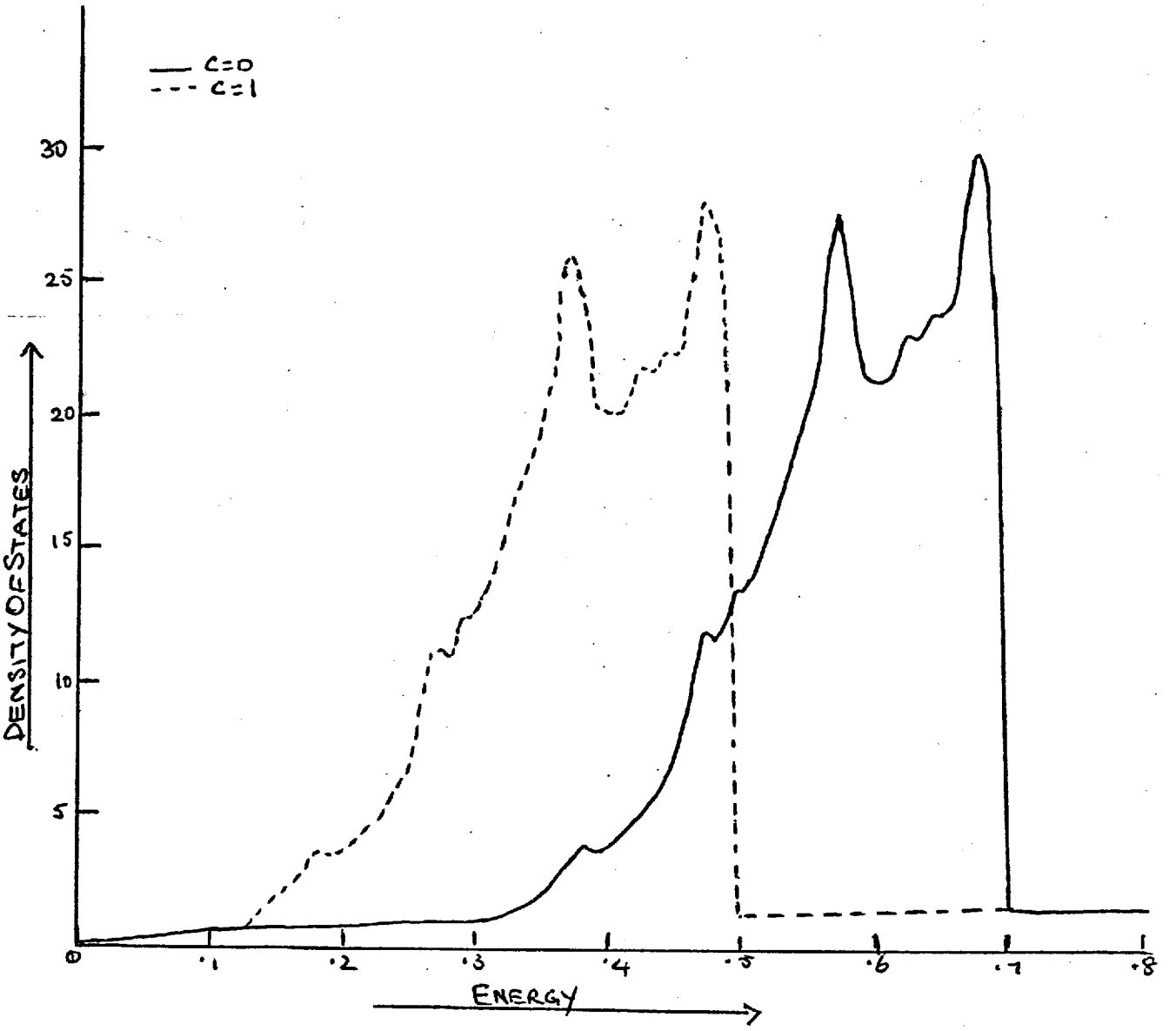

The densities of states of transition metals with E_d=.4 and .6. The area under the dotted line curve is 5.85 and that under the full line curve is 5.66.

FIGURE 3.4

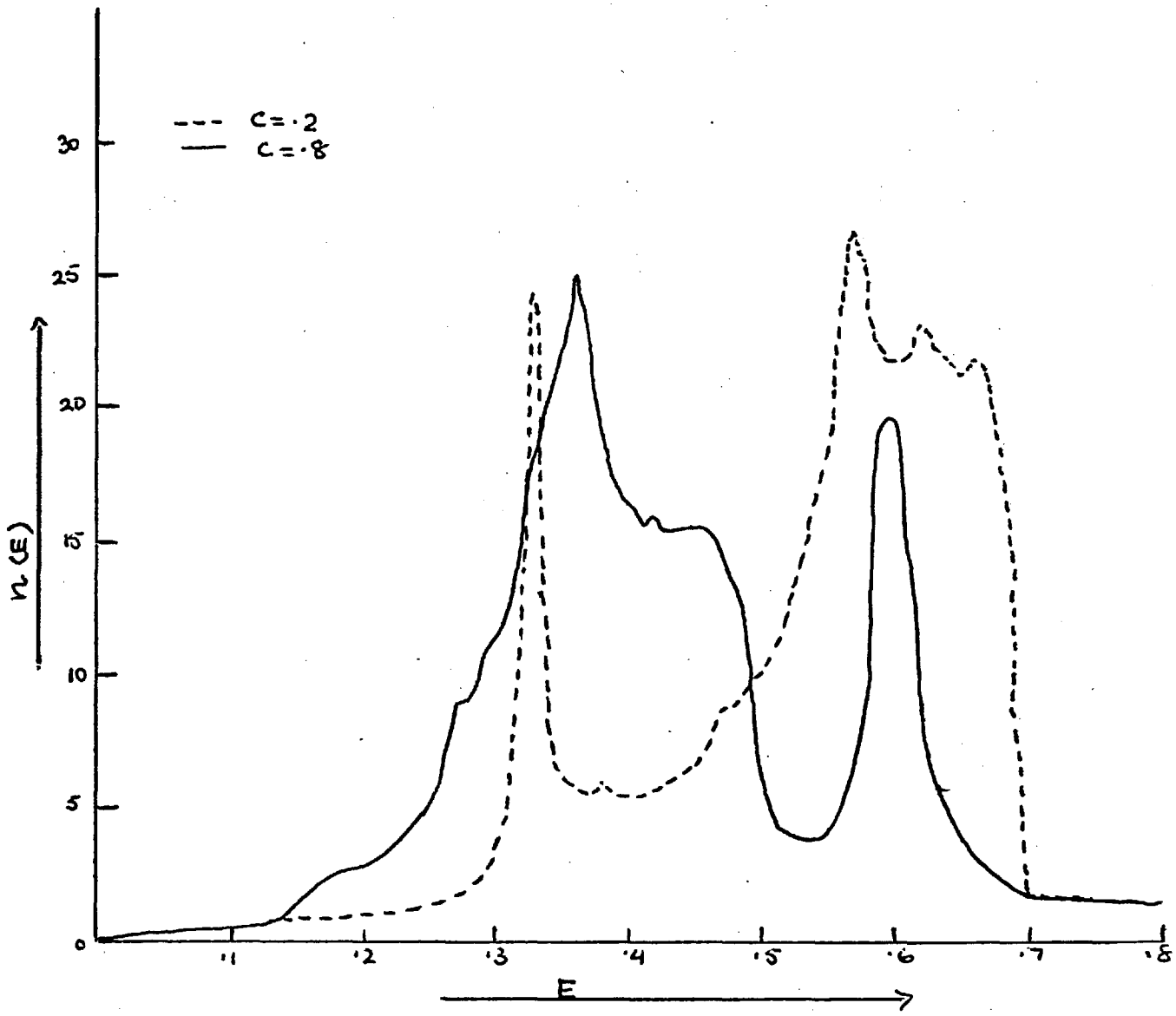

The densities of states of transition metal alloys in single site theory. The area under the dotted line curve is 5.80 and that under the full line curve is 5.68.

FIGURE 3.5

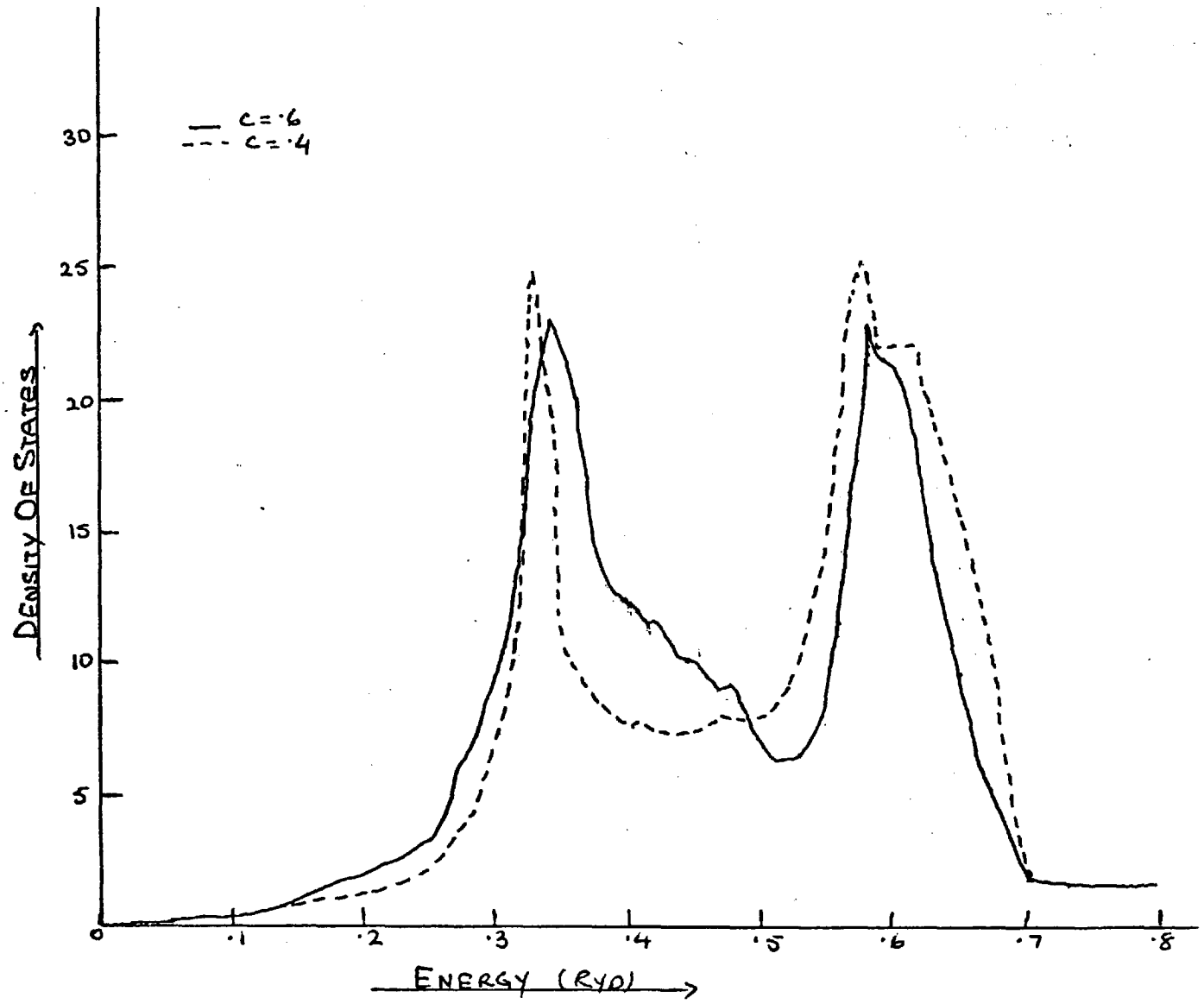

Plot of the densities of states of transition metal alloys. The area under the dotted line curve is 5.76 and that under the full line curve is 5.72.

FIGURE 3.6

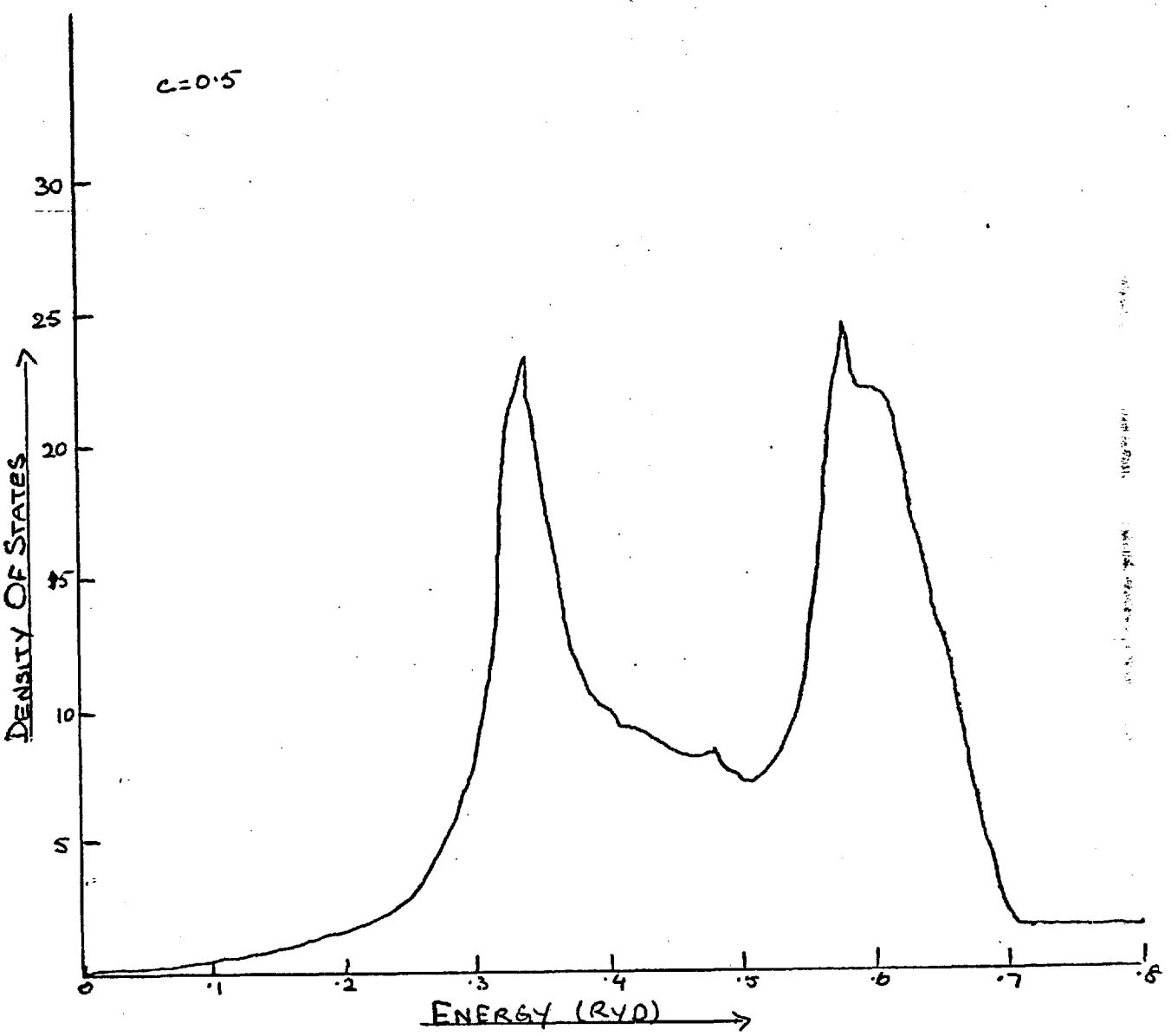

Plot of the density of states of 50–50 transition metal alloy in single site theory. The area under the curve is 5.74.

CHAPTER 4

CLUSTER THEORY FOR d-BAND ALLOYS

4.1 INTRODUCTION

In this chapter we will apply the continued fraction method to calculating the density of states of transition metal alloys in a multiple site theory. As a simplification in the calculation we will deal with the d electrons only in this chapter. The sp electrons and their hybridizing effect with the d electrons is dealt with in the next chapter. The transition metals we deal with here and in the next chapter have face-centred cubic structure, but this method can in principle be applied to the body-centred cubic and hexagonal materials also.

There are many advantages of the continued fraction technique but three of them are clear, The first is that it is not necessary to solve repeatedly sets of transcendental equations where as it is necessary in self-consistent theories. Therefore we need less computer time. The second is that there are no difficulties in conection with the analyticity of the density of states as shown by Nickel and Butler (1973). The final advantage is that the Liftshitz condition (Lifshitz 1964) on the density

of states (that the density of states is non-zero at any energy at which the pure components in the alloy has a non-zero density of states) can be satisfied.

The cluster theory method calculates the density of states for all possible configurations of a central cluster of atoms (the atoms outside the cluster are treated in an average approximation) and then an average density of states is calculated by adding together the density of states for each configuration multiplied by the multiplicity of the configuration (which is calculated using symmetry arguments) and a suitable probability weighting.

In the next section we discuss the formulation of the density of states equation for the d electrons of the transition metal alloys. In section 4.3 we present the numerical results and conclude this chapter.

4.2 THE d ELECTRON DENSITY OF STATES.

The disordered Hamiltonian which we are using is given by

$$H = H_1 + H_2 \tag{4.1}$$

where

$$H_1 = \sum_{\substack{i \neq j \\ mm'}} A^{ij} \; c^{+}_{im} c_{jm'}$$

$$H_2 = \sum_{\substack{i \\ m}} d_o^{A,B} \; c_{im} c_{im} \tag{4.2}$$

where c^{+}_{im} and c_{im} are respectively creation and annihalition operators

for the electrons on site i with angular momentum m . $d_o^{A,B}$ is equal to E_A or E_B depending on whether the central site is occupied by an A type or a B type atom in the particular configuration being considered. $A^{ij}_{mm'}$ are the elements of the hopping matrices for the electrons with angular momentum m and m′ between the sites i and j. These are infact the Slater and Koster (1954) two centre energy integrals and are given in terms of direction cosines in Table 4.1. The central atom and its twelve nearest neighbours in a face-centred cubic structure are pictorially represented by figure 4.1. The values of the direction cosines for the twelve sites as labelled in figure 4.1 are given in Table 4.2.

The problem we are dealing with here is considerably more difficult than the problem of single band cluster theory. Consequently in order to get tractable result it is necessary to make severer approximations. Nevertheless our result is the first cluster calculation on degenerate d band alloys to prove feasible. The guiding principles in making these approximations are:

(i) That our results should reduce for the pure materials to those of Haydock et al (1975).

(ii) That the diagonal matrix elements on the central atom and its twelve nearest neighbours should be treated as nearly exactly as possible.

(iii) That the Lifshitz condition should be satisfied.

The first steps in deriving the result are closely analogous

to those used in Jacobs (1974, Cubiotti et al 1975) for a single band cluster theory. However it is necessary almost immediately to make an additional approximation due to the degeneracy of the d band. We begin by writing down our basis functions. There are five Wannier functions of different angular momentum on each atom. Consequently the initial basis function $|0\rangle$ on the central atom in the single band theory is replaced by five basis functions $|0\rangle_m$ in the d band theory distinguished by different values of the index m. The same is true for all additional basis functions generated from the set $\{|0\rangle_m\}$ by repeated operation of the terms H_1 and H_2 of the Hamiltonian. The basis set we use is then as follows:

$$
\left.
\begin{aligned}
&|0\rangle_m && m = 1,2,3,4,5 \\
&|1,0\rangle_m = N_{10}^m \left[H_1 |0\rangle_m - OT \right] \\
&\qquad = N_{10}^m \sum_{i=nn} A_{mm'}^{oi} |i\rangle_{m'} \\
&|2,0\rangle_m = (N_{20}^m)' \left[H_1 |1,0\rangle_m - OT \right] \\
&\qquad = N_{20}^m \sum_{\substack{i,j=2nn \\ m'm''}} A_{mm'}^{oi} A_{m'm''}^{ij} |j\rangle_{m''} \\
&|1,1\rangle_m = N_{11}^m \left[H_2 |1,0\rangle_m - OT \right]
\end{aligned}
\right\} \qquad (4.3)
$$

{ All further kets are treated in a crude approximation analogous to that applied to the higher kets $|3,0\rangle$ and $|2,1\rangle$ in Jacobs (1974), Cubiotti et al (1975) }.

In this set of basis functions each ket is orthogonalised to the previous kets and each ket is normalized by the factor N to unity. The notation $|i,j\rangle$ for the elements of the basis set (4.3)

serves to indicate that the element $|i,j\rangle$ is constructed from the ket $|0\rangle$ by i pperations of H_1 and j of H_2 . (This notation is ambiguous beyond a certain level. The ambiguity of notation will not affect us here , because we make our approximations before that level).

In basis set (4.3) the normalizing factors are calculated as follows:

$$1 = {}_m\langle 0,0 \,|\, 1,0\rangle_m = (N_{10}^m)^2 \sum_{\substack{i=nn \\ m'}} A^{0i}_{mm'} A^{i0}_{m'm} \tag{4.4}$$

$$\text{or} \quad (N_{10}^m)^{-2} = \sum_{\substack{i=nn \\ m'}} A^{0i}_{mm'} A^{i0}_{m'm} \tag{4.5}$$

$$1 = {}_m\langle 2,0 \,|\, 2,0\rangle_m = (N_{20}^m)'^2 \sum_{\substack{i,k=nn \\ m'm_1}} \sum_{\substack{j=2+3nn \\ m_2}} A^{0i} A^{ij} A^{jk} A^{k0}_{mm'm_1m_2m_2m}$$

$$\text{or} \quad (N_{20}^m)'^{-2} = \sum_{\substack{i,k=nn \\ m'm_1}} \sum_{\substack{j=2+3nn \\ m_2}} A^{0i}_{mm'} A^{ij}_{m'm_1} A^{jk}_{m_1m_2} A^{k0}_{m_2m} \tag{4.6}$$

$$N_{20}^m = N_{10}^m (N_{20}^m)' \tag{4.7}$$

The kets $|0\rangle_m$, $|1,0\rangle_m$ and $|2,0\rangle_m$ are easy to handle. The ket $|1,1\rangle_m$, however is difficult to handle because it depends on all configurations of A and B atoms on the twelve sites of the nearest neighbour shell. We include the effects of this ket by reasoning by analogy with the single band theory of Jacobs (1974) and Cubiotti et al (1975). In this theory the part of the continued fraction which depends on the ket $|1.1\rangle$, ignoring the broadening terms, may be written as follows:

$$\frac{1}{\langle 1,0|H|1,0\rangle - E - \dfrac{|\langle 10|H|11\rangle|^2}{\langle 11|H|11\rangle - E}} = \frac{6}{\dfrac{3-Z}{6}\delta - E - \dfrac{(6-Z)Z\delta^2/36}{-\dfrac{(3-Z)\delta}{6} - E}}$$

$$= 6 \quad \frac{-(3-Z)\delta/6 - E}{(-\frac{\delta}{2}+E)(\frac{\delta}{2}+E)}$$

$$= \frac{6-Z}{\frac{\delta}{2}-E} + \frac{Z}{-\frac{\delta}{2}-E} \qquad (4.8)$$

{where equation (4.8) follows from equations (7), (8) and (15) of Jacobs (1974), Z is the number of atoms of type B in the nearest neighbour shell (i.e Z ranges from 0 to 6) }.

In this expression we see that the ket $|1,1\rangle$ has a vital role in ensuring that the band structure has no singularities in the region between the bands centred at $-\frac{\delta}{2}$ and $\frac{\delta}{2}$, which would otherwise be implied by the denominator of

$$\frac{1}{\langle 10|H|10\rangle - E} = \frac{6}{\frac{3-Z}{6}\delta - E} \qquad (4.9)$$

In our degenerate d band case E_A takes the place of $+\frac{\delta}{2}$ and E_B that of $-\frac{\delta}{2}$, and the numerators and denominators are respectively adjusted by terms proportional to ω^2 and ω (where ω is half the bandwidth) so that the result is as good as possible in the limits Z=0 Or 6. The proceedure is carried out in more detail below:

The secular equation for basis set (4.3) is given by:

$$\begin{vmatrix} \langle 0|H|0\rangle_{m,m'} - E\delta_{mm'} & \langle 0|H|10\rangle_{m,m'} & 0 & 0 \\ \langle 10|H|0\rangle_{m,m'} & \langle 10|H|10\rangle_{m,m'} - E\delta_{mm'} & \langle 10|H|11\rangle_{m,m'} & 0 \\ 0 & \langle 11|H|10\rangle_{m,m'} & \langle 11|H|11\rangle_{m,m'} - E\delta_{mm'} & \langle 11|H|20\rangle_{m,m'} \\ 0 & 0 & \langle 20|H|11\rangle_{m,m'} & F_{mm'}(\text{approx}) \end{vmatrix} \tag{4.10}$$

Now folding all the matrix elements of the matrix(4.10) into the first and using the above reasoning by analogy with the s band multiple site theory we get

$$G_{mm'} = \Big[(d_0^{A,B} - E)\delta_{mm'} - \sum_{\substack{i=nnA \\ m''m_1}} A^{0i}_{mm''} G^{A}_{m''m_1} A^{i0}_{m_1m'} - \sum_{\substack{i=nnB \\ m''m_1}} A^{0i}_{mm''} G^{B}_{m''m_1} A^{i0}_{m_1m'} \Big]^{-1} \tag{4.11}$$

where

$$d_0^{A,B} = x E_A + (1-x) E_B \tag{4.12}$$

where x is the number of atoms of type A on the central site ($x = 0$ or 1). E_A and E_B are the centres of the bands for A and B type materials respectively. The summation $\sum_{i=nnA}$ means sum over the nearest neighbour sites which are occupied by atoms of type A only, similarly $\sum_{i=nnB}$ means sum over the nearest neighbour sites occupied by B atoms. $G^{A}_{m''m_1}$ and $G^{B}_{m''m_1}$ are defined by the following equations:

$$G^{A}_{m''m_1} = \left[\left\{ A3_{m''m_1} + E_A - E - A4_{m''m_1} \bar{F}_{m_1 m_1} A4_{m_1 m''} \right\} \delta_{m''m_1}\right]^{-1} \qquad (4.13)$$

$$G^{B}_{m''m_1} = \left[\left\{ A3_{m''m_1} + E_B - E - A4_{m''m_1} \bar{F}_{m_1 m_1} A4_{m_1 m''} \right\} \delta_{m''m_1}\right]^{-1} \qquad (4.14)$$

where

$$A3_{m''m_1} = \left[\sum_{\substack{i=nn \\ m'''}} \sum_{\substack{j=nn \\ m_2}} A^{oi}_{m''m'''} A^{ij}_{m'''m_2} A^{jo}_{m_2 m_1}\right]\left[\sum_{\substack{i=nn \\ m_3}} A^{oi}_{m''m_3} A^{io}_{m_3 m_1}\right]^{-1} \qquad (4.15)$$

$$A4_{m''m_1} = \left[\sum_{\substack{i=nn \\ m_2}} \sum_{\substack{j=2+3 \\ m_3}} \sum_{\substack{k=nn \\ m_4}} A^{oi}_{m''m_2} A^{ij}_{m_2 m_3} A^{jk}_{m_3 m_4} A^{ko}_{m_4 m_1}\right]^{\frac{1}{2}}\left[\sum_{\substack{i=nn \\ m_5}} A^{oi}_{m''m_5} A^{io}_{m_5 m_1}\right]^{-\frac{1}{2}} \qquad (4.16)$$

$$\bar{F}_{m_1 m_1}(E) = c\, FD(L, E_A - E) + (1-c)\, FD(L, E_B - E) \qquad (4.17)$$

$$FD(L,E) = \left[a(L,3) - E - b(L,3)\, FD(3,E)\right]^{-1} \qquad (4.18)$$

where c is the concentration of the A atoms and $a(L,3)$ and $b(L,3)$ are the Haydock's coefficients*, L refering to the symmetry of the d bands ; L equal to 1 means that the coefficients are for degenerate set $\{xy, yz, zx\}$ and L equal to 2 means the coefficients are for $\{x^2-y^2,\ 3z^2-r^2\}$ orbitals. $F(3,E)$ is defined iteratively in terms of Haydock's coefficients $a(L,N)$ and $b(L,N)$ (given in Table 4.3) in the following way:

We are grateful to Roger Haydock for sending us the numerical values of the coefficients used in his continued fraction technique.

$$F(N,E) = \left[a(L,N+1) - E - b(L,N+1)\,F(N+1,E)\right]^{-1} \qquad (4.19)$$

$$F(15,E) = \frac{(E+a_\infty) \pm \sqrt{E^2 - 4b_\infty}}{2b_\infty} \qquad (4.20)$$

where $F(15,E)$ is the termination to the continued fraction at the fifteenth level. b_∞^2 is related to half bandwidth of the d bands, a_∞ and b_∞ are given in Table 4.3. The sign in equation (4.20) is selected so as to have the correct analytic behaviour. Because of the 3-fold and 2-fold degeneracy of the Haydocks coefficients, the elements of the diagonal matrix $\bar{F}_{m,m_1}$ also show the same behaviour.

After computing $A3_{m''m_1}$ and $A4_{m''m_1}$ wesee that these are also diagonal matrices with three fold and two fold degenerate elements on each main diagonal. This means that $G^A_{m''m_1}$ and $G^B_{m''m_1}$ given by equations (4.13) and (4.14) are diagonal matrices with the same property. We can use these facts to simplify the last two terms in equation (4.11). If G^{1A} and G^{1B} are elements from the triply degenerate set and G^{2A} and G^{2B} are the elements from the doubly degenerate set of $G^A_{m''m_1}$ and $G^B_{m''m_1}$ respectively then

$$G_{mm'} = \Big[(d_o^{A,B} - E)\delta_{mm'} - \Big\{G^{1A}\sum_{\substack{i=n\wedge A\\ m''}} A^{0i}_{mm''}A^{i0}_{m''m'} + G^{2A}\sum_{\substack{i=n\wedge A\\ m''}} A^{0i}_{mm''}A^{i0}_{m''m'}$$

$$+ G^{1B}\sum_{\substack{i=n\wedge B\\ m''}} A^{0i}_{mm''}A^{i0}_{m''m'} + G^{2B}\sum_{\substack{i=n\wedge B\\ m''}} A^{0i}_{mm''}A^{i0}_{m''m'}\Big\}\Big]^{-1} \qquad (4.21)$$

The only difficult task in the above equation is to evaluate the summations $\sum_{\substack{i=n\wedge A\\ m''}} A^{0i}_{mm''}A^{i0}_{m''m'}$ and $\sum_{\substack{i=n\wedge B\\ m''}} A^{0i}_{mm''}A^{i0}_{m''m'}$. The first sum can be very easily calculated on the computer for different

configurations of A atoms on the nearest neighbour sites, then the second sum can be evaluated from the relation

$$\sum_{\substack{i=nn \\ m''}} A^{oi}_{mm''} A^{io}_{m''m'} = \sum_{\substack{i=nnA \\ m''}} A^{oi}_{mm''} A^{io}_{m''m'} + \sum_{\substack{i=nnB \\ m''}} A^{oi}_{mm''} A^{io}_{m''m'} \qquad (4.22)$$

as we have already calculated the sum on the right hand side {equations (4.15) and (4.16) :}.

Thus if n is the number of configurations of the A atoms in the nearset neighbour shell, M_n is the multiplicity of the particular configuration n (both of which are estimated by symmetry arguments), and y is the number of A atoms in the nearest neighbour shell then the average Green function is given by

$$\langle o|G|o\rangle_{m'} = \sum_{x=0}^{1} \sum_{n=1}^{66} \left[G^{x,n}_{mm'} \right] M_n c^{x+y} (1-c)^{13-x-y} \qquad (4.23)$$

Hence the d dand density of states for transition metal alloys is given by

$$n(E) = \frac{Im}{\pi} Tr \langle o|G|o\rangle_{m'} \qquad (4.24)$$

4.3 DISCUSSION OF NUMERICAL RESULTS AND CONCLUSION.

The calculations in section 4.2 are done for arbitrary transition metal alloys with E_A= .2 ryd and E_B= .5 ryd. The band width for both A and B materials is .2 rydbergs. In figure 4.2 we give the results for the d band density of states of pure A type transition metal around E_A= .2 ryd. An exactly similar curve

is obtained for the B type material around E_B= .5 ryd, which we shall not present here. We see that our method has reproduced the Haydock curve (1975), which contains much structure. This is because of the use of the Haydock's coefficient (private commiunication) in the termination of our continued fraction. This curve has a close comparision with the result of the histogram method of Pettifor (1972) and the results of the interpolation method of Gilat and Raubenheimer (1966). In figure 4.3 we give the results for c= .8 and c= .6 and in figure 4.4 for c= .4 and c= .2 for a band around E_A= .2 ryd. The curve for c=.8 shows that with the addition of a small amount of impurity, the structure at the edges of the band has disappeared, while the peaks towards the centre of the band have crudely speaking retained their positions and their heights. As the value of c is decreased further, we see that the peak at the centre of the band remaines, with humped shoulders (having a small amount of structure in them) on either side. The band has narrowed also. This narrowing of band goes as $\sqrt{c}$ at its edges. In the curve for c= .2 we see that there is a pair consisting of a sharp peak and a small peak a little shifted from the centre of the band, surrounded by symmetrical pairs of broad peaks. The pair of peaks in the centre can be understood as arising from isolated A atoms, the splitting of the peak being due to the splitting of $d(E)$ and (T) electrons in the cubic environment. The broader peaks around this central pair are due to an A atom in the centre with one, two, three or more A atoms in the nearest neighbour shell. An A atom with a single nearest neighbour of type A, for example, will give a typical bonding-antibonding density of states i.e. peaks at or near E_A-t and E_A+t (t being the hopping integral). The central peaks are shifted from

E_A due to second order perturbation theory repulsion by the bands near E_B. The shift is roughly proportional to $(1-c)t/(E_B-E_A)$.

In figure 4.5 and figure 4.6 we give the results for a d-electron density of states for a complementary band around $E_B = .5$ for various concentrations. The results are approximately a mirror reflection of the results of figures (4.3) and (4.4) if we neglect the effects of the assymmetry of the band stwucture of the pure materials.

For the sake of comparision in figure 4.7 we give the d band density of states for c= .2 when we use a broad square root termination instead of Haydocks spiky termination. It closely resembles the curve for c=.2 in figure 4.3 with the structure smoothed. This shows that the density of states for the minorty band obtained by the above method is relatively independent of the termination we use.

TABLE 4.1

ELEMENTS OF THE HOPPING MATRIX

$$A_{xy,xy} = 3l^2m^2(dd\sigma)+(l^2+m^2-4l^2m^2)(dd\lambda)+(n^2+l^2m^2)(dd\delta)$$

$$A_{xy,yz} = 3lm^2n(dd\sigma)+ln(1-4m^2)(dd\lambda)+ln(m^2-1)(dd\delta)$$

$$A_{xy,zx} = 3l^2mn(dd\sigma)+mn(1-4l^2)(dd\lambda)+mn(l^2-1)(dd\delta)$$

$$A_{xy,x^2-y^2} = \tfrac{3}{2}lm(l^2-m^2)(dd\sigma)+2lm(m^2-l^2)(dd\lambda)+\tfrac{1}{2}lm(l^2-m^2)(dd\delta)$$

$$A_{xy,3z^2-r^2} = \sqrt{3}lm\left[n^2-\tfrac{1}{2}(l^2+m^2)\right](dd\sigma)-2\sqrt{3}lmn^2(dd\lambda)+\tfrac{1}{2}\sqrt{3}lm(1+n^2)(dd\delta)$$

$$A_{yz,x^2-y^2} = \tfrac{3}{2}mn(l^2-m^2)(dd\sigma)-mn\left[1+2(l^2-m^2)\right](dd\lambda)+mn\left[1+\tfrac{1}{2}(l^2-m^2)\right](dd\delta)$$

$$A_{zx,x^2-y^2} = \tfrac{3}{2}nl(l^2-m^2)(dd\sigma)+nl\left[1-2(l^2-m^2)\right](dd\lambda)-nl\left[1-\tfrac{1}{2}(l^2-m^2)\right](dd\delta)$$

$$A_{x^2-y^2,x^2-y^2} = \tfrac{3}{4}(l^2-m^2)^2(dd\sigma)+\left[l^2+m^2-(l^2-m^2)^2\right](dd\lambda)+\left[n^2+\tfrac{1}{4}(l^2-m^2)^2\right](dd\delta)$$

$$A_{x^2-y^2,3z^2-r^2} = \tfrac{1}{2}\sqrt{3}(l^2-m^2)\left[n^2-\tfrac{1}{2}(l^2+m^2)\right](dd\sigma)+\sqrt{3}n^2(m^2-l^2)(dd\lambda)$$

$$+\tfrac{1}{4}\sqrt{3}(1+n^2)(l^2-m^2)(dd\delta)$$

$$A_{3z^2-r^2,3z^2-r^2} = \left[n^2-\tfrac{1}{2}(l^2+m^2)\right]^2(dd\sigma)+3n^2(l^2+m^2)(dd\lambda)+\tfrac{3}{4}(l^2+m^2)^2(dd\delta)$$

TABLE 4.2

nn	DIRECTION COSINES		
	l	m	n
1	$1/\sqrt{2}$	0	$1/\sqrt{2}$
2	$-1/\sqrt{2}$	0	$1/\sqrt{2}$
3	$-1/\sqrt{2}$	0	$-1/\sqrt{2}$
4	$1/\sqrt{2}$	0	$-1/\sqrt{2}$
5	$-1/\sqrt{2}$	$-1/\sqrt{2}$	0
6	$1/\sqrt{2}$	$-1/\sqrt{2}$	0
7	$1/\sqrt{2}$	$1/\sqrt{2}$	0
8	$-1/\sqrt{2}$	$1/\sqrt{2}$	0
9	0	$1/\sqrt{2}$	$1/\sqrt{2}$
10	0	$-1/\sqrt{2}$	$1/\sqrt{2}$
11	0	$-1/\sqrt{2}$	$-1/\sqrt{2}$
12	0	$1/\sqrt{2}$	$-1/\sqrt{2}$

TABLE 4.3

Haydocks coeffients for 3-fold and 2-fold degenerate d orbitals

L=1 $\{xy, yz, zx\}$

N	$a(L,N)$	$b(L,N)$
3	-0.268442E-01	0.277508E-02
4	-0.226108E-01	0.223218E-02
5	-0.233802E-01	0.248629E-02
6	-0.233476E-01	0.268609E-02
7	-0.199578E-01	0.202226E-02
8	-0.183525E-01	0.282562E-02
9	-0.208408E-01	0.210848E-02
10	-0.233035E-01	0.218709E-02
11	-0.215445E-01	0.220476E-02
12	-0.186115E-01	0.191775E-02
13	-0.179980E-01	0.188479E-02
14	-0.113130E-01	0.232730E-02
15	-0.191887E-01	0.181939E-02

TABLE 4.3 CONTINUED

L=2 $\{x^2-y^2, 3z^2-r^2\}$

N	a(L,N)	b(L,N)
3	-0.129238E-01	0.198260E-02
4	-0.134164E-01	0.188169E-02
5	-0.155777E-01	0.200111E-02
6	-0.188541E-01	0.221760E-02
7	-0.200979E-01	0.209972E-02
8	-0.196472E-01	0.172915E-02
9	-0.111317E-01	0.215488E-02
10	-0.184626E-01	0.170182E-02
11	-0.101740E-01	0.188401E-02
12	-0.111907E-01	0.166363E-02
13	-0.160846E-01	0.179735E-02
14	-0.108216E-01	0.186812E-02
15	-0.177737E-01	0.173759E-02

a_∞ = -0.0183 ; b_∞ = 0.00245

FIGURE 4.1

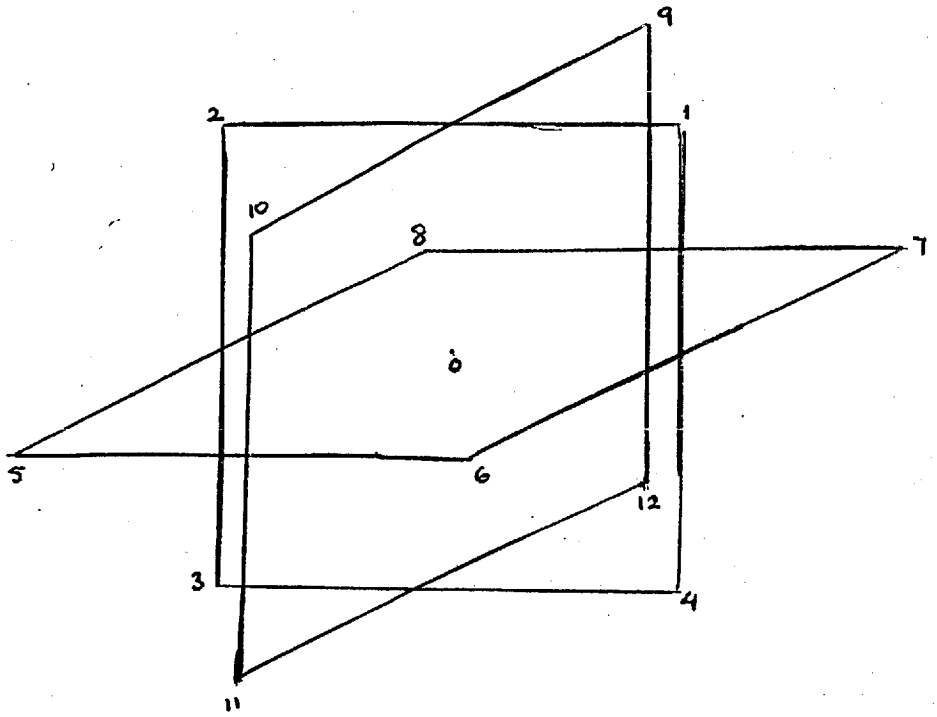

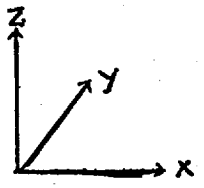

FIGURE 4.2

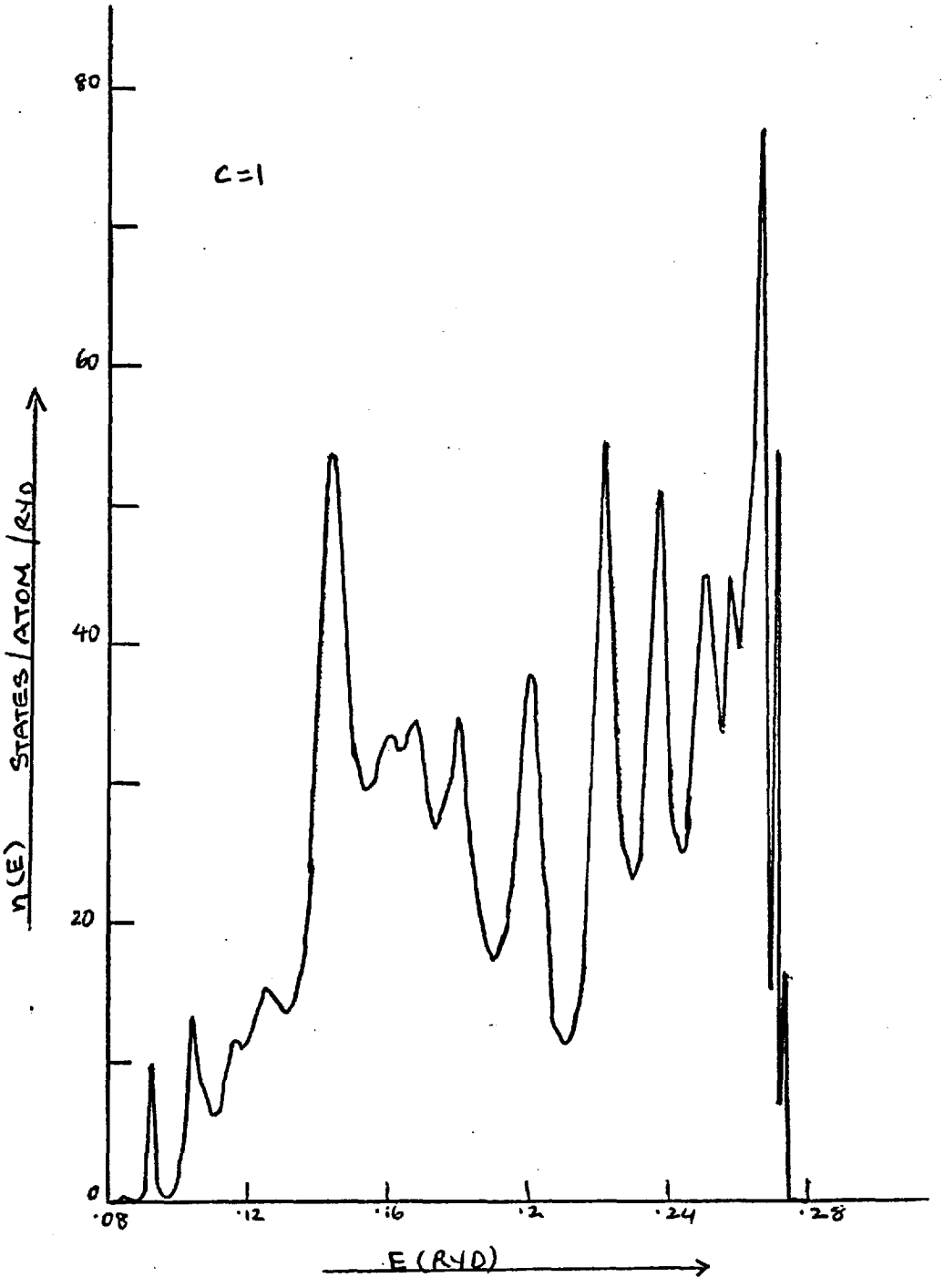

Plot of the d band density of states of pure material in cluster theory around $E_d = .2$

FIGURE 4.3

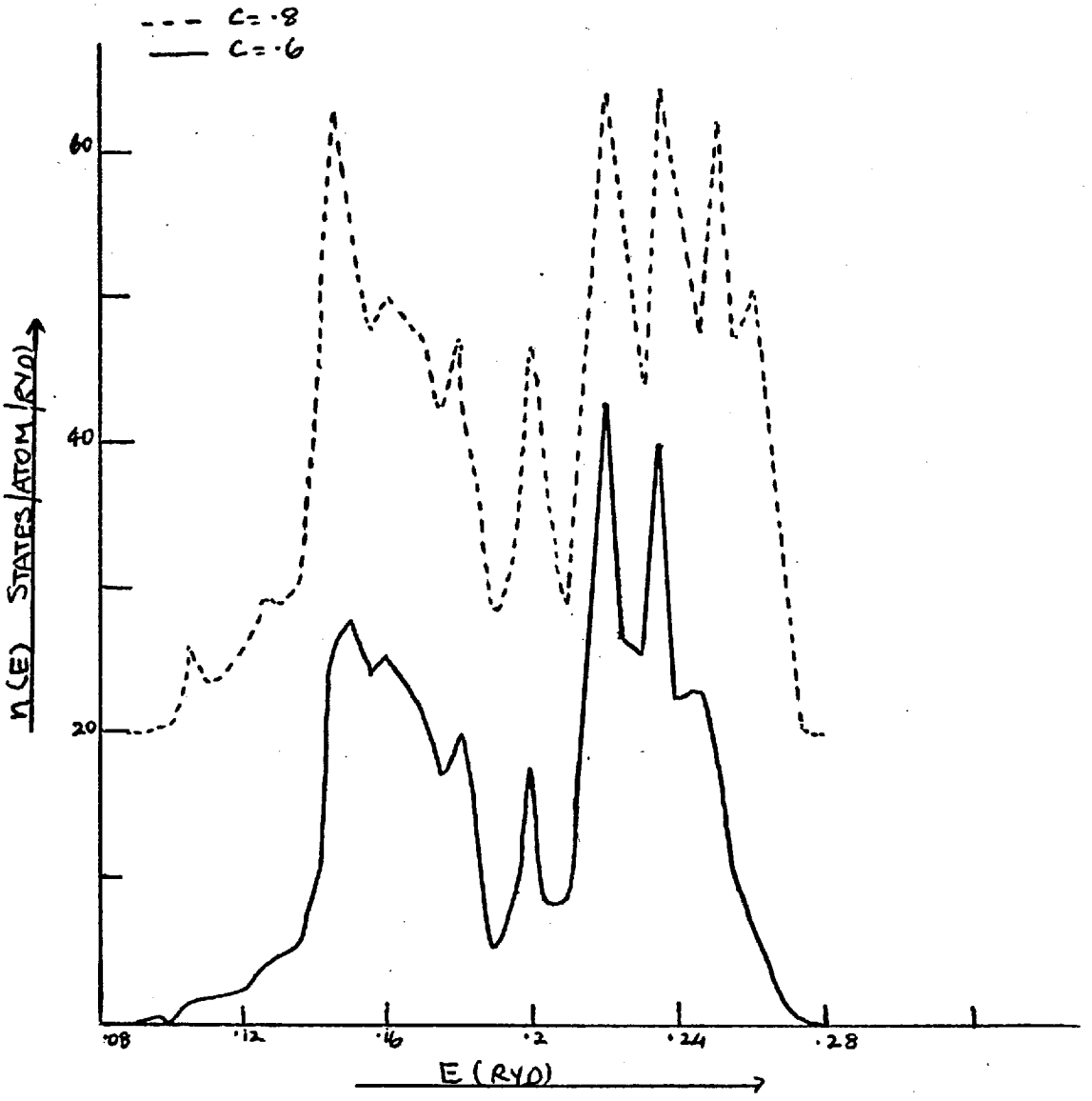

Plot of the d band density of states of transition metal alloy in cluster theory. The origin of curves for different concentration is shifted upwards.

FIGURE 4.4

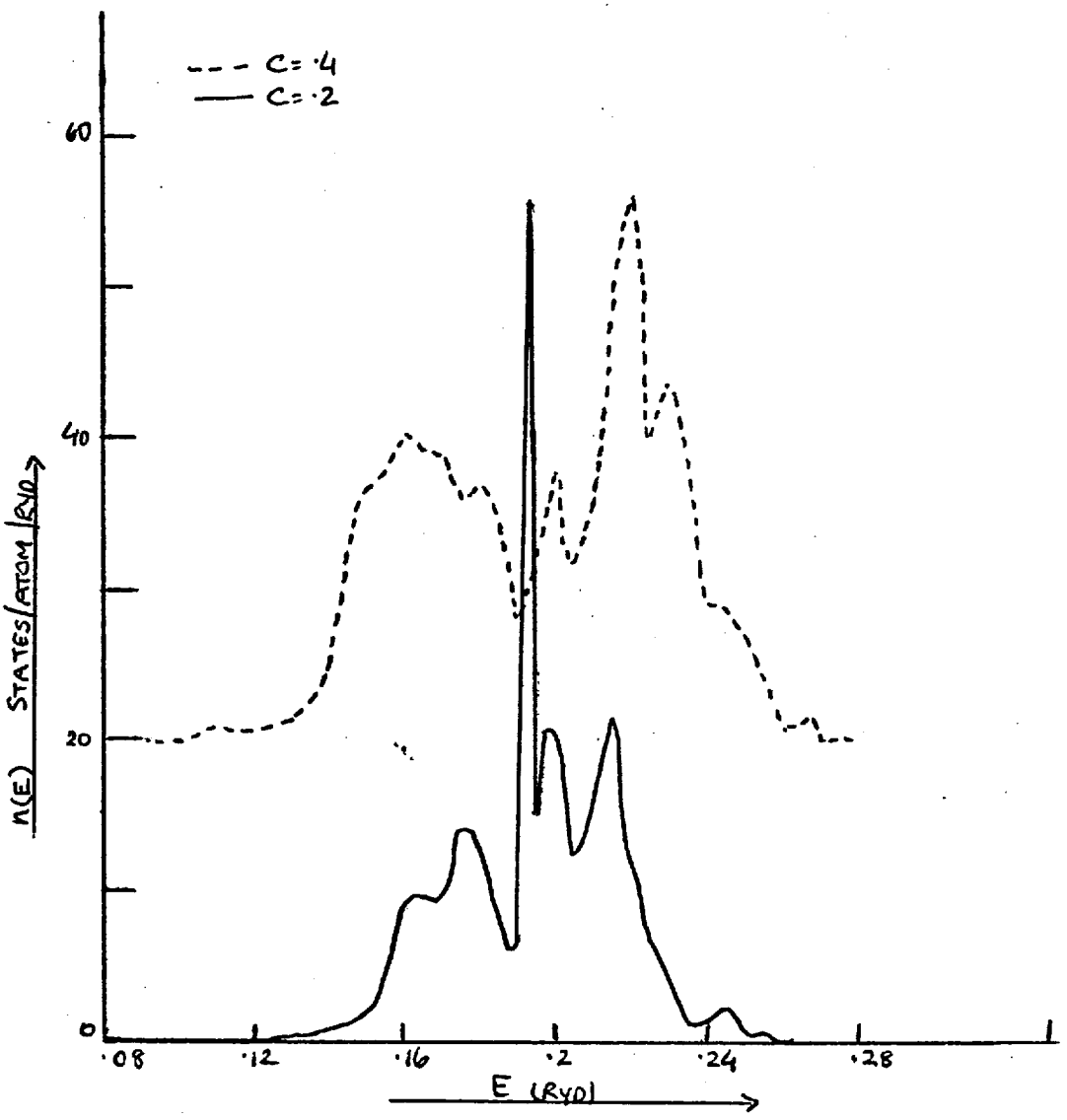

Plot of the d band density of statesof the component of alloy around E_d=.2. The origin of the curve for c=.4 is shifted upwards.

FIGURE 4.5

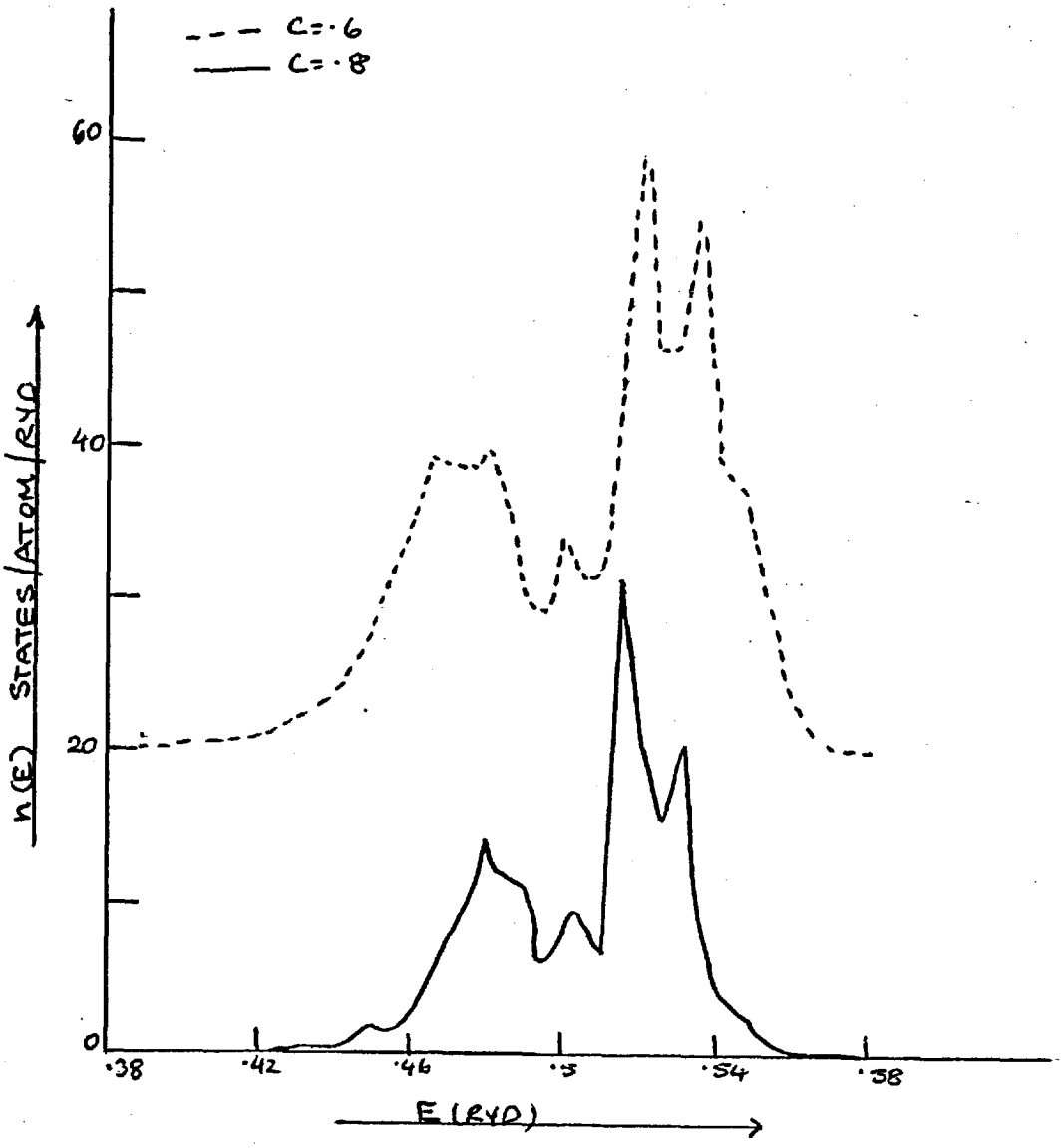

Plot of the d band density of states for c= .6 and c= .8. The origin of the curves is shifted upwards for different concentrations.

FIGURE 4.6

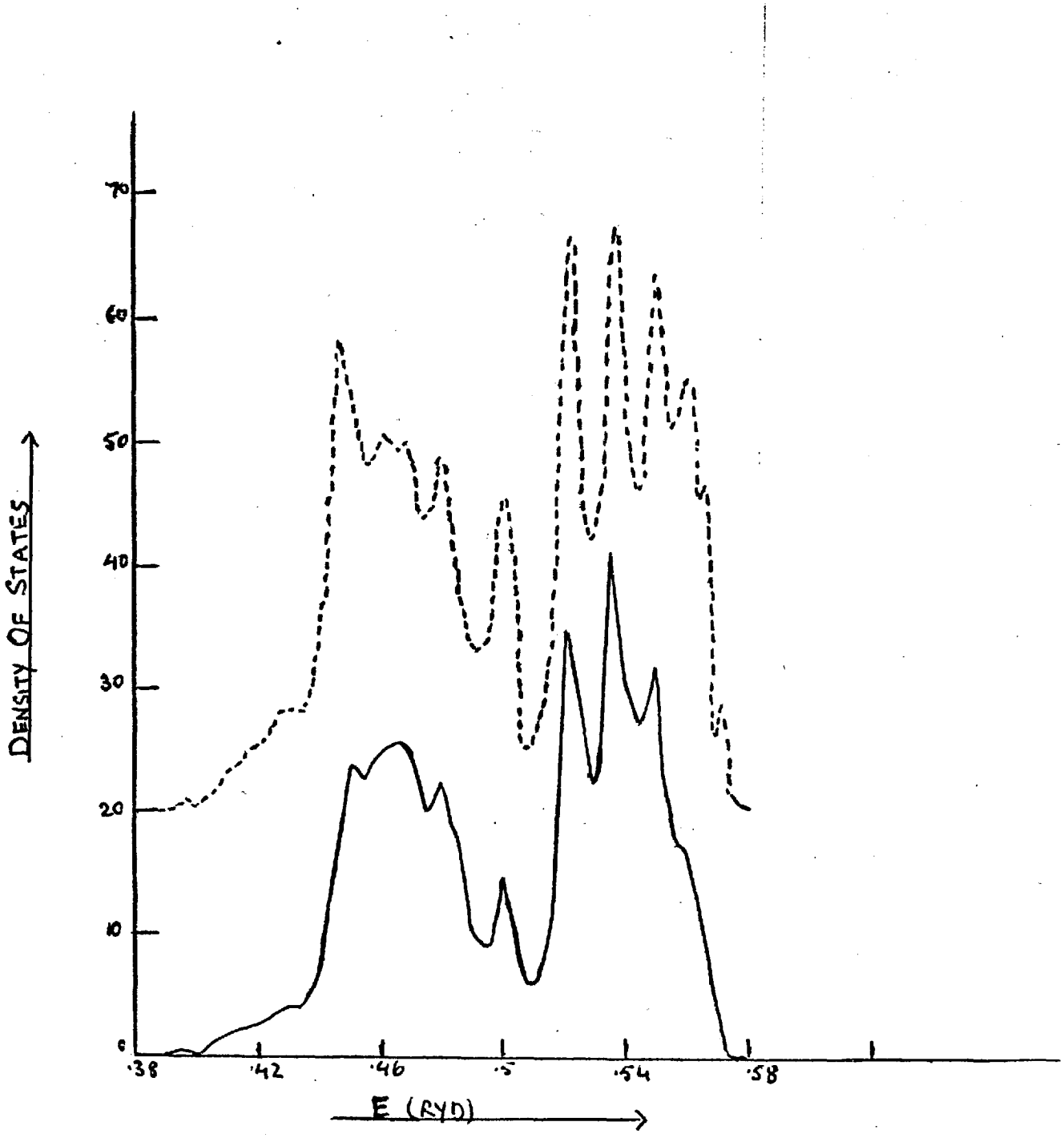

Density of states of d band transition metal alloy. The full line curve is for c=.4 and the dotted line curve is for c=.2.

FIGURE 4.7

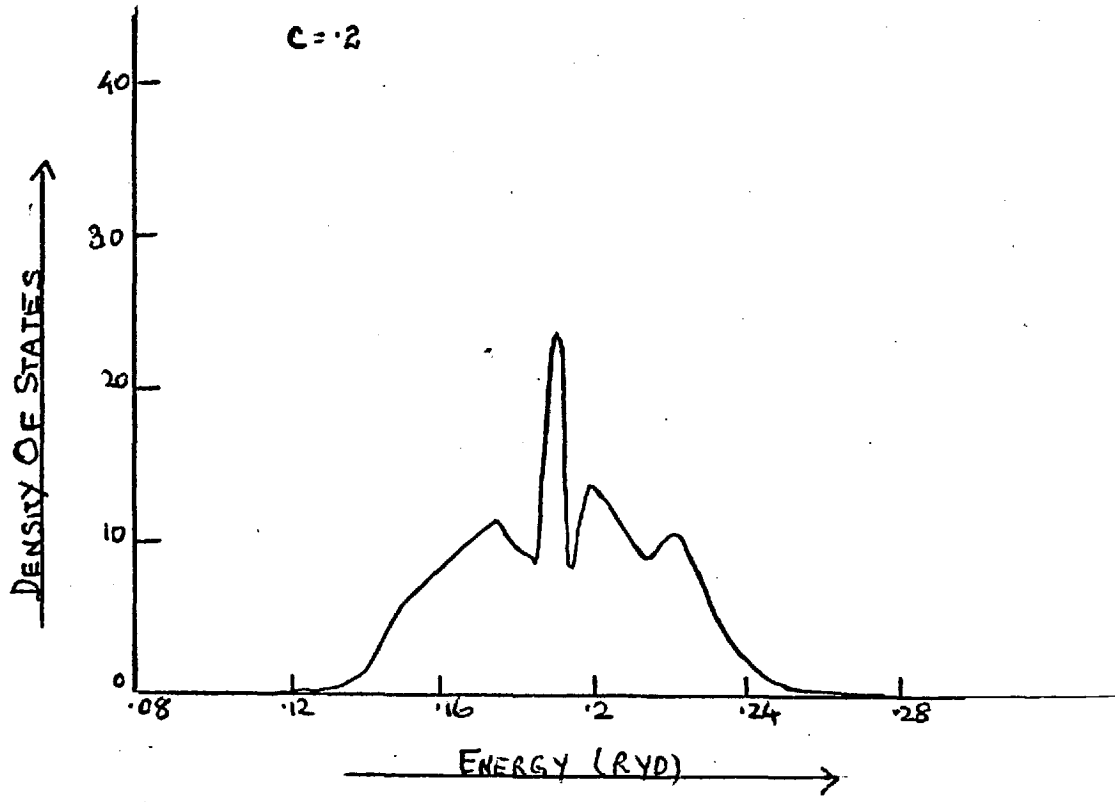

Plot of the d band density of states of minority band, when a smooth square root termination to the continued fraction is used.

CHAPTER 5

CLUSTER THEORY OF TRANSITION METAL ALLOYS

5.1 INTRODUCTION

In chapter 3 we applied the continued fraction method to realistic transition metal alloys in a very simple approximation, in chapter 4 we went a step further and carried out the calculation in cluster theory, but neglected the hybridizing effects. In this chapter we will do the hardest and the final model calculations of the transition metal alloys. Here we consider a more realistic model of transition metals, where the d bands cross and hybridize with the s band; that is to say we take into account the sp density of states and the hybridizing effects. In the calculations of this chapter we will use the discussion of chapter 1 (about the KKR matrix), the results of chapter 2(modification of Lloyds expression) and chapter 4 (calculations of d electron density of states).

In the next section we will show how the KKR secular equation for transition metals can be written when we abandon the Bloch representation and how we can split the result into a tight binding part in site representation hybridizing with an infinite plane wave matrix. The tight binding part will turn out to be the same as calculated in chapter 4. The hybridization part

is calculated in section 5.3. In section 5.4 we will do the final calculation for the density of states of the realistic transition metal alloys. In the last section of this chapter we will present the numerical results.

5.2 KKR MATRIX

The secular equation for transition metals in Bloch representation is given by (Hubbard 1967, Jacobs 1968)

$$\left| T_{mm'}(\underset{\sim}{k}) - E\delta_{mm'} - \sum_{g} \frac{\Gamma_m^*(\underset{\sim}{k}+\underset{\sim}{g})\,\Gamma_{m'}(\underset{\sim}{k}+\underset{\sim}{g})}{|\underset{\sim}{k}+\underset{\sim}{g}|^2 - E} \right| = 0 \qquad (5.1)$$

where $T_{mm'}(\underset{\sim}{k})$ is the 5x5 tight binding Slater and Koster (1954) matrix in Bloch representation and is given by Table 3.2. $\Gamma_m^*(\underset{\sim}{k}+\underset{\sim}{g})$ and $\Gamma_{m'}(\underset{\sim}{k}+\underset{\sim}{g})$ are the hybridization matrices. $\underset{\sim}{g}$ is a reciprocal lattice vector. ($\underset{\sim}{k}$ is an argument of the matrix elements here and not a matrix index).

According to Heine (1967) the above equation can be unfolded and rewritten as follows:

$$\begin{vmatrix} T_{mm'}(\underset{\sim}{k}) - E\delta_{mm'} & \Gamma_m^*(\underset{\sim}{k}+\underset{\sim}{g}) \\ \Gamma_{m'}(\underset{\sim}{k}+\underset{\sim}{g}) & [|\underset{\sim}{k}+\underset{\sim}{g}|^2 - E]\delta_{gg'} \end{vmatrix} = 0 \qquad (5.2)$$

This is a nine by nine matrix.

Transforming equation (5.2) into the site representation we have

$$\begin{vmatrix} T^{ij}_{mm'} - E\delta_{ij} & \Gamma_{im}(k) \\ \Gamma^{*}_{jm}(k') & (k^2-E)\delta_{kk'} \end{vmatrix} = 0 \qquad (5.3)$$

where

$$\Gamma_{im}(k) = \frac{1}{\sqrt{N}} \Gamma_m(\underset{\sim}{k}+\underset{\sim}{g})\, e^{i\underset{\sim}{k}\cdot\underset{\sim}{t}_i} \qquad (5.4)$$

This is an infinite matrix, because we have abandoned the Bloch theorem the wave vector $\underset{\sim}{k}$ can have any value, and is a matrix index.

In equation (5.3) $T^{ij}_{mm'}$ is the tight binding d matrix between the sites i ahd j. $\Gamma_{im}(k)$ and $\Gamma^{*}_{jm}(k)$ are the hybridization matrices between the tight binding d wave functions and the free electron wave functions. $(k^2-E)\delta_{kk'}$ is the free electron matrix. N is the number of lattice sites.

The matrix given by equation (5.3) can be symbolically represented as

$$\begin{bmatrix} D & A & E \\ A^{*} & B & F \\ E^{*} & F^{*} & C \end{bmatrix} \qquad (5.5)$$

where D is the diagonal d electron 5x5 matrix at the central site, A is the 5x5(N-1) hopping matrix betweem the central site and the

other sites, B is the matrix for the d electrons on the other sites, E is the hybridization matrix between the d electrons on the central site and plane wave, F is the hybridization matrix between the d electrons on the other sites and the plane wave and C is the plane wave matrix. A^*, E^*, and F^* are the complex congugates of A, E and F respectively.

In matrix (5.4), folding the sub-matrix B into the sub-matrix

$$\begin{bmatrix} D & E \\ E^* & C \end{bmatrix} \tag{5.6}$$

we get

$$\begin{bmatrix} D-AB^{-1}A^* & E-AB^{-1}F \\ E^*-F^*B^{-1}A & C-F^*B^{-1}F \end{bmatrix} \tag{5.7}$$

There are two reasons for folding B first rather than C. The first is we can separate out the tight binding part from the hybridization part. The second reason is we can express the tight binding part in a form in which it has already been evaluated in chapter 4.

Finally folding everything into the first element of the matrix we get

$$\left[(D-AB^{-1}A^*)-\{(E-DB^{-1}F)(C-F^*B^{-1}F)\ (E^*-F^*B^{-1}D^*)\}\right] \tag{5.8}$$

where the first term is the tight binding d electron term, while the second term gives the hybridization correction.

The reciprocal of expression (5.8) is one diagonal element

of the inverse matrix (i.e one diagonal element of the Green function), hence we can use it to calculate the density of states.

5.3 HYBRIDIZATION CORRECTION

The last term of equation (5.8) in curly brackets gives the hybridization correction to the tight binding matrix. To calculate this we will first evaluate the inverse matrix $(C-F^{*}B^{-1}F)$, where C is the plane wave matrix given by

$$C = (k^2-E)\delta_{kk'} \tag{5.9}$$

F is the hybridization matrix given by

$$F = \Gamma_{im}(k) = \frac{1}{\sqrt{N}} A_H j_2(kR_H) Y_L(\hat{k}) f_c(k) e^{i\underset{\sim}{k}\cdot\underset{\sim}{t}_i} \tag{5.10}$$

$$= \Gamma_{om}(k) e^{i\underset{\sim}{k}\cdot\underset{\sim}{t}_i} \tag{5.11}$$

where A_H and R_H are Mueller's (1967) hybridization coefficients and $f_c(k)$ is the Mueller's cut-off factor. j_2 is the spherical Bessel function and $Y_L(\hat{k})$ is the spherical Harmonics. B is the matrix which correspond to sites other than the central. In calculating the hybridization we make an approximation for B, which corresponds to taking average medium outside the central site with a fraction c of atoms of type A and a fraction (1-c) of type B. This approximation can be justified by the reasoning that d electrons on the central atom hybridize with the freely moving sp electrons, which in turn hybridize with d electrons on sites anywhere else in the lattice. Because there are infinite number of sites available for this second hybridization, the average approximation

is likely to be reasonably accurate. B^{-1} is approximated by

$$B^{-1} = \frac{c}{E_A - E - \Delta} + \frac{1-c}{E_B - E - \Delta} \qquad (5.12)$$

where Δ is a small broadening introduced to make the result analytical and is discussed later.

Now the inverse matrix $(C - F^* B^{-1} F)^{-1}$ can be evaluated as follows:

$$(C - F^* B^{-1} F) = (k^2 - E)\delta_{kk'} - \sum_{\substack{i \neq 0 \\ m}} \Gamma^*_{im}(k) \left[\frac{c}{E_A - E - \Delta} + \frac{1-c}{E_B - E - \Delta} \right] \Gamma_{im}(k') \qquad (5.13)$$

$$= (k^2 - E)\delta_{kk'} - \sum_{i m} \Gamma^*_{im}(k) \left[\frac{c}{E_A - E - \Delta} + \frac{1-c}{E_B - E - \Delta} \right] \Gamma_{im}(k') \qquad (5.14)$$

$$+ \sum_m \Gamma^*_{0m}(k) \left[\frac{c}{E_A - E - \Delta} + \frac{1-c}{E_B - E - \Delta} \right] \Gamma_{0m}(k')$$

Approximating the sum over the site index i by an integral in the above equation we have

$$C - F^* B^{-1} F = (k^2 - E)\delta_{kk'} - \left[\sum_m \frac{1}{\Omega} \int d^3 r_i \, e^{i(k - k') \cdot r_i} \right] \Gamma^*_{0m}(k) \Gamma_{0m}(k') \times$$

$$\left[\frac{c}{E_A - E - \Delta} + \frac{1-c}{E_B - E - \Delta} \right] + \sum_m \Gamma^*_{0m}(k) \left[\frac{c}{E_A - E - \Delta} + \frac{1-c}{E_B - E - \Delta} \right] \Gamma_{0m}(k') \qquad (5.15)$$

where Ω is the volume of the unit cell. Now if N is the number of unit cells then

$$\int d^3 r_i \, e^{i(k - k') \cdot r_i} = N\Omega \, \delta_{kk'} \qquad (5.16)$$

Hence we can write equation (5.15) as

$$C - F^{*} B^{-1} F = \left[(k^2 - E) - \sum_m \sqrt{N}\, \Gamma^{*}_{0m}(k) \sqrt{N}\, \Gamma_{0m}(k') \left\{ \frac{c}{E_A - E - \Delta} + \frac{1-c}{E_B - E - \Delta} \right\} \right] \delta_{kk'}$$

$$+ \sum_m \Gamma^{*}_{0m}(k) \left\{ \frac{c}{E_A - E - \Delta} + \frac{1-c}{E_B - E - \Delta} \right\} \Gamma_{0m}(k') \qquad (5.17)$$

Let

$$\Gamma'_{0m}(k) = \sqrt{N}\, \Gamma_{0m}(k) . \qquad (5.18)$$

$$\left.
\begin{aligned}
f^{*}_m(k) &= \Gamma_{0m}(k) \sqrt{\frac{c}{E_A - E - \Delta} + \frac{1-c}{E_B - E - \Delta}} \\
f_m(k') &= \Gamma_{0m}(k') \sqrt{\frac{c}{E_A - E - \Delta} + \frac{1-c}{E_B - E - \Delta}}
\end{aligned}
\right\} \qquad (5.19)$$

$$\mathcal{D}(k) = k^2 - E - \sum_m \Gamma'^{*}_{0m}(k)\, \Gamma'_{0m}(k) \left\{ \frac{c}{E_A - E - \Delta} + \frac{1-c}{E_B - E - \Delta} \right\} \qquad (5.20)$$

$$\left.
\begin{aligned}
f'^{*}_m(k) &= \frac{1}{\sqrt{N}} f^{*}_m(k) \\
f'_m(k') &= \frac{1}{\sqrt{N}} f_m(k')
\end{aligned}
\right\} \qquad (5.21)$$

Then equation (5.17) gives

$$\left[C - F^{*} B^{-1} F \right]^{-1} = \left[\mathcal{D}(k)\, \delta_{kk'} + \sum_m f^{*}_m(k)\, f_m(k') \right]^{-1} \qquad (5.22)$$

By Taylors expansion

$$\left[C - F^{*} B^{-1} F \right]^{-1} = \mathcal{D}^{-1}(k) \delta_{kk'} - \mathcal{D}^{-1}(k) \sum_n f^{+}_m(k)\, f_m(k')\, \mathcal{D}^{-1}(k')$$

$$+ \mathcal{D}^{-1}(k) \sum_m f^{*}_m(k) \sum_{k''} f_m(k'')\, \mathcal{D}^{-1}(k'') \sum_{m'} f^{*}_{m'}(k'')\, f_{m'}(k')\, \mathcal{D}^{-1}(k')$$

$$+ \cdots \qquad (5.23)$$

$$= \tilde{D}^{-1}(k)\delta_{kk'} - \tilde{D}^{-1}(k)\sum_{m m'} f_m^*(k)\Big[\delta_{mm'} + \sum_{k''} f_m(k'')\tilde{D}^{-1}(k'')f_{m'}^*(k'')\Big]^{-1} \times$$
$$f_{m'}(k')\tilde{D}^{-1}(k') \qquad (5.24)$$

$$= \tilde{D}^{-1}(k)\delta_{kk'} - \tilde{D}^{-1}(k)\sum_{m m'} f_m^*(k)\Big[\delta_{mm'} + \frac{N\Omega}{(2\pi)^3}\int d^3k'' f_m(k'')\tilde{D}^{-1}(k'')f_{m'}^*(k'')\Big]^{-1} \times$$
$$f_{m'}(k')\tilde{D}^{-1}(k') \qquad (5.25)$$

where

$$\sum_k \longrightarrow \frac{N\Omega}{(2\pi)^3}\int d^3k$$

The standard result used in equation (5.23) and (5.24) is given in appendix B. If we denote the integral occuring in equation (5.25) by $g_{mm'}$ {this integral will be evaluated later in section 5.3(i)} then we can rewrite equation (5.25) as

$$\Big[C - F^*B^{-1}F\Big]^{-1} = \tilde{D}^{-1}(k)\delta_{kk'} - \tilde{D}^{-1}(k)\sum_{m m'} f_m^*(k)\Big[\delta_{mm'} + g_{mm'}\delta_{m,m'}\Big]^{-1} f_{m'}(k')\tilde{D}^{-1}(k') \qquad (5.26)$$

Returning to the hybridization correction term of equation (5.8), we see that it can be broken up into four terms. In the following pages we will calculate each of them separately.

5.3(i) FIRST CORRECTION TERM

The first correction term in equation (5.8) is in proper notation given by

$$\left.\begin{aligned}
&\sum_{kk'} E_{ok}\Big[C - F_{ki}^* B_{ij}^{-1} F_{jk'}\Big]^{-1}_{kk'} E_{k'o}^* \\
&= \sum_{kk'} \Gamma_{om}(k)\Big[C - F_{ki}^* B_{ij}^{-1} F_{jk'}\Big]^{-1} \Gamma_{om}^*(k') \\
&= \frac{1}{B^{-1}}\Big\{\sum_{kk'}\Big[f_m(k)\Big\{\tilde{D}^{-1}(k)\delta_{kk'} - \sum_{m_1 m''}\tilde{D}^{-1}(k)\delta_{kk'}f_{m_1}(k)\Big[\delta_{m_1 m''} + g_{m_1 m''}\delta_{m_1 m''}\Big]^{-1} \times \\
&\qquad f_{m''}(k')\tilde{D}^{-1}(k')\Big\} f_{m'}^*(k')\Big]\Big\}
\end{aligned}\right\} \qquad (5.27)$$

$$= \frac{1}{B^{-1}}\Big[f_m(k)\, \bar{D}^{-1}(k)\, \delta_{kk'} f^{*}_{m'}(k) - \sum_{m_1 m''} \sum_{k} f_m(k)\, \bar{D}^{-1}(k)\, f^{*}_{m_1}(k) \times$$

$$\left[\delta_{m_1 m''} + g_{m_1 m''} \delta_{m_1 m''}\right]^{-1} \sum_{k'} f_{m''}(k')\, \bar{D}^{-1}(k') f^{*}_{m'}(k') \Big\} \qquad (5.28)$$

$$= \frac{1}{B^{-1}} \Big[g^{(E)}_{mm'} \delta_{mm'} - \sum_{m_1 m''} g^{(E)}_{mm_1} \delta_{mm_1} \left[\delta_{m_1 m''} + g_{m_1 m''} \delta_{m_1 m''}\right]^{-1} g_{m'' m'} \delta_{m'' m'} \qquad (5.29)$$

(we can drop the summation over m and m'', because all the matrices are diagonal). Thus

$$= \frac{1}{B^{-1}} \Big[g^{(E)}_{mm'} \Big/ 1 + g^{(E)}_{mm'} \Big] \delta_{mm'} \qquad (5.30)$$

Now we evaluate the integral $g^{(E)}_{mm'}$ given by

$$g^{(E)}_{mm'} = \frac{N\Omega}{(2\pi)^3} \int d^3k\, f_m(k)\, \bar{D}^{-1}(k) f^{*}_{m'}(k) \qquad (5.31)$$

$$= \frac{\Omega}{(2\pi)^3} B^{-1} \int d^3k\, \Gamma'_{Om}(k)\, \bar{D}^{-1}(k)\, \Gamma'^{*}_{Om'}(k) \qquad (5.32)$$

[using equations (5.18) and (5.19).]

Substituting the values of $\Gamma'_{Om}(k)$ and $\bar{D}^{-1}(k)$ from equations (5.11) and (5.20) respectively we have

$$g^{(E)}_{mm'} = P(E) \int d^3k\, \frac{j_2^2(kR_H) f_c^2(k) Y_L(k) Y^{*}_{L'}(k)}{k^2 - E'} \qquad (5.33)$$

$$= P(E) \int dk\, \frac{k^2 j_2^2(kR_H) f_c^2(k)}{k^2 - E'}\, \delta_{LL'} \qquad (5.34)$$

where

$$P(E) = \frac{\Omega B^{-1}}{(2\pi)^3} A_H^2 \qquad (5.35)$$

$\Omega = a^3/4$ (a is a lattice constant)

and

$$E' = E + \sum_m \Gamma'^{*}_{om}(k)\Gamma'_{om}(k)\left[\frac{c}{E_A - E - \Delta} + \frac{1-c}{E_B - E - \Delta}\right]\delta_{kk'} \qquad (5.36)$$

The broadening Δ in $\tilde{D}^{-1}(k)$ (occuring in E') will henceforth be ignored. The reason is $\tilde{D}^{-1}(k)$ occurs only in integrals, and the effects of this broadening are significant only in the neighbourhood of the singularities of the integrand. These effects are nearly symmetrically disposed around the singularities and consequently give only a small effect on the integral. With this approximation and the substitution of values of $\Gamma'^{*}_{om}(k)$ and $\Gamma'_{om}(k)$ we can rewrite equation (5.36) as

$$E' = E + A_H^2 j_2^2(kR_H) f_c^2(k)\left[\frac{c}{E_A - E - \Delta} + \frac{1-c}{E_B - E - \Delta}\right]\delta_{LL'} \qquad (5.37)$$

E' can be made independent of k by fixing the value of $f_c(k)$ and $j_2(kR_H)$ at a certain point $k = k_o$ in k-space; and it can be shown that it does not make difference to the shift of the energy bands. Therefore

$$E' = E + A_H^2 j_2^2(k_oR_H) f_c^2(k_o)\left[\frac{c}{E_A - E - \Delta} + \frac{1-c}{E_B - E - \Delta}\right]\delta_{LL'} \qquad (5.38)$$

Returning to equation (5.34) we will now discuss the Mueller cut-off factor $f_c(k)$. It should be selected such that only the lowest one or two plane waves hybridize with the d bands and thus ensure that the d bands given by the interpolation scheme

preserves the correct symmetry based degeneracies. Let

$$f_c(k) = e^{-\alpha(k-k_0)^2} \tag{5.39}$$

This will be equal to one at $k=k_0$ and will be virtually zero after a certain value of k. Having thus defined all the quantities occuring in equation (5.34) we can now proceed with the calculation of $g^{(E)}_{mm'}$. For this we will introduce a small broadening $i\epsilon$ in the denominator of equation (5.34) to make the function analytic.

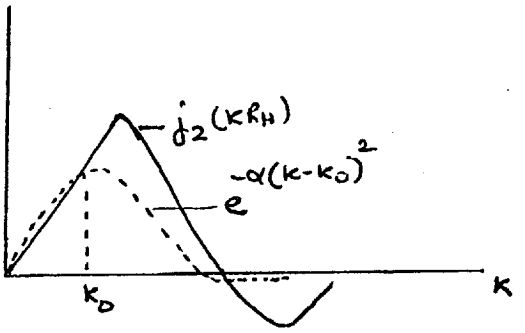

Substituting the value of $f_c(k)$ in equation (5.34) we have

$$g_{mm'}(E) = P(E)\int_0^\infty k^2 dk \; \frac{j_2^2(kR_H)\, e^{-2\alpha(k-k_0)^2}}{k^2 - E' - i\epsilon}\, \delta_{LL'} \tag{5.40}$$

$$= P(E)\int_0^\infty dk \; \frac{E'\, j_2^2(\sqrt{E'}R_H)\, e^{-2\alpha(\sqrt{E'}-k_0)^2}}{k^2 - E' - i\epsilon}\, \delta_{LL'}$$

$$+ P(E)\int_0^\infty dk \; \frac{k^2 j_2^2(kR_H) e^{-2\alpha(k-k_0)^2} - E' j_2^2(\sqrt{E'}R_H) e^{-2\alpha(\sqrt{E'}-k_0)^2}}{k^2 - E' - i\epsilon}\, \delta_{LL'} \tag{5.41}$$

It should be noted that the sum over k extends from o to ∞, because by alloying we have destroyed the translational symmetry of the lattice, so now there are no boundary conditions on k.

The first integral $F_{mm'}$ of $g_{mm'}$ is solved analytically by the use of complex analysis as follows:

$$F_{mm'} = P(E)\int_0^\infty dk\, E' j_2^2(\sqrt{E'}R_H)\frac{1}{2\sqrt{E'}}\left[\frac{1}{k-\sqrt{E'}} - \frac{1}{k+\sqrt{E'}}\right] e^{-2\alpha(\sqrt{E'}-k_0)^2}\delta_{LL'}$$

$$= \frac{P(E)}{2\sqrt{E'}} e^{-2\alpha(\sqrt{E'}-k_0)^2} j_2^2(\sqrt{E'}R_H)\int_{-\infty}^{\infty}\frac{dk}{k-\sqrt{E'}-i\epsilon}\delta_{LL'}$$

$$= \frac{i\pi}{2\sqrt{E'}} P(E)\, e^{-2\alpha(\sqrt{E'}-k_0)^2} j_2^2(\sqrt{E'}R_H)\,\delta_{LL'} \qquad (5.42)$$

The last equation is obtained by Principals Parts integration, the real part of $F_{mm'}$ being zero. This proves that the first integral of $g_{mm'}^{(E)}$ has only the imaginary part.
The second integral of $g_{mm'}^{(E)}$ can be calculated numerically. This is real , its imaginary part is zero. Hence the final expression for $g_{mm'}$ is

$$g_{mm'}(E) = P(E)\left[\frac{i\pi}{2\sqrt{E'}} e^{-2\alpha(\sqrt{E'}-k_0)^2} j_2^2(\sqrt{E'}R_H)\right.$$

$$\left. + \int_0^\infty dk\, \frac{k^2 j_2^2(kR_H)e^{-2\alpha(k-k_0)^2} - E' j_2^2(\sqrt{E'}R_H)e^{-2\alpha(\sqrt{E'}-k_0)^2}}{k^2-E'-i\epsilon}\delta_{LL'}\right] \qquad (5.43)$$

Thus the first correction term given by equation (5.30) is now clearly known and it turns out to be diagonal , with all elements equal.

5.3(ii) SECOND CORRECTION TERM

The second correction term from equation (5.8) is

$$\sum_{kk'}\sum_{ij}\sum_{i'j'}\left\{E_{ok}\left[C - F^*_{ki}\, B^{-1}_{ij}\, F_{jk'}\right]^{-1}_{kk'}\left[F^*_{k'i'}\, B^{-1}_{i'j}\, A^*_{j'0}\right]_{k'0}\right\}$$

$$= \sum_{kk'}\sum_{ij}\left\{\Gamma_{om}(k)\left[C - F^*_{ki}\, B^{-1}_{ij}\, F_{jk'}\right]^{-1}_{kk'}\left[\Gamma^*_{jm}(k')\, B^{-1}_{j'j}\, A^*_{j'0}\right]_{k'0}\right\}$$

$$= \sum_{kk'}\sum_{ij}\left\{\frac{f_m(k)}{B^{-1}}\left[\bar{D}^{-1}(k)\delta_{kk'} - \bar{D}^{-1}(k)\sum_{m_1 m''} f^*_{m_1}(k)\left[\delta_{mm''}\right.\right.\right.$$

$$\left.\left.\left. + \frac{N\Omega}{(2\pi)^3}\int d^3k''\, f_{m_1}(k'')\bar{D}^{-1}(k'') f^*_{m''}(k'')\right]^{-1} f_{m''}(k')\bar{D}^{-1}(k') f^*_{m'}(k')\, e^{-ik'\cdot r_j}\, B^{-1} A^*_{j0}\right] \qquad (5.44)$$

The last expression is obtained by using equations (5.19) and (5.25) and the fact that the matrix $\mathcal{B}^{-1}$ is a diagonal matrix between the site indices.

Carrying out the simplifications of the second correction term we have equation (5.44) equal to

$$\sum_j \left\{ \left[\sum_k f_m(k) \mathcal{D}^{-1}(k) f^*_{m'}(k') e^{-ik'\cdot r_j} \delta_{kk'} - \sum_{m,m''} \sum_k f_m(k) \mathcal{D}^{-1}(k) f^*_{m_1}(k) \times \right.\right.$$

$$\left.\left. \left[\delta_{m,m''} + g_{m,m''} \delta_{m,m''} \right]^{-1} \sum_{k'} f_{m''}(k') \mathcal{D}^{-1}(k') f^*_{m'}(k') e^{-ik'\cdot r_j} \right] A^*_{jo} \right.$$

$$= \sum_j \left\{ \left[\frac{N\Omega}{(2\pi)^3} \int d^3k\, f_m(k) \mathcal{D}^{-1}(k) f^*_{m'}(k) e^{-ik\cdot r_j} - \sum_{m,m''} \left[\frac{N\Omega}{(2\pi)^3} \int d^3k\, f_m(k) \mathcal{D}^{-1}(k) f^*_{m_1}(k) \times \right.\right.\right.$$

$$\left.\left.\left. \left[\delta_{m,m''} + g_{m,m''} \delta_{m,m''} \right]^{-1} \frac{N\Omega}{(2\pi)^3} \int d^3k'\, f_{m''}(k') \mathcal{D}^{-1}(k') f^*_{m'}(k') e^{-ik'\cdot r_j} \right] \right\} A^*_{jo} \qquad (5.45)$$

$$= \sum_j \left\{ \left[\frac{\Omega}{(2\pi)^3} \int d^3k\, f'_m(k) \mathcal{D}^{-1}(k) f'^*_m(k) e^{-ik\cdot r_j} - \sum_{m,m'} \left[\frac{\Omega}{(2\pi)^3} \int d^3k\, f'_m(k) \mathcal{D}^{-1}(k) f'^*_{m_1}(k) \times \right.\right.\right.$$

$$\left.\left.\left. \left[\delta_{m,m''} + g_{m,m''} \delta_{m,m''} \right]^{-1} \frac{\Omega}{(2\pi)^3} \int d^3k'\, f'_{m''}(k') \mathcal{D}^{-1}(k') f'^*_{m'}(k') e^{-ik'\cdot r_j} \right] \right\} A^*_{jo} \qquad (5.46)$$

$$= \sum_j \left\{ I_{LL'}(E, r_j) - \sum_{m,m'} g^{(E)}_{mm_1} \delta_{m_1 m'} \left[\delta_{m,m''} + g_{m,m''} \delta_{m,m''} \right]^{-1} I^{(E,r_j)}_{L''L'} \right\} A^*_{jo} \qquad (5.47)$$

$$= \sum_j \left\{ I_{LL'}(E, r_j) \Big/ \left(1 + g^{(E)}_{mm'} \delta_{mm'} \right) \right\} A^*_{jo} \qquad (5.48)$$

where

$$g_{mm'}(E) = \frac{N\Omega}{(2\pi)^3} \int d^3k''\, f_m(k'') \mathcal{D}^{-1}(k'') f^*_{m'}(k'') \qquad (5.49)$$

This factor is the same as occuring in the first correction term and has already been evaluated there {equation (5.43)}; and

$$\underline{I}_{LL'}(E,\underline{r}_j) = \frac{\Omega}{(2\pi)^3}\int d^3k\, f'_m(k)\, \mathcal{D}^{-1}(k)\, f'^{*}_{m'}(k)\, e^{-i\underline{k}\cdot\underline{r}_j} \qquad (5.50)$$

Using equations (5.19), (5.20) and (5.10) we have

$$\underline{I}_{LL'}(E,\underline{r}_j) = \frac{\Omega B^{-1} A_H^2}{(2\pi)^3}\int d^3k\, \frac{j_2^2(kR_H)Y_L(\underline{k})Y^*_{L'}(\underline{k}')\, e^{-i\underline{k}\cdot\underline{r}_j} e^{-2\alpha(k-k_0)^2}}{k^2-E'} \qquad (5.51)$$

$$= P(E)\int d^3k\, \frac{j_2^2(kR_H)Y_L(\underline{k})Y^*_{L'}(\underline{k}')\, e^{-i\underline{k}\cdot\underline{r}_j} e^{-2\alpha(k-k_0)^2}}{k^2-E'} \qquad (5.52)$$

where as before ignoring the broadening Δ in $\mathcal{D}^{-1}(k)$ we define

$$\left.\begin{aligned} P(E) &= \Omega B^{-1} A_H^2/(2\pi)^3 \\ E' &= E + A_H^2 j_2^2(k_0R_H) f_c(k_0)\left[\frac{c}{E_A-E} + \frac{1-c}{E_B-E}\right]\delta_{LL'} \\ f_c(k) &= e^{-\alpha(k-k_0)^2} \end{aligned}\right\} \qquad (5.53)$$

Using the following expansion for the exponential in equation (5.52) (Messiah 1964)

$$e^{-i\underline{k}\cdot\underline{r}_j} = 4\pi\sum_{\ell''=0}^{\infty}\sum_{m''=-\ell''}^{\ell''}(i)^{\ell''} j_{\ell''}(kr_j)Y_{L''}(\underline{r}_j)Y^*_{L''}(\underline{k}) \qquad (5.54)$$

where $Y_{L''}(\underline{k})$ etc. are the real spherical harmonics. These are derived from the complex spherical harmonics $y_{L''}$ by the relation:

$$\left.\begin{aligned} Y^m_\ell &= \frac{1}{\sqrt{2}}\left[y^m_\ell + \bar{y}^m_\ell\right] \\ Y^{-m}_\ell &= \frac{-i}{\sqrt{2}}\left[y^m_\ell - \bar{y}^m_\ell\right] \end{aligned}\right\} \qquad (5.55)$$

The real spherical harmonics used in these calculations are given in Table 5.1.

Therefore

$$I_{LL'}(E,r_j) = 4\pi P(E)\sum_{l''=0}^{\infty}\sum_{m''=-l''}^{l''}(i)^{l''}\int dk\,k^2\,\frac{j_2^2(kR_H)\,Y_{L''}(r_j)\,j_{l''}(kr_j)\,C_{LL'L''}\,e^{-2\alpha(k-k_0)^2}}{k^2-E'-i\epsilon} \qquad (5.56)$$

where

$$C_{LL'L''} = \int d\Omega\, Y_L(k)\,Y_{L'}^{*}(k)\,Y_{L''}^{*}(k)$$

are the Clebsch- Gordon coefficients for the real spherical harmonics and are given in Table 5.2.

The integral $I_{LL'}$ {equation (5.56)} as it stands looks rather formidable and non-analytic but by rewritting it into two parts and adding a small broadening $i\epsilon$ in the denominator we will see that one of it can be done analytically and other on the computer very easily.

$$I_{LL'}(E,r_j) = 4\pi P(E)\sum_{l''=0}^{\infty}\sum_{m''=-l''}^{l''}(i)^{l''}Y_{L''}(r_j)\,C_{LL'L''}\left[\int_0^{\infty}dk\,\frac{E'j_2^2(\sqrt{E'}R_H)\,e^{-2\alpha(\sqrt{E'}-k_0)^2}}{k^2-E'-i\epsilon}\,j_{l''}(\sqrt{E'}r_j)\right.$$

$$\left.+\int_0^{\infty}dk\,\frac{k^2j_2^2(kR_H)\,e^{-2\alpha(k-k_0)^2}\,j_{l''}(kr_j) - E'j_2^2(\sqrt{E'}R_H)\,e^{-2\alpha(\sqrt{E'}-k_0)^2}\,j_{l''}(\sqrt{E'}r_j)}{k^2-E'-i\epsilon}\right] \qquad (5.57)$$

$$= 4\pi P(E)\sum_{l''=0}^{\infty}\sum_{m''=-l''}^{l''}(i)^{l''}Y_{L''}(r_j)\,C_{LL'L''}\left[\frac{i\pi}{2}\sqrt{E'}\,j_2^2(\sqrt{E'}R_H)\,e^{-2\alpha(\sqrt{E'}-k_0)^2}\,j_{l''}(\sqrt{E'}r_j)\right.$$

$$\left.+\int_0^{\infty}dk\,\frac{k^2j_2^2(kR_H)\,e^{-2\alpha(k-k_0)^2}\,j_{l''}(kr_j) - E'j_2^2(\sqrt{E'}R_H)\,e^{-2\alpha(\sqrt{E'}-k_0)^2}\,j_{l''}(\sqrt{E'}r_j)}{k^2-E'-i\epsilon}\right] \qquad (5.58)$$

Because of the property of the Clebsch Gordon coefficients, l'' can have even values only, therefore the first term in the above equation is imaginary and can be evaluated for a fixed r_j, the integral part of it is purely real and is computed numerically. r_j is the nearest neighbour vector and for a face-centred cubic there are twelve nearest neighbours with $|r_j| = \frac{a}{\sqrt{2}}$, where 'a' is a lattice constant.

After substituting the values of $I_{LL'}(E,\underset{\sim}{r}_j)$ in equation (5.48) and summing over all j we see that the second correction term turns out to be diagonal also, with three elements equal and other two equal to each other.

5.3(iii) THIRD CORRECTION TERM

The third hybridization correction term from equation (5.8) is

$$\left[A_{oi}\,\bar{B}^{1}_{ii}\,F_{ik}\right]_{ok}\left[C-F^{*}_{ki}\,\bar{B}^{-1}_{ii}\,F_{ik'}\right]^{-1}E^{*}_{k'o}$$

which is clearly the transpose of the second correction term.

5.3 (iv) FOURTH CORRECTION TERM

The last hybridization correction term from equation (5.8) is

$$\left[A_{oi}\,\bar{B}^{-1}_{ii}\,F_{ik}\right]\left[C-F^{*}_{ki}\,\bar{B}^{-1}_{ii}\,F_{ik'}\right]^{-1}_{kk'}\left[F^{*}_{k'j}\,\bar{B}^{-1}_{jj}\,A^{*}_{jo}\right]_{k'o}$$

$$=\sum_{kk'}\sum_{ij}\frac{1}{B^{-1}}\Big[A_{oi}\,\bar{B}^{-1}f_{n}(k)\,e^{i\underset{\sim}{k}\cdot\underset{\sim}{r}_i}\Big\{\bar{D}^{-1}(k)\delta_{kk'}-\sum_{m,m''}\bar{D}^{-1}(k)f_{m''}(k)\times$$

$$\left[\delta_{mm''}+g_{m''m,n''m_1}\delta_{n''m_1}\right]^{-1}f^{*}_{m_1}(k')\,\bar{D}^{-1}(k')\Big\}f^{*}_{m'}(k')\,e^{-i\underset{\sim}{k}'\cdot\underset{\sim}{r}_j}\bar{B}^{-1}A^{*}_{jo} \qquad (5.59)$$

$$=\sum_{ij}\bar{B}^{-1}A_{oi}\Big[\frac{\Omega}{(2\pi)^3}\int d^3k\,f'_{m}(k)\,\bar{D}^{-1}(k)\,f'^{*}_{m}(k)\,e^{i\underset{\sim}{k}\cdot(\underset{\sim}{r}_i-\underset{\sim}{r}_j)}$$

$$-\frac{\Omega}{(2\pi)^3}\sum_{\substack{m''\\ m_1}}\int d^3k\,f'_{m}(k)\,\bar{D}^{-1}(k)\,f'^{*}_{m''}(k)\,e^{i\underset{\sim}{k}\cdot\underset{\sim}{r}_i}\left[\delta_{m''m_1}+g^{(E)}_{m''m_1}\delta_{m''m_1}\right]^{-1}\times$$

$$\frac{\Omega}{(2\pi)^3}\int d^3k'\,f'_{m_1}(k')\,\bar{D}^{-1}(k')\,f'^{*}_{m'}(k')\,e^{-i\underset{\sim}{k}'\cdot\underset{\sim}{r}_j}\Big]A^{*}_{jo} \qquad (5.60)$$

$$=\sum_{ij}\bar{B}^{-1}A_{oi}\left[K_{LL'}(E,\underset{\sim}{r}_i,\underset{\sim}{r}_j)-\sum_{L''L_1}I_{L''L_1}(E,\underset{\sim}{r}_i)\left[\delta_{m''m_1}+g_{m''m_1,m''m_1}\delta_{m''m_1}\right]^{-1}I^{-1}_{L_1L'}(E,\underset{\sim}{r}_j)\right]A^{*}_{jo} \qquad (5.61)$$

$$= \sum_{ij} B^{-1} A_{oi} \left[K_{LL'}(E, r_i, r_j) - \sum_{L''} I_{LL''}(E, r_i) \left[1 + g_{m''m''}(E) \right]^{-1} I_{L''L'}(E, r_j) \right] A^{*}_{jo} \qquad (5.62)$$

where $I_{LL'}(E, r_i)$ is the same as given by equation (5.58) and $g_{m''m''}(E)$ is given by equation (5.43), (for transition metals only l=2 component of the angular momentum contributes); and

$$K_{LL'}(E, r_i, r_j) = \frac{\Omega}{(2\pi)^3} \int d^3k \, f'_m(k) \, \bar{D}^{-1}(k) \, f'^{*}_{m'}(k) \, e^{i k \cdot (r_i - r_j)}$$

$$= \frac{\Omega}{(2\pi)^3} B^{-1} A_H^2 \int d^3k \, \frac{j_2^2(kR_H) Y_L(k) Y_{L'}(k) \, e^{-2\alpha(k-k_0)^2} \, e^{i k \cdot (r_i - r_j)}}{k^2 - E' - i\epsilon} \qquad (5.63)$$

It should be noted that the broadening Δ is ignored in $\bar{D}^{-1}(k)$ for the same reason as before. Using the following expansion

$$e^{i k \cdot (r_i - r_j)} = 4\pi \sum_{l''=0}^{\infty} \sum_{m''=-l''}^{l''} (i)^{l''} j_{l''}(k|r_i - r_j|) Y_{L''}(r_i - r_j) Y^{*}_{L''}(k) \qquad (5.64)$$

we can write the above equation as

$$K_{LL'}(E, r_i, r_j) = 4\pi P(E) \sum_{l''=0}^{\infty} \sum_{m''=-l''}^{l''} (i)^{l''} Y_{L''}(r_i - r_j) \, C_{LL'L''} \int dk \, \frac{k^2 j_2^2(kR_H) \, e^{-2\alpha(k-k_0)^2} \, j_{l''}(k|r_i - r_j|)}{k^2 - E - i\epsilon} \qquad (5.65)$$

Doing the same procedure with this integral as we have done with the previous integrals we get

$$K_{LL'}(E, r_i, r_j) = 4\pi P(E) \sum_{l''=0}^{\infty} \sum_{m''=-l''}^{l''} (i)^{l''} Y_{L''}(r_i - r_j) \, C_{LL'L''} \left[\frac{i\sqrt{E'}}{2} j_2(\sqrt{E'} R_H) \, e^{-2\alpha(k-k_0)^2} \, j_{l''}(\sqrt{E'}|r_i - r_j|) \right.$$

$$\left. + \int_0^{\infty} dk \, \frac{k^2 j_2^2(kR_H) \, e^{-2\alpha(k-k_0)^2} \, j_{l''}(k|r_i - r_j|) - E' j_2^2(\sqrt{E'} R_H) \, e^{-2\alpha(\sqrt{E'}-k_0)^2} \, j_{l''}(\sqrt{E'}|r_i - r_j|)}{k^2 - E' - i\epsilon} \right]$$

(5.66)

$\underline{r}_i$ and $\underline{r}_j$ are the vectors to the nearest neighbour sites, $C_{LL'L''}$ are the Clebsch Gordon coefficients.

After substituting this into equation (5.62), we noticed that $|\underline{r}_i - \underline{r}_j| = R_n$ where n has five values; and if we evaluate the sum over the site indices i and j (i and j both go from 1to 12) corresponding to the different values of n first and then the sum over l'', m'' and n, the computer time is reduced tremendously. The complete calculation shows that the fourth correction term is also diagonal, with diagonal elements falling into two groups.

Before ending this section we will discuss the broadening Δ introduced in B^{-1} occuring in the function $\rho(E)$ of integrals $g_{mm'}(E)$, $I_{LL'}$ and $K_{LL'}$. The function of this is to keep B^{-1} analytical i.e it does not below up at $E=E_A$ or $E=E_B$. B^{-1} is given by equation

$$B^{-1} = \frac{c}{E_A - E - \Delta} + \frac{1-c}{E_B - E - \Delta} \qquad (5.67)$$

where

$$\Delta(E) = c\,F(E_A - E) + (1-c)\,F(E_B - E) \qquad (5.68)$$

$$F(E) = \left(E^2 \pm \sqrt{E^2 - 4zt^2}\right)/2zt^2 \qquad (5.69)$$

The sign of the last equation is chosen to get the correct high energy limit of $F(E)$ i.e

$$F(E) \to -\frac{1}{E} \quad \text{as} \quad E \to \pm\infty \qquad (5.70)$$

$4zt^2$ in equation (5.70) gives the band width of the density of states of the metal.

Thus we have calculated the hybridization correction completely and it turns out to be a diagonal matrix. We will use these results in the next section to calculate the density of states of transition metal alloys.

5.4 DENSITY OF STATES TRANSITION METAL ALLOYS

We now know equation (5.8) completely, because the tight binding part (i.e $D-AB^{-1}A^{*}$) has already been calculated in chapter 4 and is explicitly given by $G_{mm'}$ of equation (4.21); the four contributions to the hybridization have been numerically evaluated in section 5.3. It has been shown by a number of authors (Heine 1967, Hubbard 1967, Jacobs 1968 and Pettifor 1969) as discussed in chapter 1 that the inverse of the secular equation for transition metals (given by equation (5.1) or (5.8)) is the same as the inverse matrix in Lloyds expression of chapter 2. Precisely

$$\left[t_L^{-1}+G^{+}\right]^{-1}=\left[T_{mm'}^{(k)}-ES_{mm'}-\sum_{g}\frac{\Gamma_m^{*}(k+g)\,\Gamma_{m'}(k+g)}{|k+g|^2-E}\right]^{-1} \qquad (5.71)$$

$$=\left[(D-AB^{-1}A^{*})-(E-DB^{-1}F)(C-F^{*}B^{-1}F)(E^{*}-F^{*}B^{-1}D^{*})\right]^{-1} \qquad (5.72)$$

Therefore we can use the modified Lloyds expression for the density of states given by equation (2.33) of chapter 2 to calculate the density of states of transition metal alloys. The explicit equations we use are given by

$$n(E)=n_0(E)+\frac{1}{\pi}\mathrm{Im}\,\mathrm{Tr}\left[t_2^{-1}\dot{\alpha}t_2^{-1}-2\beta t_2^{-1}-\frac{d}{dE}t_2^{-1}\right]\overline{\langle 0|G|0\rangle_m}, \qquad (5.73)$$

where

$$\overline{\langle 0|G|0\rangle}_{m m'} = \left[\sum_{x=0}^{1}\sum_{n=1}^{66} \langle 0|G^{xn}|0\rangle_{m m'} M_n c^{x+y}(1-c)^{13-x-y}\right] \qquad (5.74)$$

$$\langle 0|G^{xn}|0\rangle_{m m'} = G_{m m'} - h_{m m'} \qquad (5.75)$$

In these equations α, β and t_2^{-1} are the same quantities as defined in chapter 3 and the values of the parameters used in their calculations are given in Table 3.1. x is the number of A atoms on the central site. n is the number of configurations of atoms on the twelve nearest neighbouring sites. M_n is the multiplicity of configuration n. y is the number of A atoms in the nearest neighbour shell. The number y depends on n. c is the concentration of A atoms . $G_{mm'}$ is the tight binding matrix calculated in chapter 4 and $h_{mm'}$ is the hybridization correction calculated in section 5.3.

5.5 DISCUSSION

In this section we will discuss the numerical results obtained for the real transition metal alloy AB with E_A = .2ryd and E_B = .5 ryd.

In figure 5.1 we give the results for the density of states for B type material. A similar result is obtained for A type transition metal which is not presented here. We notice two effects on the d band density of states(figure 4.2) by taking into account its hybridization with the free electron band. The first is that the

d band as a whole has become wider, the second is that some of the states have been taken from the top of the band and pushed towards the bottom. This curve is similar to those obtained before by interpolation or histogram methods (Gilat and Raubenheimer 1966), though the density of states above the top of the d band seems rather low.

In figure 5.2 we present the results for an alloy with a small concentration of A atoms in a B matrix. In a stretched out energy scale we see for the minority band a two peak structure in the middle with humped shoulders on either sides. The shoulder towards the top of the band, which corresponds to antibonding state of the electrons lying near the boundary of the Brillioun zone, is compressed downwards. This is due to the fact that the hybridization effects are strong near the edges of the zone. The pair of peaks near E_A=.2 is due to states on isolated A atoms , and these are split because of the cubic environment of isolated A atoms. The peaks are shifted relative to those for unhybridized d bands because of hybridization effects.

In figure 5.3 we present the results for c=.3, and we see that the A band has grown at the expense of B band. This A band is slightly shifted from the centre of the d band for pure A material due to band repulsion effects. Figure 5.4 gives the result for 50% alloy.

In figure 5.5 we present the results for the density of states when c=.7. The A band has now a great deal of structure in it, while

B band is comparatively smooth and shows the beginning of the three peak structure. The band repulsion effects in the B band are more visible now than when c was smaller.

In figure 5.6 we give the results for c=.9 with an expanded scale for the minority band. We again see a two peak structure and asymmetrical pair of humped shoulders. The reason for asymmetry and the splitting of the central peak being the as for c=0.1.

Thus we have been able to present a cluster theory for transition metal alloys, which is tractable and numerically feasible. The structure that appears in the density of states for the minority band can be for the most part explained in terms of simple and easily understood physical ideas. The effects of hybridization however are not yet completely understood.

The computer time taken to calculate one point on the graph for pure material is about 3 seconds and for an alloy about 5 seconds on CDC 7814.

TABLE 5.1

The real spherical harmonics

$$Y_0^0 = \sqrt{1/4\pi}$$

$$Y_2^e = \sqrt{5/16\pi}\ (3\cos^2\theta - 1)$$

$$Y_2^1 = -\sqrt{15/4\pi}\ \sin\theta\ \cos\theta\ \sin\phi$$

$$Y_2^{-1} = -\sqrt{15/4\pi}\ \sin\theta\ \cos\theta\ \cos\phi$$

$$Y_2^2 = \sqrt{15/16\pi}\ \sin^2\theta\ \cos 2\phi$$

$$Y_2^{-2} = \sqrt{15/16\pi}\ \sin^2\theta\ \sin 2\phi$$

$$Y_4^0 = \sqrt{9/256\pi}\ (35\cos^4\theta - 30\cos^2\theta + 3)$$

$$Y_4^1 = -\sqrt{45/32\pi}\ (7\cos^2\theta - 3)\ \sin\theta\ \cos\theta\ \sin\phi$$

$$Y_4^{-1} = -\sqrt{45/32\pi}\ (7\cos^2\theta - 3)\ \sin\theta\ \cos\theta\ \cos\phi$$

$$Y_4^2 = \sqrt{45/64\pi}\ (7\cos^2\theta - 1)\ \sin^2\theta\ \cos 2\phi$$

$$Y_4^{-2} = \sqrt{45/64\pi}\ (7\cos^2\theta - 1)\ \sin^2\theta\ \sin 2\phi$$

$$Y_4^3 = -\sqrt{315/32\pi}\ \sin^3\theta\ \cos\theta\ \sin 3\phi$$

$$Y_4^{-3} = -\sqrt{315/32\pi}\ \sin^3\theta\ \cos\theta\ \cos 3\phi$$

$$Y_4^4 = \sqrt{315/256\pi}\ \sin^4\theta\ \cos 4\phi$$

$$Y_4^{-4} = \sqrt{315/256\pi}\ \sin^4\theta\ \sin 4\phi$$

$$Y_l^m = 1/\sqrt{2}\ (\mathcal{Y}_1^m + \mathcal{Y}_1^{-m})$$

$$Y_l^{-m} = -i/\sqrt{2}\ (\mathcal{Y}_1^m - \mathcal{Y}_1^{-m})$$

where $\mathcal{Y}$ is the complex spherical harmonic.

TABLE 5.2

THE NON-ZERO CLEBSCH GORDON COEFFICIENTS $C_{LL'L''}$ USED IN OUR CALCULATIONS.

L	L′	L″	$C_{LL'L''}$	L	L′	L″	$C_{LL'L''}$
2-2	2-2	0 0	$\sqrt{1/4\pi}$	2 1	2 2	4 1	$\sqrt{5/392\pi}$
2-2	2-2	2 0	$-\sqrt{5/49\pi}$	2 1	2 0	2 1	$\sqrt{5/196\pi}$
2-2	2-2	4 0	$\sqrt{1/196\pi}$	2 1	2 0	4 1	$\sqrt{15/98\pi}$
2-2	2-2	4 4	$-\sqrt{5/28\pi}$	2-1	2-1	0 0	$\sqrt{1/4\pi}$
2-2	2 1	2-1	$\sqrt{15/196\pi}$	2-1	2-1	2 0	$\sqrt{5/196\pi}$
2-2	2 1	4-1	$-\sqrt{5/392\pi}$	2-1	2-1	2 2	$\sqrt{15/196\pi}$
2-2	2 1	4-3	$-\sqrt{5/56\pi}$	2-1	2-1	4 0	$-\sqrt{4/49\pi}$
2-2	2-1	2 1	$\sqrt{15/196\pi}$	2-1	2-1	4 2	$\sqrt{5/49\pi}$
2-2	2-1	4 3	$\sqrt{5/56\pi}$	2-1	2 2	2-1	$\sqrt{15/196\pi}$
2-2	2-1	4 1	$-\sqrt{5/392\pi}$	2-1	2 2	4-1	$-\sqrt{5/392\pi}$
2-2	2 2	4-4	$\sqrt{5/28\pi}$	2-1	2 2	4-3	$\sqrt{5/56\pi}$
2-2	2 0	2-2	$-\sqrt{5/49\pi}$	2-1	2 0	2-1	$\sqrt{5/196\pi}$
2-2	2 0	4-2	$\sqrt{15/196\pi}$	2-1	2 0	4-1	$\sqrt{15/98\pi}$
2 1	2 1	0 0	$\sqrt{1/4\pi}$	2 2	2 2	0 0	$\sqrt{1/4\pi}$
2 1	2 1	2 0	$\sqrt{5/196\pi}$	2 2	2 2	2 0	$-\sqrt{5/49\pi}$
2 1	2 1	2 2	$-\sqrt{15/196\pi}$	2 2	2 2	4 0	$\sqrt{1/196\pi}$
2 1	2 1	4 0	$-\sqrt{4/49\pi}$	2 2	2 2	4 4	$\sqrt{5/28\pi}$
2 1	2 1	4 2	$-\sqrt{5/49\pi}$	2 2	2 0	2 2	$-\sqrt{5/49\pi}$
2 1	2-1	2-2	$\sqrt{15/196\pi}$	2 2	2 0	4 2	$\sqrt{15/196\pi}$
2 1	2-1	4-2	$\sqrt{5/49\pi}$	2 0	2 0	0 0	$\sqrt{1/4\pi}$
2 1	2 2	2 1	$-\sqrt{15/196\pi}$	2 0	2 0	2 0	$\sqrt{5/49\pi}$
2 1	2 2	4 3	$\sqrt{5/56\pi}$	2 0	2 0	4 0	$\sqrt{9/49\pi}$

This Table is symmetric between L and L′

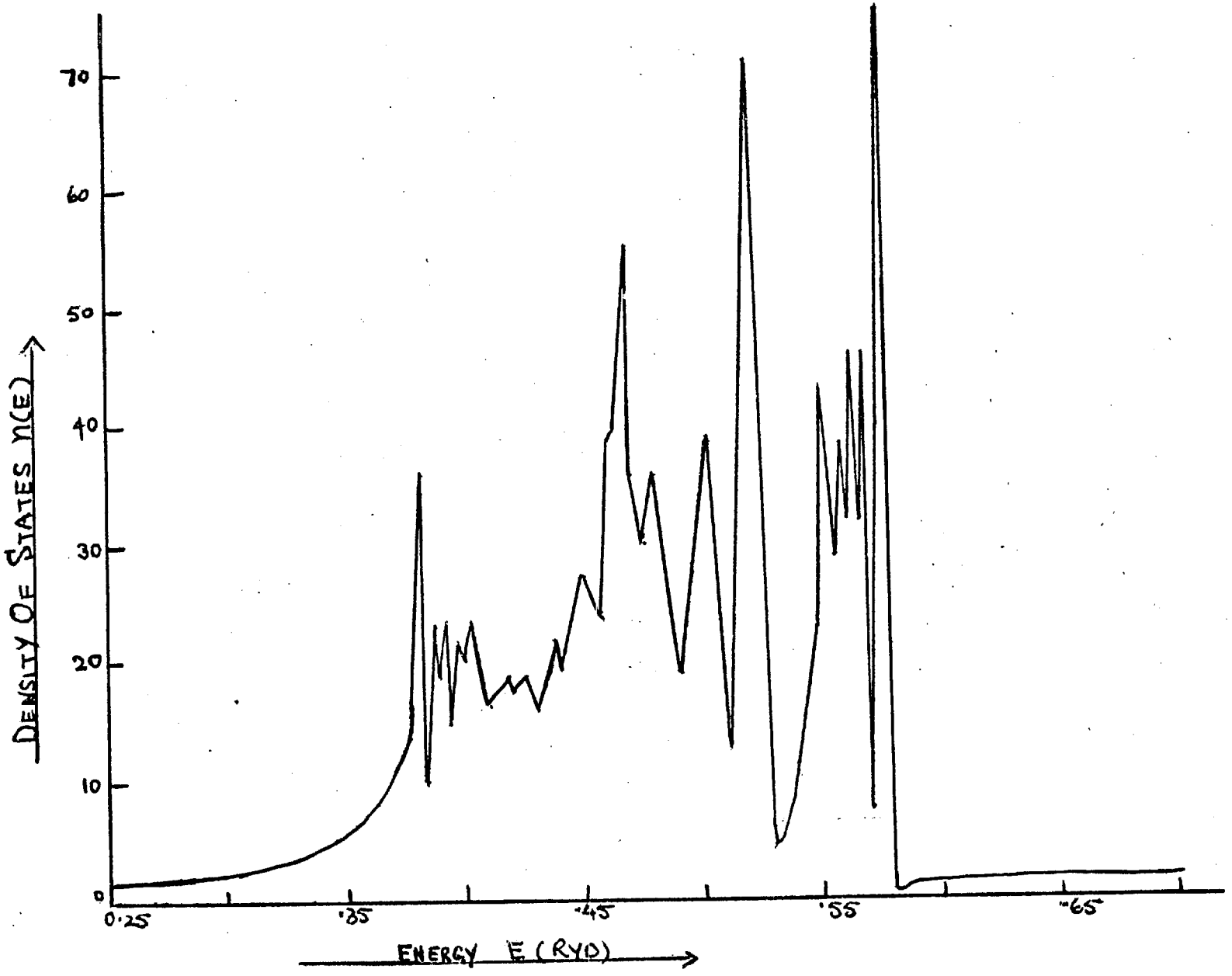

FIGURE 5.1

Plot of the density of states of pure real transition metal.

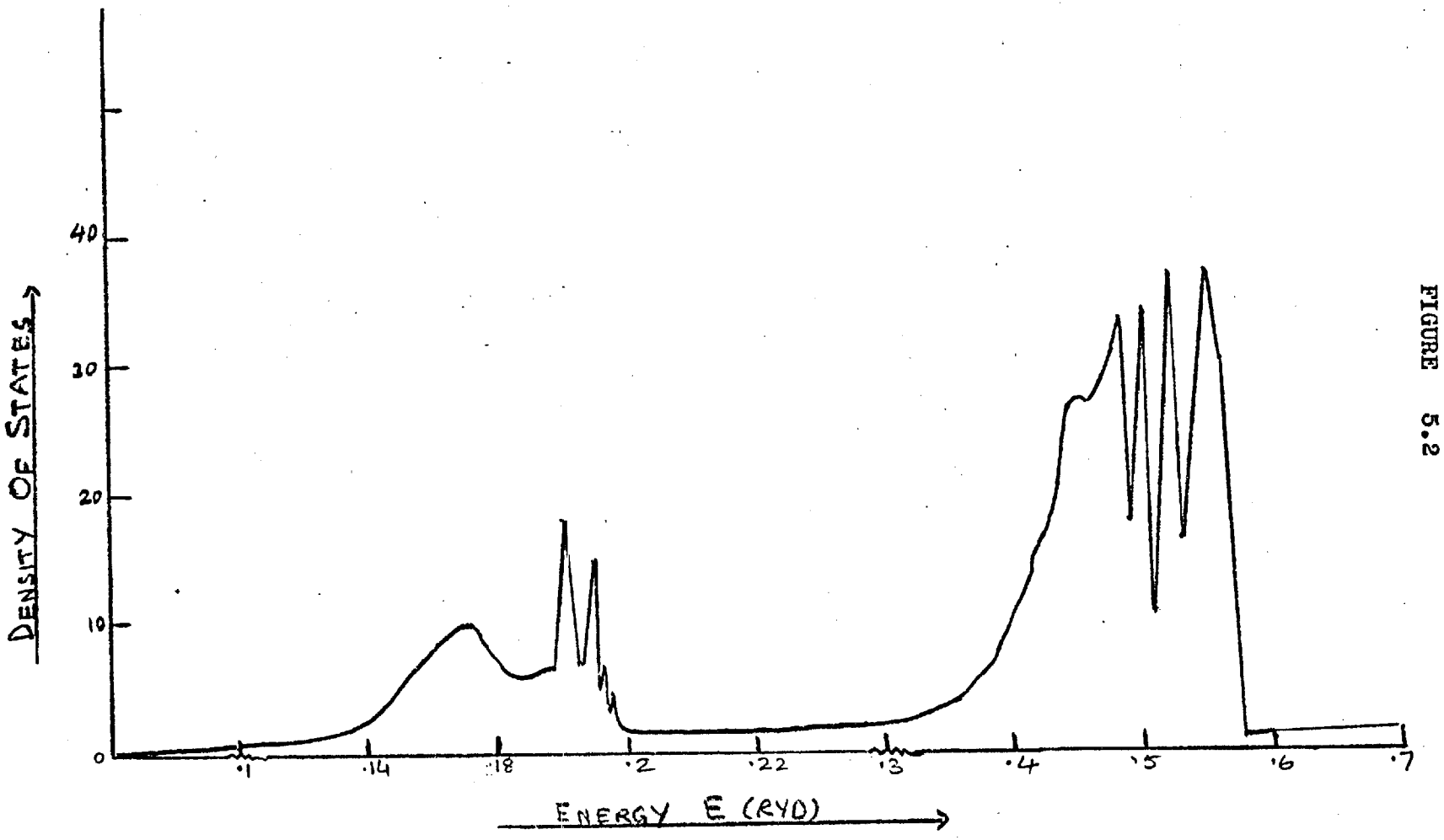

FIGURE 5.2

Plot of the density of states of transition metal alloy. The energy scale between .1 and .3 ryd is extended to see the details of the structure in the minority band.

FIGURE 5.3

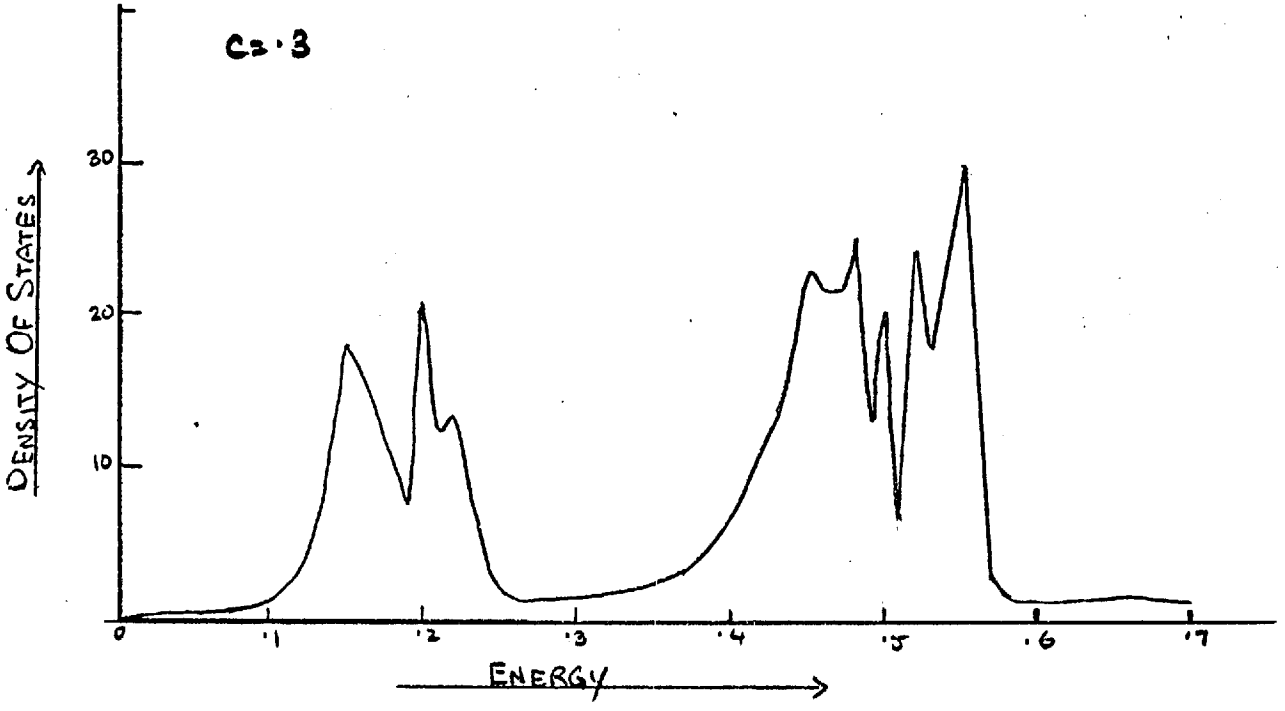

Plot of the density of states of transition metal alloy.

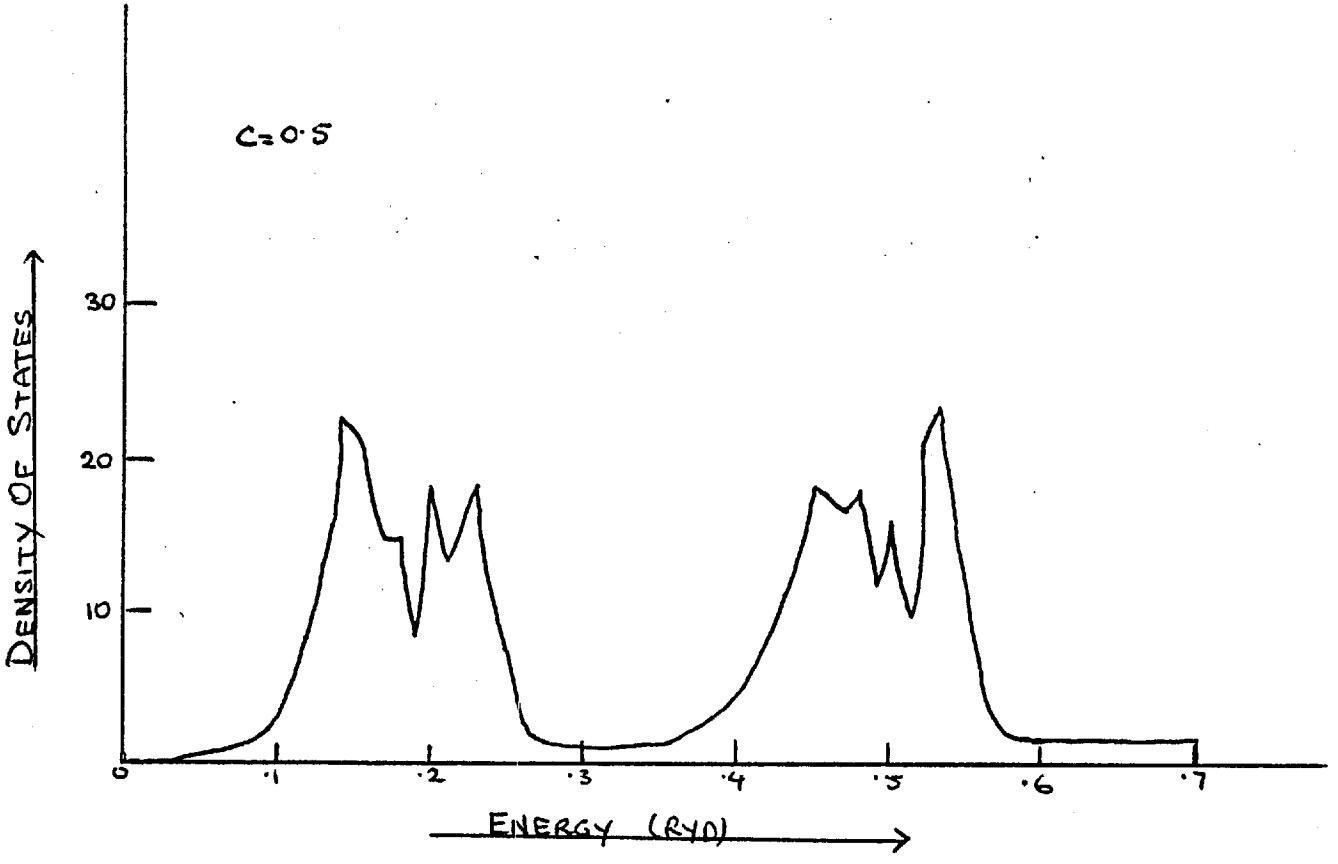

FIGURE 5.4

Density of states of 50-50 transition metal alloy in cluster theory.

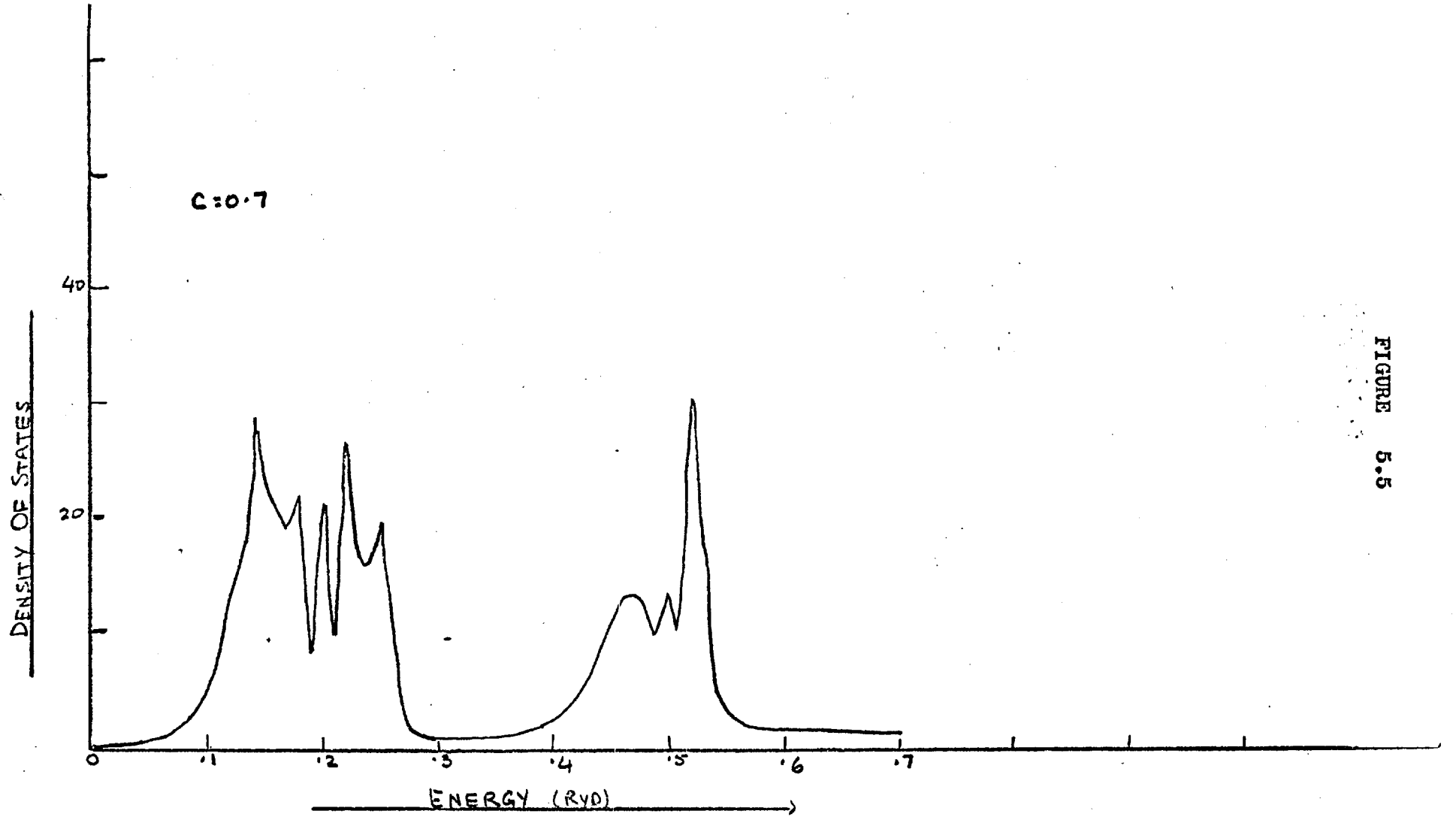

FIGURE 5.5

Plot of the density of states of transition metal alloy. Minority band is around E_d=.5ryd.

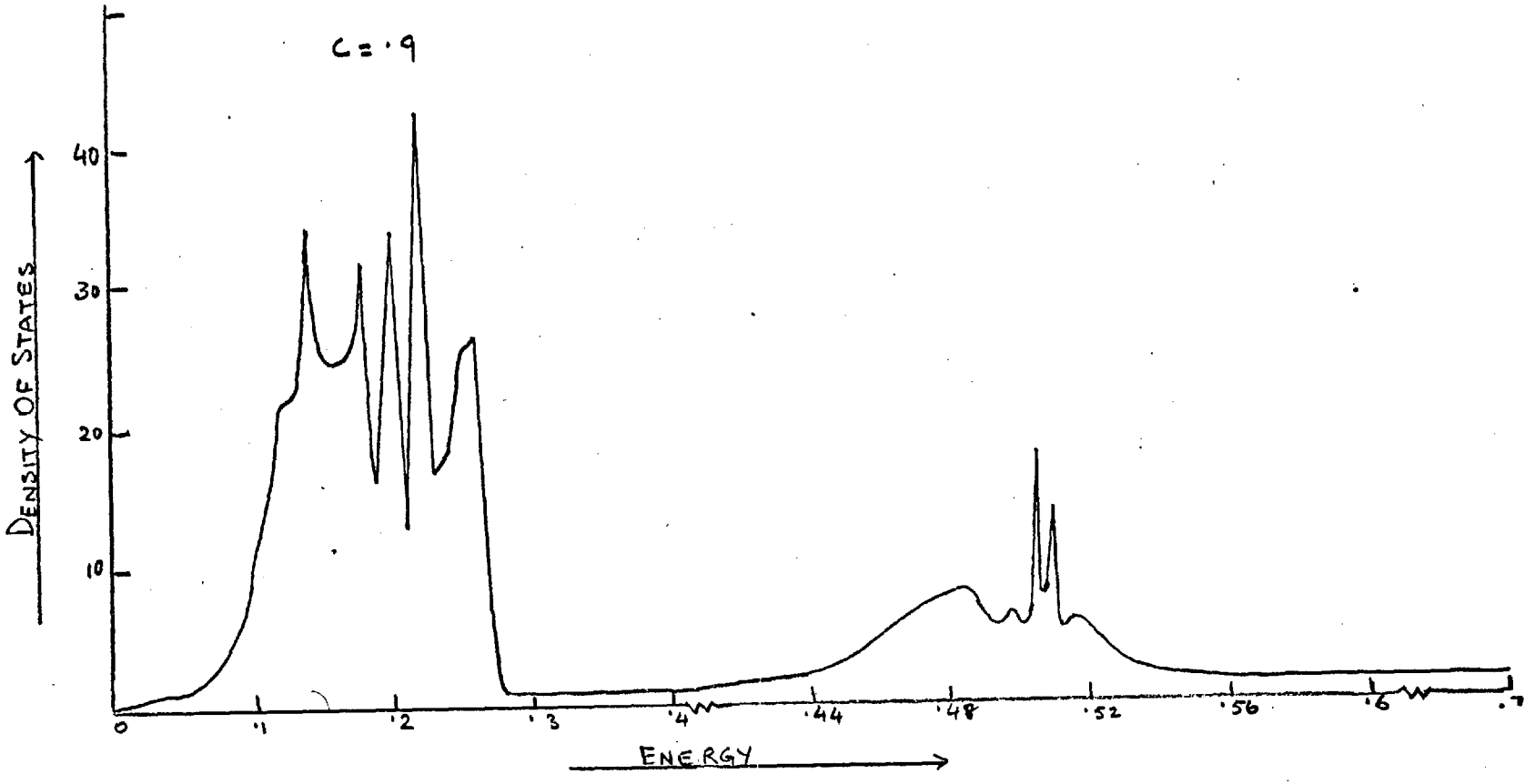

FIGURE 5.6

Plot of the density of states of transition metal alloy. The energy scale between .4 and .6 ryds. is extended to show the details of the structure in the minority band

CHAPTER 6

APPLICATIONS

6,1 INTRODUCTION

The purpose of this chapter is two fold. The first is to apply the model calculations of the previous chapters to more realistic alloys and the second is to demonstrate the flexibility of the continued fraction technique by dealing with a very disordered material viz. dilute disordered Heisenberg ferromagnet. The density of states of metals and their alloys can be used to explain many of their physical properties. The electronic specific heat coefficient at low temperature is one of them and is related to density of states at Fermi-energy. The calculations of the density of states for transition metal alloys in a single site approximation(chapter 3) and in a cluster theory(chapter 4) are used to calculate the low temperature specific heat coefficient γ for Ni-Pt alloys as a fundtion of concentration of nickel. The results obtained in a single site approximation after taking into account the phonon enhancement factor are in close agreement with the experimental results until the critical concentration. Experimentally at the critical concentration real Ni becomes ferromagnetic and the electronic specific heat coefficient for the ferromagnetic alloys decreases rapidly(Beille et al 1974). We have, however, carried out the calculations for the model paramagnetic alloys in this concentration regime and γ is found in these calculations to be approximately constant. The result obtained for γ in cluster theory, when we do not take into account the

hybridization of the d bands with the s band, are not in such good agreement with the experiment. This is due to two reasons as explained later in the chapter.

In the second half of this chapter we will discuss the usefulness of the continued fraction technique and its merits in simplifying complicated problems. As an illustration to the above points we will apply the continued fraction method to a completely disordered Heisenberg ferromagnet. The result we get for the density of states are compared with those obtained by Harris et al(1974) and Tahir Kheli(1972,1975). We shall now outline the remainder of this chapter. In the next section we will give a brief review of the experimental results and theoretical calculations of the low temperature specific heat coefficient γ for Ni-Pt alloys. In section 6.3 we will present our calculations of γ for Ni-Pt alloys in a single site theory and in section 6.4 we will discuss the results obtained by the above method. In section 6.5 we will use the cluster theory to calculate γ and will discuss the results obtained. In section 6.6 we shall briefly outline the theory of Heisenberg ferromagnet. Section 6.7 will be devoted to setting up the Model Hamiltonian for the disordered dilute Heisenberg ferromagnet and finding an expression for the density of states which can be easily used for the numerical calculations. In the last section of this chapter we will discuss the results of 6.7.

6.2 EXPERIMENTAL RESULTS AND REVIEW OF THE THEORY FOR ELECTRONIC SPECIFIC HEAT COEFFICIENT FOR Ni-Pt ALLOYS.

There have been many studies, both experimental and theoretical

of the disordered Ni-Pt alloys. These alloys display a high value of specific heat at certain critical concentration. The low temperature specific heat is given by the following equation

$$C = \gamma T + \beta T^3 + \ldots \qquad (6.1)$$

where T is the absolute temperature and γ and β are the low temperature specific heat coefficients(terms involving higher powers of T are neglected because they are small). Beille et al (1974) experimently measured the low temperature specific heat coefficient γ of Ni-Pt alloys as a function of Ni concentration. Their results are presented by solid circles on figures 6.2 and 6.3. The fall in γ when $c > .42$ is due to ferromagnetic splitting between the up and down spin bands. Infact pure Ni is a strong ferromagnetic and has a very small up spin density of states $n_\uparrow(E_F)$ and the electronic specific heat coefficient of value $7.1\ mJ/mole\,k^2$ is mainly associated with the down spin density of states $n_\downarrow(E_F)$.

Both nickel and platinum have a face-centred cubic structure and this face-centred cubic structure is retained in their alloys. This property of these alloys make the theoretical study of them much easier. Alben and Wohlfarth (1974) have calculated the low temperature specific heat coefficient for a ferromagnetic Ni-Pt alloy using the coherent potential approximation. They found that even after taking into account the phonon enhancement factor(Andersen 1970), the gradient of their curve was much smaller than that of the experimental curve (Beille et al 1974). Alben et al ascribed this discrepancy to two causes. The first is that the density of states they used for pure Pt is only roughly derived from the density of states of Ni(which is in

itself approximate, Hasegawa 1972). The second is that the lattice constant and hence the hopping matrix elements between Ni and Pt sites in an alloy are assumed independent of concentration, while according to Heine(1967), the hopping matrix elements should depend on the lattice constant, which is of course not constant. In the next three sections the density of states of Ni-Pt alloy is calculated using a more appropriate density of states for pure Pt and making all the parameters concentration dependent. The low temperature specific heat coefficient γ is obtained from the density of states by the relation(one electron theory):

$$\gamma = \frac{1}{3}\pi^2 k_B^2 N(E_F) \qquad (6.2)$$

where k_B is Boltzmans constant ($\frac{1}{3}\pi^2 k_B^2 = .35\,(m\,J)^2 k^{-2}$) and $N(E_F)$ is the density of states at the Fermi energy. The results so obtained are then compared with the experimental results and those of the CPA (Alben and Wolfarth 1974).

6.3 THE SINGLE SITE THEORY

The method used in this section is the same as that in chapter 3, but with the following difference. The calculations in chapter 3 are only model calculations so most of the parameters are concentration independent, but here we are doing more realistic calculations so we must take account of the proper concentration dependence of the various parameters.

We have from equation (3.26)

$$n(E) = n_0(E) - \frac{I_m}{\pi} \mathrm{Tr}\left\{ c D_N \left[\frac{c D_N}{K^N_{2m2m'}} + \frac{(1-c) D_P}{K^P_{2m2m'}} + (1-c) t^{-1}_{2N} - (1-c) t^{-1}_{2P} \right]^{-1} + (1-c) D_P \left[\frac{(1-c) D_P}{K^P_{2m2m'}} + \frac{c D_N}{K^N_{2m2m'}} + c t^{-1}_{2P} - c t^{-1}_{2N} \right]^{-1} \right\} \quad (6.3)$$

where the suffix N stands for Ni and P for Pt, c is the concentration of Ni atoms, $n_0(E)$ is the free electron density of states, t^{-1}_{2N} and t^{-1}_{2P} depend on the phase shifts on Ni and Pt sites respectively, D_N and D_P depend on t^{-1}_{2N} and t^{-1}_{2P}, and the equations defining these quantities precisely will be given later in this section.

The imaginary parts of $K^N_{2m2m'}$ and $K^P_{2m2m'}$ are related to the density of states of pure Ni and pure Pt respectively(as explained and shown in section 3.3(ii)). The densities of states of pure Ni and Pt are calculated as follows.

The model Hamiltonian(Hubbard 1967, Heine 1967, Jacobs 1968, Pettifor 1969) derived from Korringa(1947) Kohn and Rostoker(1954) method is used to calculate the E and T components of the density of states of a transition metal (as already described in section 3.3(ii)) Assuming that the basic structure of the density of states for all transition metals is the same, we have adjusted the above density of states so that it gives a pure Ni bandwidth of 0.3 rydbergs and a pure Pt bandwidth of 0.6 rydbergs. The Fermi level is selected so that there are 6 d holes in the Ni band and 3 d holes in the Pt band(Alben et al 1974) and the band structures are shifted so that the Fermi levels coincide. Figure 6.1 shows the densities of states of Ni and Pt calculated by this method.

To calculate the real parts of $K^N_{2m2m'}$ and $K^P_{2m2m'}$ we take the Hilbert transform of the imaginary parts of $K^N_{2m2m'}$ and $K^P_{2m2m'}$

in the same way as given in chapter 3.

If a_N and a_P are the lattice constants of Ni and Pt, then the lattice constant for the alloy is given by

$$a(c) = c a_N + (1-c) a_P \tag{6.4}$$

If w_N and w_P are the half bandwidths of pure Ni and Pt, then the half bandwidths of Ni and Pt in the alloy are given by the following formulae(Heine 1967)

$$\left.\begin{aligned} w_N(c) &= w_N \left(a_N/a(c)\right)^5 \\ w_P(c) &= w_P \left(a_P/a(c)\right)^5 \end{aligned}\right] \tag{6.5}$$

The centres of Ni and Pt d bands also vary with the concentration to keep the number of d holes constant. If E_F is the Fermi energy then the varition of the centres of Ni and Pt d bands in an alloy are given by the following equations

$$E_d^N = E_F - w_N(c)\,(1 - F_N) \tag{6.6}$$

$$E_d^P = E_F - w_P(c)\,(1 - F_P) \tag{6.7}$$

where F_N and F_P are factors selected so as to give the correct number of d holes in Ni and Pt bands.

We now return to the quantities which depend on the phase shifts and we shall see that these are also concentration dependent.

$$t_{2N}^{-1} = K \cot \eta_{2N} - iK$$
$$t_{2P}^{-1} = K \cot \eta_{2P} - iK \qquad (6.8)$$

where (Pettifor 1969)

$$\cot \eta_{2N} = (E_d^N - E)/K C_N j_2^2(Kr_c)$$
$$\cot \eta_{2P} = (E_d^P - E)/K C_P j_2^2(Kr_c) \qquad (6.9)$$

and

$$C_N = \tfrac{1}{2} W_{Ni} / K_d^N j_2^2(K_d^N r_c)$$
$$C_P = \tfrac{1}{2} W_{Pt} / K_d^P j_2^2(K_d^P r_c) \qquad (6.10)$$

$$K_d^N = \sqrt{E_d^N}$$
$$K_d^P = \sqrt{E_d^P}$$
$$K = \sqrt{E} \qquad (6.11)$$

$$r_c = c r_N + (1-c) r_P$$
$$r_N = a_N/2\sqrt{2}$$
$$r_P = a_P/2\sqrt{2} \qquad (6.12)$$

$$ra_N = .39\, a_N$$
$$ra_P = .39\, a_P \qquad (6.13)$$

(r_N and r_P are the radii of inscribed sheres of Wigner Seitz cell and ra_N and ra_P are the radii of the spheres, having the same volume as the unit cell)

j_2 is the spherical Bessel function. W_{Ni} and W_{Pt} are the nickel and platinum d resonance band widths (Hubbard 1969).

The function D_N and D_P which occur in equation (6.3) are given by

$$D_N = \frac{d}{dE} t_{2N}^{-1} - 2\beta t_{2N}^{-1} - t_{2N}^{-1} \alpha t_{2N}^{-1}$$

$$D_P = \frac{d}{dE} t_{2P}^{-1} - 2\beta t_{2P}^{-1} - t_{2P}^{-1} \alpha t_{2P}^{-1} \qquad (6.14)$$

where the α and β are defined in equations (3.21) and (3.22), we redefine them here for this particular case as:

$$\left.\begin{aligned} \alpha &= \tfrac{1}{2}(ra_c)^3 \left[j_2^2(kra_c) - j_1(kra_c) j_3(kra_c) \right] \\ \beta &= \tfrac{1}{2} k^2 (ra_c)^3 \left[j_1(kra_c) n_1(kra_c) - 3 j_2(kra_c) n_1(kra_c)/kra_c \right. \\ &\quad \left. + n_2(kra_c) j_2(kra_c) - 2 j_1(kra_c) n_1(kra_c)/kra_c \right] - ika \end{aligned}\right\} \qquad (6.15)$$

where

$$ra_c = c\, ra_N + (1-c)\, ra_P \qquad (6.16)$$

The derivative of t matrix with respect to E are given by the equations

$$\frac{d}{dE} t_{2N}^{-1} = \frac{-1}{C_N j_2^2(kr_c)} - \frac{j_1(kr_c)}{j_2(kr_c)} \frac{r_c}{k} t_{2N}^{-1} + 3 t_{2N}^{-1}/E - i/2k \qquad (6.17)$$

$$\frac{d}{dE} t_{2P}^{-1} = \frac{-1}{C_P j_2^2(kr_c)} - \frac{j_1(kr_c)}{j_2(kr_c)} \frac{r_c}{k} t_{2P}^{-1} + 3 t_{2P}^{-1}/E - i/2k \qquad (6.18)$$

We now know all the quantities occurring in equation (6,3) and their dependence on concentration. Therefore we can use equation(6.3) for numerical computation of the density of states and hence the low temperature specific heat coefficient (equation(6.2)) as a function of nickel concentration c. The values of the parameters used in the calculation are given in Table 6.1. The whole proceedure of calculating γ over the entire concentration range took less than 16 seconds of computer time on CDC 7314.

6.4 DISCUSSION OF RESULTS FOR γ

The computed values of γ in the single site theory are given in figure 6.2. For pure Pt we find that the value of γ is about 4.6mJ/degree^{2}mole, while experimental value is 7.3mJ/degree^{2}mole (Beille et al 1974). This is reasonable in view of the estimate of 1.6 for the phonon enhancement factor computed by Andersen(1970). If we multiply the computed values of γ by 1.6 for all concentrations we see that the theoretical curve coincides with the experimental curve very well upto the critical concentration(which is 42 atomic% of Ni) i.e the concentration after which Ni becomes ferromagnetic. Experimentally after this concentration the value of γ sharply decreases because the material becomes ferromagnetic and the $\uparrow$ spin and the $\downarrow$ spin bands split leaving a lower density of states at the Fermi-level. In the calculations we have assumed that Ni remains paramagnetic throughout the range of the concentration. Therefore we obtain a continuous increase of electronic specific heat coefficient from the value for non-magnetic Pt to the value for paramagnetic Ni.

The origin of our computed values of γ can be understood as follows:

The lattice constant of pure Pt is large and consequently when Ni is added the Ni-Ni hopping integrals are much smaller than they would be in pure Ni. That is when a small amount of Ni is added to a Pt matrix the Ni contribution to the density of states is much larger than it would be if the Ni-Ni hopping integrals had retained the value they have in pure Ni. This explains partly the fact that our single site curve has a larger initial slope than the curve obtained by Alben and Wohlfarth(1974) in CPA, where no such effects were considered. Finally near the pure Ni edge the curve for γ vs c is rather flat. This is due to the fact that the peak near the Fermi-level in pure Ni maintains its height in the alloys with low concentration of Pt. A possible explanation for this is that there are two competing effects. The first is due to the fact that the Pt-Pt hopping integral is large ($w_p \sim 0.9$ryd) in nearly pure Ni. Thus one effect of adding Pt to Ni is dilution and in the fashion of CPA this leads to a dependence of density of states on concentration proportional to $\sqrt{(1-c)}$ (c being the concentration of Pt). The second effect is due to the change in the Ni-Ni hopping integrals and the concentration dependence of this is given by Heine's R^{-5} law i.e

$$w_{N-N}(c) = w_{N-N}(0)\left[a_N/a_P\right]^5 = w_{N-N}(0)\left[\frac{1}{1+.1c}\right]^5$$

The magnitude of the density of states scales as the inverse of the bandwidth and therefore in the alloy has an additional factor $(1+0.1c)^5$. The product of this factor and the dilution factor is, to first order in c, unity. This gives a density of states and hence γ which is flat in the Ni rich region. This provides a crude explanation of the flat and steep regions of the calculated curve.

Any residual difference between our results and those of CPA must be due to differences in the alloy theory used. In particular they can be

attributed to the fact that our single site theory gives a density of states with more structure and higher peaks than the CPA.

6.5 CLUSTER THEORY

In this section we calculate the specific heat coefficient for Ni-Pt alloys following the method of chapter 4. In chapter 4 we considered the alloying behaviour of the tight binding d band densities of states of transition metals in cluster approximation. The cluster theory which we are considering here treats a cluster consisting of the central atom and the nearest neighbours exactly and the surrounding medium in an average approximation.

The method of this chapter differs slightly from that of chapter 4. As we are now doing more realistic calculations we redefine some of the quantities to take account of the hopping integrals which depend on the atoms at each end of the hop (or different bandwidths of the components or off-diagonal disorder).

We startwith equation(4.24) i.e

$$n(E) = I_m \mathrm{Tr} \frac{1}{\pi} \langle 0|G|0\rangle_{m'} \qquad (6.19)$$

where the average Green function is given by

$$\langle 0|G|0\rangle_{m'} = \sum_{x=0}^{1} \sum_{n=1}^{66} c^{13-x-y} (1-c)^{x+y} M_n G^{x,n}_{mm'} \qquad (6.20)$$

The quantities occurring in this equation are the same as defined in chapter 4 with Ni atoms taking the place of A atoms and Pt atoms that of B atoms, except $G^{x,n}_{mm'}$ which is now defined by

$$G^{x,n}_{mm'} = \left[(E_x - E)\delta_{mm'} - \frac{W_x}{W_{cu}} Gl_{mm'} \right]^{-1} \qquad (6.21)$$

where

$$E_x = x E_d^N + (1-x) E_d^P \qquad (6.22)$$

$$W_x = x W_N(c) + (1-x) W_p(c) \qquad (6.23)$$

$$Gl_{mm'} = \frac{W_N(c)}{W_{cu}} \sum_{\substack{i=nn N \\ m''m_1}} A^{oi}_{mm''} G^N_{m''m_1} A^{io}_{m_1 m'} + \frac{W_p(c)}{W_{cu}} \sum_{\substack{i=nn P \\ m''m_1}} A^{oi}_{mm''} G^P_{m''m_1} A^{io}_{m_1 m'} \qquad (6.24)$$

The parameters E_d^N and E_d^P are the centres of the Ni and Pt sub-bands in an alloy (given by equations (6.6) and (6.7)), $W_N(c)$ and $W_p(c)$ are half bandwidths of Ni and Pt in an alloy (defined by equation (6.5)), and

$$G^N_{m''m_1} = \left[\left\{ \frac{W_N(c)}{W_{cu}} A3_{m''m_1} + E_d^N - E - \frac{W_N(c)}{W_{cu}} A4_{m''m_1} \bar{F}_{m_1 m_1} A4_{m_1 m''} \right\} \delta_{m''m_1} \right]^{-1} \qquad (6.25)$$

$$G^P_{m''m_1} = \left[\left\{ \frac{W_p(c)}{W_{cu}} A3_{m''m_1} + E_d^P - E - \frac{W_p(c)}{W_{cu}} A4_{m''m_1} \bar{F}_{m_1 m_1} A4_{m_1 m''} \right\} \delta_{m''m_1} \right]^{-1} \qquad (6.26)$$

The hopping integrals $A^{ii'}_{mm'}$ (depending on ddσ, ddπ and ddδ) are taken from a calculation for copper (Jacobs 1968). To normalize these quantities to the correct hopping integrals for the Ni-Pt alloys it is necessary to divide them by the copper half bandwidth W_{cu} , and multiply them by $W_N(c)$, $W_p(c)$ or W_x as appropriate.

The quantities $A3''_{m m_1}$ and $A4''_{m m_1}$ are the same as those given in equations (4.15)and (4.16), but $\bar{F}_{m,m_1}$ is now defined as:

$$\bar{F} = c\,FD(L,Z_N) + (1-c)\,FD(L,Z_P) \qquad (6.27)$$

where

$$Z_N = (E_d^N - E)\; w_{cu} \;/w_N(c) \qquad (6.28)$$

$$Z_P = (E_d^P - E)\; w_{cu} \;/w_P(c) \qquad (6.29)$$

and c is the concentration of Ni atoms. The factor L and the functions $FD(L,Z_N)$ and $FD(L,Z_P)$ are explicitly defined in chapter 4, and they are used here without any modification. Equation (6.24) is simplified and evaluated in the same way as discussed in chapter 4. Thus we can calculate the density of states of Ni-Pt alloys and hence γ in this tight binding cluster theory. The results of the above calculations are given in figure 6.3.

The dotted line curve is the experimental (Beille 1974). The full line curve is the plot of γ as a function of nickel concentration when we consider only the d band density of states for pure Ni and Pt i.e we exclude the sp band and its hybridizing effects on the d bands. We have assumed here also that Ni remains paramagnetic throughout the concentration range. This curve is steeper than the experimental curve. The value of γ sharply rises from 7.3mJ/K^2-mole at c=0 to 22mJ/K^2-mole at c=0.6 and then it comes down slightly to 21mJ/K^2-mole at c=1. The difference between the single site and cluster theory behaviour of γ is due to two reasons. The first is that we have used very

sharply peaked densities of states for pure Ni and pure Pt(that are given by Haydock method ,1975). The second is that we have neglected the conduction band and its hybridization effects on the d bands. The first reason is probably the more important because states at the top of the band are less hybridized.

Thus we have been able to demonstrate the practical utility of our theories by applying it to a discussion of Υ for Ni-Pt alloys.

6.6 REVIEW OF THE THEORY FOR THE DISORDERED HEISENBERG FERROMAGNET

Tahir Kheli(1972) was the first to devote attention to the calculation of the magnon spectrum of a randomly diluted Heisenberg ferromagnet. This system is described by a Hamiltonian given by:

$$\mathcal{H} = -2J \sum_{rr'} p_r p_{r'} \underset{\sim}{S}_r \cdot \underset{\sim}{S}_{r'} \qquad (6.30)$$

where p_γ is a random variable assuming the values 1 or 0 depending whether the site at r is or is not occupied by a magnetic ion. The sum over r and r' is taken only over nearest neighbours on a simple cubic lattice.Tahir Kheli's approach was an effective medium approach. He applied the truncated Kohn-neighbourhood (where the dynamics of a sufficiently random many body systems may be approximated by that of a typical small neighbourhood consisting of, say, only two sites). His results show a density of states which peaks towards the lower energies. The height of the peak and its shift towards the lower energy increases with the decrease of the concentration of the magnetic

ions. He was able to get three frequency moments exactly.

Harris et al (1974) used the coherent potential approximation (CPA) in several different forms to treat this problem. Their results for the line shapes or the spectral weight functions are in good agreement with the 'exact' results(Harris 1974 , Nickel 1974). The density of states curve is, however, rather smooth and has none of the structure that we would expect. (There must be,for example,' δ' funations in the spectrum of finite weight arising from the free rotation of magnetic moments on 'isolated' magnetic ions).

Nickel(1974)has done the 'exact' calculations in an eight atom cluster theory. He used the moment expansion method. His results consist of curves for the line shapes for various concentrations of the magnetic ions. He obtained the "dangling bond effect in the line shape response. He also predicted, on general physical grounds, a multispiked structure in the density of states, that appears to be characteristic of all strongly disordered binary systems(Dean 1960, Cubiotti et al 1975). Theumann and Tahir Kheli (1975) have presented another treatment of the problem. Their result shows some improvements on the results of Harris et al (1974). It gives a density of states which is non-zero only at positive frequency and is more peaked at lower frequencies. All the above calculations were done for simple cubic materials.

In this chapter we have adapted the cluster theory for the disordered alloys(Jacobs 1974, Cubiotti et al 1975) as developed from the continued fraction method (Haydock et al 1972) to treat the dilute Heisenberg ferromagnet. We treat the central atom and the six

atoms in the nearest neighbour shell exactly; the atoms in the second and the third neighbour shells are treated less exactly and beyond that we make an average approximation. The result show much structure in the density of states and this structure increases as the concentration of magnetic ions decreases. The structure contains broadened delta functions at energies slightly shifted from integral values. There are also unbroadened delta functions at integral values of the energy. The broadened delta functions are due to partially isolated magnetic atom clusters and the unbroadened delta functions are due to completely isolated magnetic atoms. In general the results display many aspects of the dilute Heisenberg ferromagnet that cannot be adequately treated in an effective medium theory.

6.7 THE GREEN FUNCTION

Harris et al (1974) have shown that the Hamiltonian given by equation (6.30) may be written in terms of boson variables (equation 2.4 of their paper) in the form

$$h = H/2JS = \sum_{rr'} (a_r^+ - a_{r'})(a_r - a_{r'}) - \sum_{r\delta} q_r (a_r^+ - a_{r+\delta}^+)(a_r - a_{r+\delta}) \qquad (6.31)$$

where δ denotes the nearest neighbour distance and

$$q_r = 1 - p_r \qquad (6.32)$$

In this form the Hamiltonian implies that a localized excitation can only hop between nearest neighbour sites which are both occupied by magnetic ions or both are occupied by non-magnetic ions, but it cannot hop if one of them is occupied by a magnetic and other by a

non-magnetic ion. Hopping between two non-magnetic sites results in spurious excitations and these must be sub-tracted to get the true magnetic response.

We shall apply the continued fraction method developed by Jacobs(1974) to the Hamiltonian given by equation(6.30). This method expresses the diagonal matrix element of the Green function for a given configuration of magnetic ions in a continued fraction approximation. The average density of states is then obtained by multiplying the average Green function for a given configuration by the probability of occurrence of that configuration and summing the result over all configurations.

Assuming that the central site is occupied by a magnetic ion, the diagonal element of the Green function $\langle 0|G|0\rangle$ (where $|r\rangle$ is the Wannier function for site r, r=0 referring to central site) for a particular configuration is given by

$$\langle 0|G|0\rangle = \left[E - Z - \sum_{i=1}^{Z} G_i\right]^{-1} \qquad (6.33)$$

where Z is the number of magnetic ions in the nearest neighbour shell (for a simple cubic $6 \geq Z \geq 0$), i refers to the number of magnetic sites in the nearest neighbour shell and

$$G_i = t^2\left[E - x_i - (x_i - 1)\,\bar{F}(E)\right]^{-1} \qquad (6.34)$$

where t is the hopping matrix between the neighbouring sites: t is equal to one when the two nearest neighbouring sites are occupied

by magnetic atoms and is zero when either of the two or both of them are vacancies i.e $t_{AA}=1$ and $t_{AV}= t_{VV}=0$, where A refers to a magnetic site and V to a vacancy(non-magnetic site). In this way we are able to project out the spurious vacancy-vacancy interactions, x_i is the number of magnetic atoms in the nearest neighbour shell of the ith site; and $\bar{F}(E)$ gives the termination of the continued fraction appropriate to the pure magnetic component i.e

$$\bar{F}(E) = \tilde{F}(E-E_A) \tag{6.35}$$

where

$$\tilde{F}(E) = 1\cdot 8\left[E - \frac{8S}{9} F(E)\right]^{-1} \tag{6.36}$$

$$F(E) = \frac{E \pm \sqrt{E^2-36t^2}}{18t^2} \tag{6.37}$$

$$E_A = 6. \tag{6.38}$$

$\tilde{F}(E)$ ensures that we get the correct density of states for the ordered material(Jacobs 1974). The sign in equation(6.37) is chosen to give the correct high energy limit to $F(E)$i.e

$$F(E) \rightarrow \frac{1}{E} \qquad \text{as} \quad E \rightarrow \pm\infty \tag{6.39}$$

Equation (6.34) involves the approximation of hopping from the nearest

$$W_D = c^6\left[1+(1-c)c^4\right]^6 \qquad (6.44)$$

a number which increases with the increase in the value of c.

The density of states of the magnetic ions is then given by

$$\rho_m(E) = \frac{1}{\pi} I_m \overline{\langle 0|g|0\rangle} \qquad (6.45)$$

The result so obtained are plotted in figures 6.4 and 6.5. Our technique is a real space technique and is not well adapted to the calculation of self energies and line shapes.

6.8 NUMERICAL RESULTS AND DISCUSSION

Figure 6.4 gives the density of states for a pure simple cubic material with E_A=6. This result is very close to the exact result and is the same as that given by figure 2 of Jacobs(1974).

Figure 6.5 gives the magnetic density of states at different concentrations of non-magnetic ions. It is clear from this figure that there is much structure in the density of states and this structure increases with the decrease in the concentration of magnetic atoms. This structure is mainly due to nearly isolated clusters which give slightly broadened delta functions in the spectrum. These should occur, according to equations (6.33)and (6.34) near integral values of energies from 0 to 6 except 1. We do indeed see these broadened out delta functions slightly shifted from integral values of E. Unbroadened delta functions occur at integral values of E and are due to completely isolated clusters. The peak at very low energy is the low energy resonance peak. This is called the 'dangling bond' effect(i.e a

small isolated cluster of magnetic atoms is conected to an infinite magnetic material by a single hopping integral). This peak shifts towards still lower energies and becomes more and more sharp with the decrease in the concentration of the magnetic atoms. The centre of gravity of the density of states and the cut off energy (after which the density of states is effectively zero) also shifts towards lower energy with the increase in c. It is also seen that at higher values of c the weight under the curve decreases. This lost weight has gone into the delta functions due to isolated magnetic atoms and is given by equation(6.44).The lowest five moments of the density of states are correct and it is reasonable to assume that many more are well approximated in this technique.

Thus we conclude that the cluster theory developed from the continued fraction technique can be reasonably applied to the calculation of the density of states of any kind of binary system, though it cannot easily be applied to some other aspects of such systems, such as the self energies or line shapes.

TABLE 6.1

PARAMETERS USED IN THE CALCULATION OF γ

$dd\sigma$	=	-0.0296 ryd
$dd\pi$	=	0.0147 ryd
$dd\delta$	=	-0.0024 ryd
RH	=	3.592 a_B
AH	=	.8826 ryd
E_d	=	.5 ryd
a	=	6.8088 a_B
a_N	=	6.632 a_B
a_P	=	7.338 a_B
w_N	=	.15 ryd
w_P	=	.3 ryd
w_{CU}	=	.15 ryd
E_F	=	.65 ryd
F_N	=	.46
F_P	=	.39
W_{Ni}	=	0.0465 ryd
W_{Pt}	=	.08 ryd

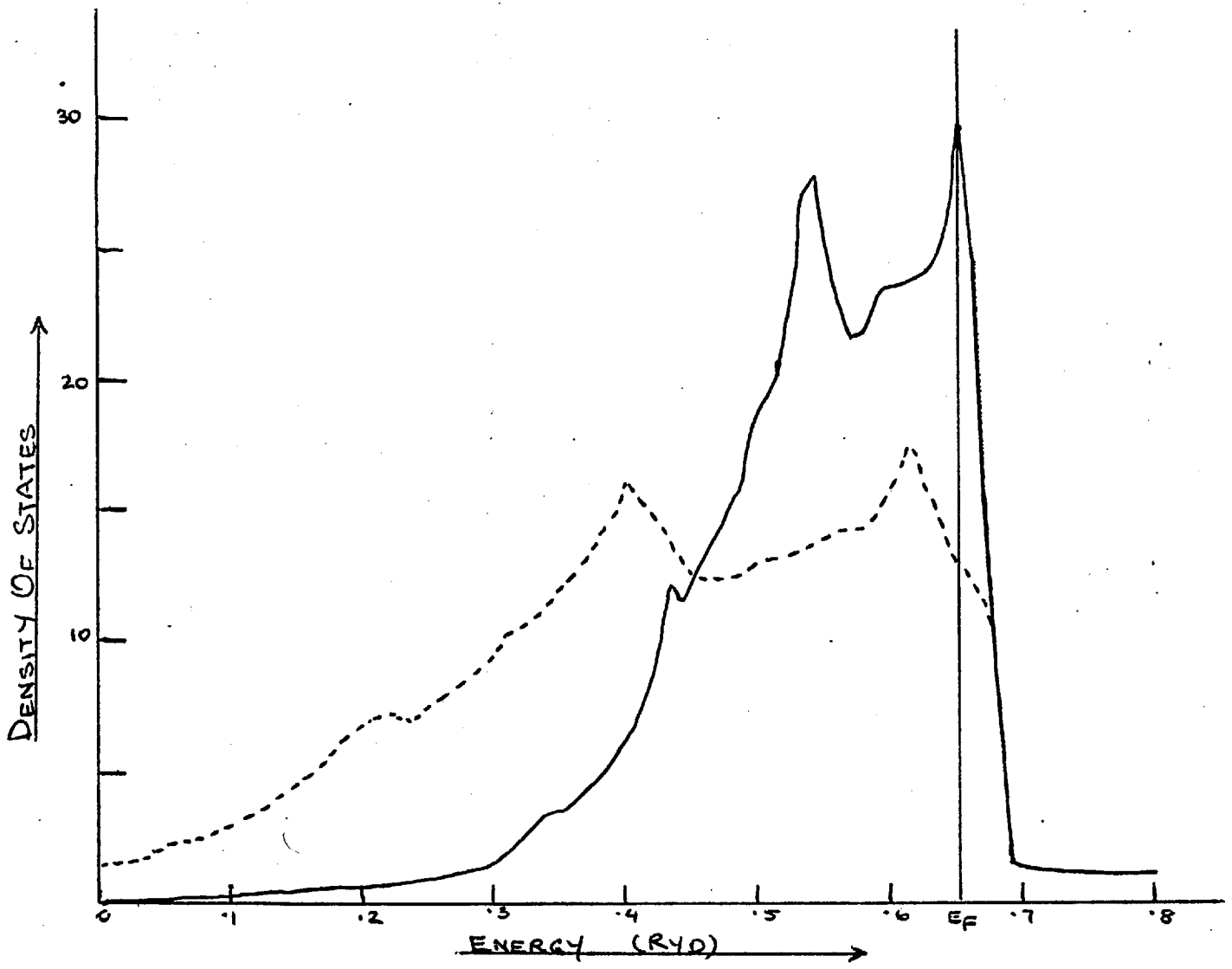

FIGURE 6.1

Plot of the densities of states of nickel(full line curve) and platinum (dotted line curve). E_F= .65

FIGURE 6.2

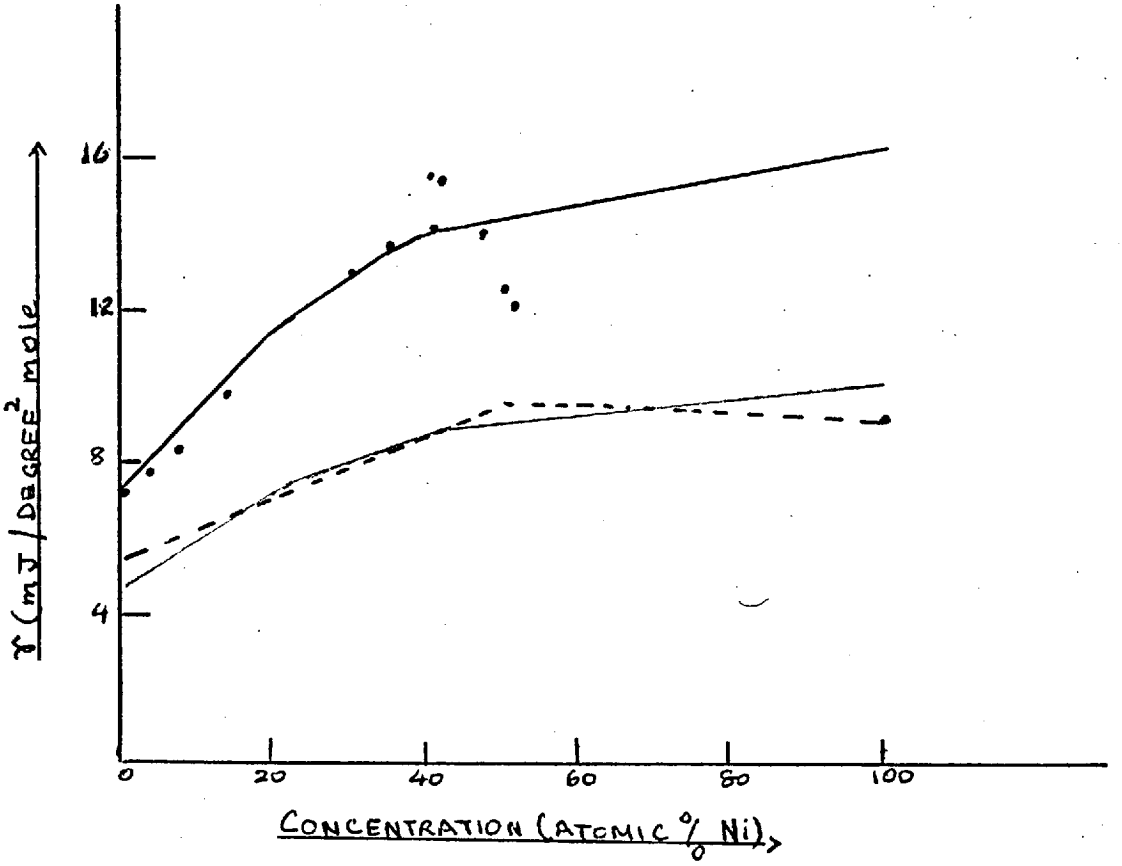

Specific heat coefficient γ for Ni-Pt alloys. Solid circles are the experimental points. Full line curves are of single site theory(dim one is without phonon enhancement factor and dark one is with phonon enhancement factor). Dashed line curve is curve b of Alben et al(1974).

FIGURE 6.3

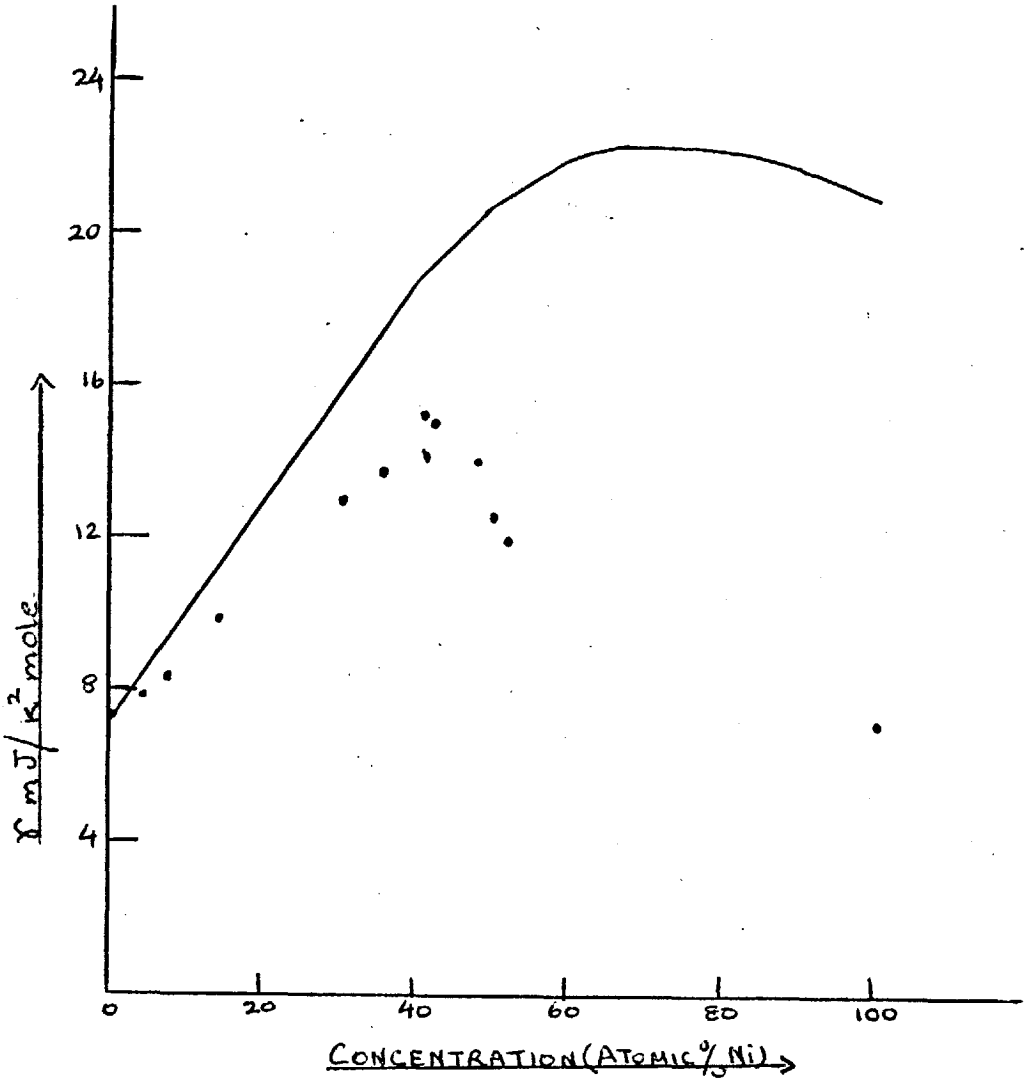

Specific heat coefficient for Ni-Pt alloys in cluster theory. The solid circles are the experimental points.

FIGURE 6.4

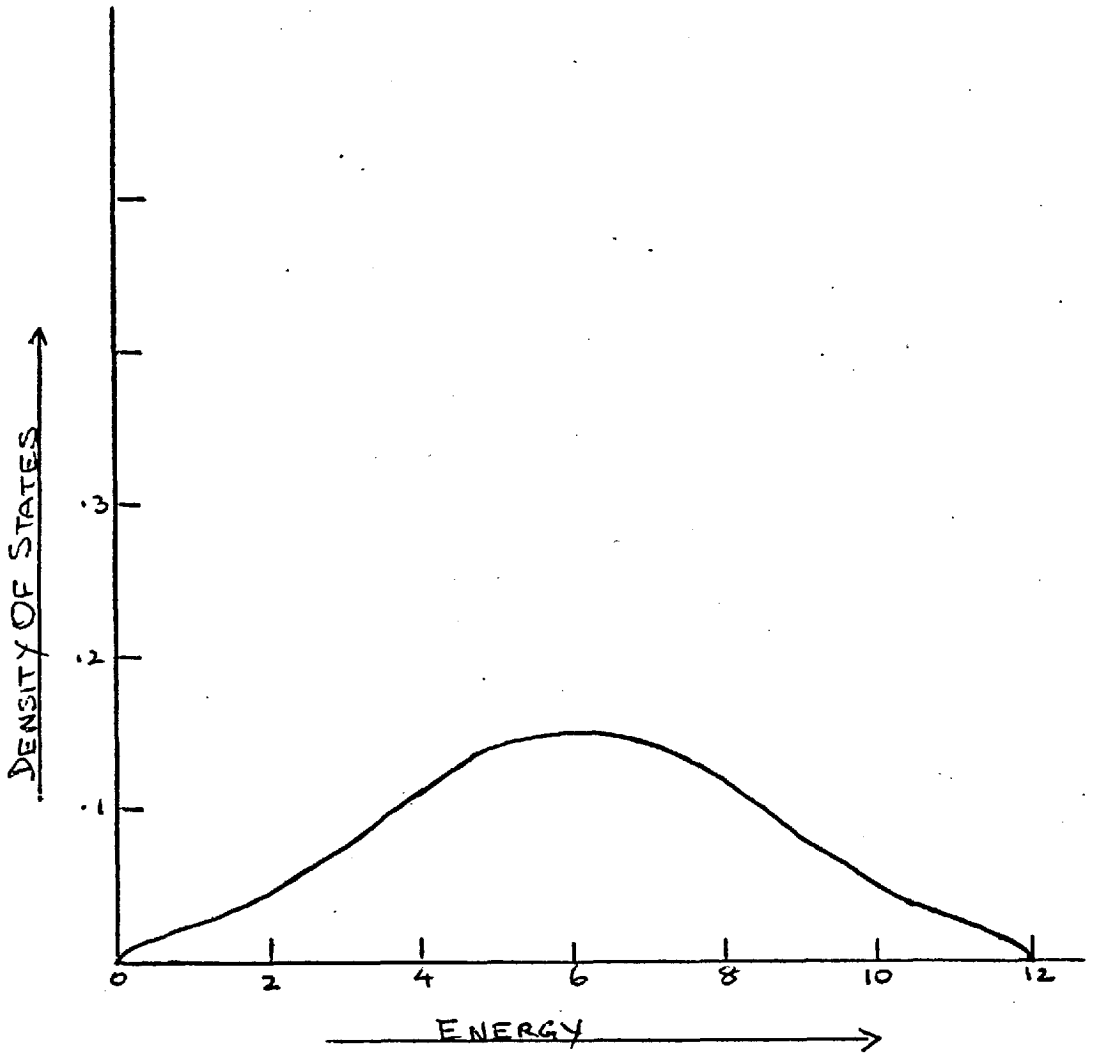

Density of states of ordered simple cubic material.

FIGURE 6.5

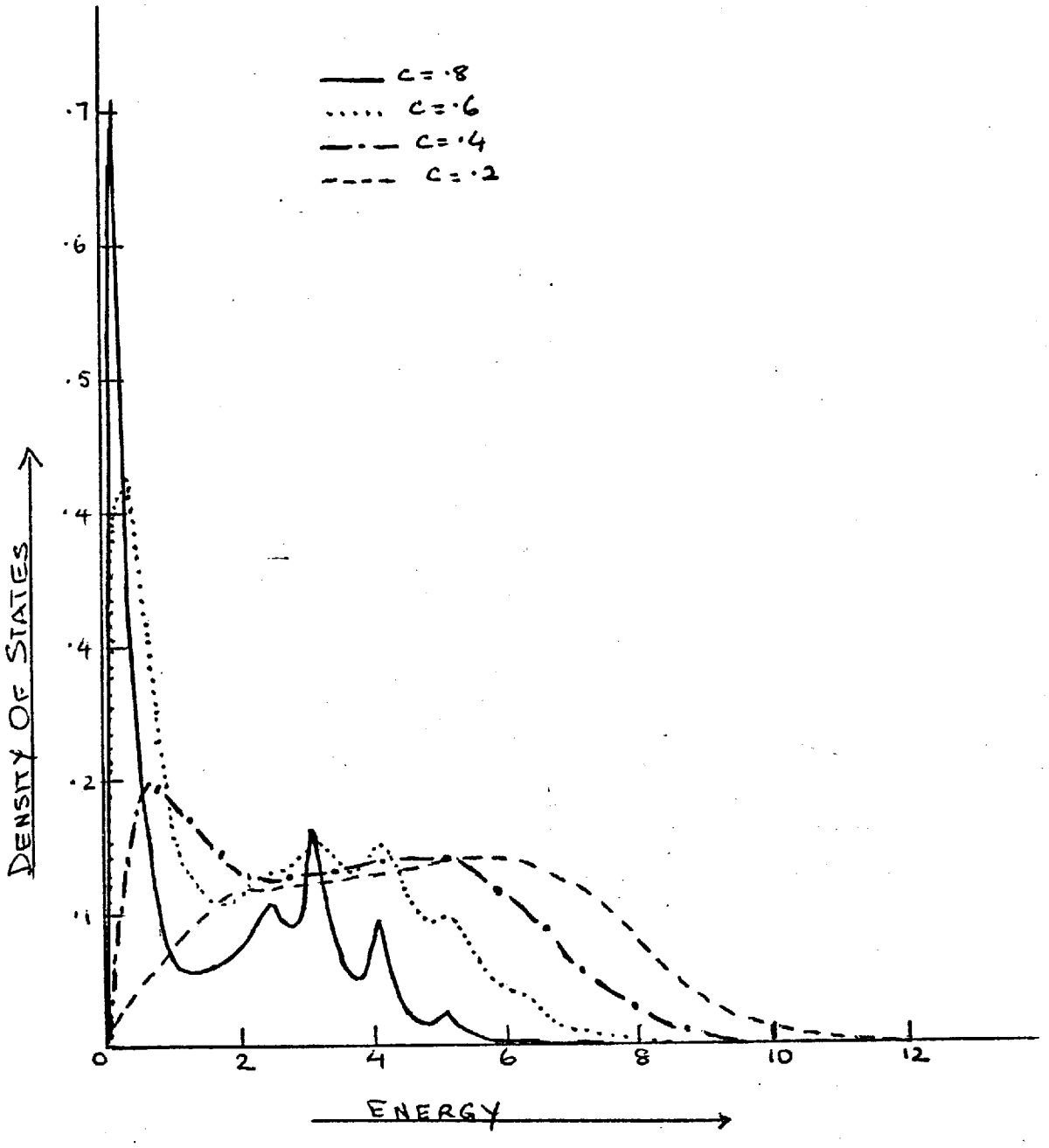

Density of states for various concentration c of non-magnetic ions.

APPENDIX A

In this appendix we will prove that the expression

$$-\frac{1}{\pi}\,\mathrm{Im}\,\mathrm{Tr}\left[\frac{d}{dE}t_\ell^{-1} - t_\ell^{-1}\alpha_\ell\, t_\ell^{-1} + 2\beta_\ell t_\ell^{-1}\right]\left[t_\ell^{-1} + G^+\right]^{-1}$$

of chapter 2 is equal to the free electron density of states $n_\ell(E)$ when $l=0$ and $l=1$.

For $l=0$ and $l=1$, the pseudopotential is weak and weakly energy dependent which means that t_o is small and weakly energy dependent, where t_o is given by

$$t_\ell^{-1} = t_o^{-1} - i\,k$$
$$t_o^{-1} = k\cot\eta_\ell$$

then

$$-\frac{1}{\pi}\,\mathrm{Im}\,\mathrm{Tr}\left[\left(\frac{d}{dE}t_\ell^{-1} - t_\ell^{-1}\alpha_\ell\, t_\ell^{-1} + 2\beta_\ell t_\ell^{-1}\right) t_\ell\,(1 + G^+ t_\ell)^{-1}\right]$$
$$= -\frac{1}{\pi}\,\mathrm{Im}\,\mathrm{Tr}\left[\left(\frac{d}{dE}t_\ell^{-1}\right)t_\ell - t_\ell^{-1}\alpha_\ell + 2\beta_\ell - \left(\frac{d}{dE}t_\ell^{-1}\right)t_\ell G^+ t_\ell - \alpha_\ell G^+ - 2\beta_\ell G^+ t_\ell + \cdots\right]$$

The first and fourth terms terms are equal to zero, partly because $t_o \to o$ and partly due to the weak energy dependence of t_ℓ .The last two terms are also equal to zero because G^+ has zero trace. Thus we are left with following two terms

$$-\frac{1}{\pi}\,\mathrm{Im}\,\mathrm{Tr}\left[-t_\ell^{-1}\alpha_\ell + 2\beta_\ell\right]$$

$$= \frac{1}{\pi}\,\mathrm{Tr}\left[\alpha_\ell K\right]$$

$$= \frac{1}{\pi}\left[\alpha_0 K + 3\alpha_1 K\right] = n_0(E)$$

APPENDIX B

This appendix lists several standard results which are used in this thesis. They are given without proof. Definitions of the functions used are given by Messiah (1961); but it should be noted that we have used opposite sign convention for spherical Neumann function $n_\ell(x)$ and spherical Hankel function $h_\ell(x)$ which is defined by Messiah.

$$\int h_\ell^+(x) j_\ell(x) x^2 dx$$

$$= \tfrac{1}{2}x^3\left[j_{\ell-1}(x) h_{\ell-1}^+(x) - \frac{\ell+1}{x} j_\ell(x) h_{\ell-1}^+(x)\right.$$

$$\left. + j_\ell(x) h_\ell^+(x) - \frac{\ell}{x} j_{\ell-1}(x) h_\ell^+(x)\right] - \frac{\ell}{2} \qquad (B1)^*$$

$$\int j_\ell^2(x) x^2 dx = \tfrac{1}{2}x^3\left[j_\ell^2(x) - j_{\ell-1}(x) j_{\ell+1}(x)\right] \qquad (B2)^*$$

$$j_{\ell+1}(x) + j_{\ell-1}(x) = \frac{2\ell+1}{x} j_\ell(x) \qquad (B3)^+$$

$$j_\ell(x) n_{\ell-1}(x) - j_{\ell-1}(x) n_\ell(x) = x^{-2} \qquad (B4)^*$$

$$\ell j_{\ell-1}(x) - (\ell+1) j_{\ell+1}(x) = (2\ell+1)\frac{d}{dx} j_\ell(x) \qquad (B5)^*$$

$$h_\ell^+(x) = n_\ell(x) - i j_\ell(x) \qquad (B6)$$

+ See Messiah (1961) vol. 1 p 490

* See Morse and Feshbach (1953) part II p 1573-74

Appendix B continued.

Consider in general $(A-B)^{-1}$, where A is a diagonal matrix and B is a non-diagonal matrix then it should satisfy the following relation:

$$(A-B)^{-1}(A-B) = I \tag{1}$$

where I is a unitary matrix.

If we write $(A-B)^{-1}$ in the form

$$(A-B)^{-1} = A^{-1} + A^{-1}BA + A^{-1}BA^{-1}BA^{-1} + \cdots\cdots\cdots \tag{2}$$

then we see that relation (1) is satisfied, this means that expansion (2) of $(A-B)^{-1}$ is correct. This is a geometric series and its sum is given by

$$(A-B)^{-1} = A^{-1} + A^{-1}B(1+A^{-1}B + A^{-1}BA^{-1}B\cdots\cdots)\,A^{-1} \tag{3}$$

This is the expansion we use in chapter 5 with

$$A = D(k)\,\delta_{kk'}$$

$$B = \sum_m f_m(k)\,f_m(k')$$

REFERENCES

Alben R., Blume M., Krakauer H. Schwartz L. 1975 Phys. Rev. B 12 4090

Alben R., Wohlfarth E.P., Phys.Lett. 49A 271

Andersen O.K., 1970 Phys. Rev. B2 883

Beille J., Bloch D., and Kuentzler R., 1974 Solid State Commun.14 963

Cubiotti G., Donato E., Jacobs R.L., 1975 J.Phys. F 5 2068

Cubiotti G., Donato E., Giuliano E.S.,and Ruggeri R. 1973 J.Phys.C6 L202 .

Dean P., 1960 Proc. R.Soc. A 254 507

Ham F.S., and Segall B., 1961 Phys Rev. 124 1786

Harris A.B., Leath P.L., Nickel B.G. and Elliot R.J., 1974 J.Phys.C7 1693

Harris A.B., 1974 J. Phys. C 7 1671

Hasegawe H., and Kanamori J., 1971 J.Phys. Soc. Japan 31 382; 1972 33 1599

Haydock R., Heine V. and Kelly M.J., 1972 J.Phys.C5 2845

1975 J.Phys. C 8 2591

Haydock R. and Johannes R.L., 1975 J.Phys.F 5 2055

Heine V., 1967 Phys.Rev. 153 673

Hodges L., Enrehreich H. and Lang N.D., 1966 Phys.Rev. 152 505

Householder 1964 The Theory Of Matrices in Numerical Analysis. Blaisdall

Hubbard J., 1969 J.Phys.C 2 1222

Jacobs R.L., 1968 J.Phys. C 1 492

Jacobs R.L., 1973 J. Phys. F 3 933

Jacobs R.L., 1974 J.Phys. F 4 1351

Kohn W. and Rostoker N., 1954 Phys Rev. 94 1111

Korringa J., 1947 Physica 13 392

Lifshitz I.M., 1964 Adv.Phys. 13 483

Lloyd P., 1967 Proc. Phy. Soc. 90 207

Lloyd P. and Smith P.V., 1071 Adv.Phys 21 69

Messiah A.,1961,Quantum Mechanics (Amsterdam; North Holland)

Morse and Feshbach 1953 Methods of Theoretical Physics(Mcgrew Hill)

Mueller F.M., 1967 Phys.Rev 153 659

Nickel B.G., 1974 J.Phys.C 7 1719

Nickel B.G., Butler W.H., 1973 Phys.Rev Lett. 30 373

Pettifor D.G., 1969 J.Phys.C 2 1051

Pettifor D.G., 1970 J.Phys. C 3 367

Pettifor D.G., 1972 (private communication)

Slater J.C. and Koster G.F., Phys.Rev. 94 1498

Tahir Kheli R.A., 1972 Phys.Rev B6 2808

Theumann A. and Tahir Kheli R.A., 1975, B12 1796 Phy Rev.

Velicky B. Kirkpatric S. and Enhreureich H., 1968 Phys.Rev. 175 747

J. Phys. F: Metal Phys., Vol. 5, September 1975. Printed in Great Britain. © 1975.

The density of states of a one-dimensional binary alloy by continued fractions

N Zaman and R L Jacobs

Mathematics Department, Imperial College, London SW7 2AZ

Received 13 December 1974

Abstract. The density of states of a one-dimensional disordered alloy is calculated by a continued fraction technique and the results are found to agree well with those of the selfconsistent theory of Butler and with the exact density of states obtained from the Schmidt integral equation technique.

The continued fraction method due to Haydock *et al* (1972) which has previously been successfully applied by Jacobs (1974) to a three-dimensional disordered alloy is now applied to a one-dimensional system. In our method a central cluster of seven atoms is treated exactly, a further pair of atoms is treated approximately and all other atoms more approximately still.

The model Hamiltonian for a disordered alloy is

$$H = H_1 + H_2 \tag{1}$$

where

$$H_1 = \sum_{i \neq j} t_{ij} c_i^+ c_j \qquad H_2 = \sum_i \epsilon_i n_i \tag{2}$$

and where c_i and n_i are creation and number operators for electrons on site i and t_{ij} is the hopping integral between the sites i and j which is taken to be equal to a constant, t, for nearest neighbours and zero otherwise. The disorder is confined to the second term H_2 in the Hamiltonian where ϵ_i can take the values $\pm \frac{1}{2}\delta$ depending on whether site i is assigned the value A or B in the particular configuration considered.

The orthonormalized basis set is generated by the method of Haydock *et al* (1972) as modified by Jacobs (1974) and is given by

$$\begin{aligned}
&|0) = |0\rangle \\
&|1,0) = (1/\sqrt{2})(|\bar{1}\rangle + |1\rangle) && |0,1) = 0 \\
&|2,0) = (1/\sqrt{2})(|\bar{2}\rangle + |2\rangle) && |0,2) = 0 \\
&|1,1)_1 = 0 && |1,1)_2 = (1/\sqrt{2})(|\bar{1}\rangle - |1\rangle) \\
&|1,1)_3 = (1/\sqrt{2})(|\bar{1}\rangle - |1\rangle) && |1,1)_4 = 0 \\
&|3,0) = (1/\sqrt{2})(|\bar{3}\rangle + |3\rangle) && |4,0) = (1/\sqrt{2})(|\bar{4}\rangle + |4\rangle) \\
&|2,1)_{14} = 0 && |2,1)_{23} = (1/\sqrt{2})(|\bar{2}\rangle - |2\rangle) \\
&|3,1)_{14} = 0 && |3,1)_{23} = (1/\sqrt{2})(|\bar{3}\rangle - |3\rangle).
\end{aligned} \tag{3}$$

The notation $|i,j)$ for the elements of the basis set serves to indicate that the element $|i,j)$ is constructed from the ket $|0)$ by i operations of H_1 and j of H_2. The suffixes on some of these kets indicate that they depend on the arrangement of atoms. For example the ket $|1,1\rangle$ vanishes if the arrangement of atoms on the nearest neighbour shell is symmetrical, ie of type 1 ≡ ACA or type 4 ≡ BCB, where C denotes the central atom. If the arrangement is of type 2 ≡ ACB or type 3 ≡ BCA then the ket $|1,1\rangle$ does not vanish. The ket $|2,1\rangle$ however will vanish only if the arrangement of atoms on the second nearest neighbour shell is of type 1 or 4 *and* the arrangement on the nearest neighbour shell is also of type 1 or 4. Similarly the ket $|3,1\rangle$ will vanish only if the arrangements of atoms on the first, second and third nearest neighbour shells are all of type 1 or 4. The notation $|n\rangle$ or $|\bar{n}\rangle$ refers to a Wannier function centred about an atom n units to the right or left of the central atom.

The secular equation with this basis set is given by the matrix shown in table 1, where a 1×1 matrix in the first position on the main diagonal is linked by 1×1 matrices to a 1×1 matrix in the second position which in turn is linked by 1×2 and 2×1 matrices to a 2×2 matrix on the main diagonal. After this the pattern repeats itself. All other elements are zero. Here

$$\begin{aligned} E_v &= -v\tfrac{1}{2}\delta + (1-v)\tfrac{1}{2}\delta \\ E_w &= [-w\tfrac{1}{2}\delta + (2-w)\tfrac{1}{2}\delta]/2 \qquad E_x = [-x\tfrac{1}{2}\delta + (2-x)\tfrac{1}{2}\delta]/2 \\ E_y &= [-y\tfrac{1}{2}\delta + (2-y)\tfrac{1}{2}\delta]/2 \qquad E_z = [-z\tfrac{1}{2}\delta + (2-z)\tfrac{1}{2}\delta]/2 \end{aligned} \tag{4}$$

where v is the number of atoms of type B on central site, ie $v = 0$ or 1; w, x, y and z are the number of atoms of type B on first, second, third and fourth sites respectively and they all can take on the values 0, 1 or 2.

It should be noted that some off-diagonal matrix elements depend on the relative arrangement of A and B atoms on symmetrical sites about the central atom. This is manifested for example in the sign of the fourth element of the second row, which is negative if the configuration in the nearest neighbour shell is of type 2 and positive if the configuration is of type 3. If the configuration is of type 1 or 4 the sign is irrelevant because the element goes to zero on account of the factor $[w(2-w)]^{\frac{1}{2}}$.

The continued fraction is correct up to the fourth nearest neighbour shell but is continued further with an average of the continuation appropriate to the two pure components,

$$\bar{F}(E) = cF(E - \tfrac{1}{2}\delta) + (1-c)\,F(E + \tfrac{1}{2}\delta) \tag{5}$$

with

$$F(x) = [x \pm (x^2 - 4t^2)^{\frac{1}{2}}]/2t^2. \tag{6}$$

The sign is chosen so that $F(x) \to 1/x$ as $x \to \pm\infty$.

The density of states is given by

$$\rho(E) = -(1/\pi)\,\mathrm{Im}\,\overline{\langle 0|\,G\,|0\rangle}. \tag{7}$$

The diagonal element of the Green function is obtained by folding the matrix elements referring to a given shell of neighbours into those referring to the adjacent nearer shell and by ending at the central atom. The bar indicates averaging over all possible configurations. This is done by finding the diagonal element of the Green function for a particular configuration and then multiplying by the probability of occurrence of the configuration and summing the result over all configurations.

Table 1. The matrix used to derive the continued fraction. Beyond the eight level the matrix is treated approximately.

$E_v - E$	$(2t)^{\frac{1}{2}}$	0	0	0	0	0	0	0	0
$(2t)^{\frac{1}{2}}$	$E_w - E$	t	$\pm\frac{1}{2}\delta[w(2-w)]^{\frac{1}{2}}$	0	0	0	0	0	0
0	t	$E_x - E$	0	t	$\pm\frac{1}{2}\delta[x(2-x)]^{\frac{1}{2}}$	0	0	0	0
0	$\pm\frac{1}{2}\delta[w(2-w)]^{\frac{1}{2}}$	0	$E_w - E$	0	t	0	0	0	0
0	0	t	0	$E_y - E$	0	t	$\pm\frac{1}{2}\delta[y(2-y)]^{\frac{1}{2}}$	0	0
0	0	$\pm\frac{1}{2}\delta[x(2-x)]^{\frac{1}{2}}$	t	0	$E_x - E$	0	t	0	0
0	0	0	0	t	0	$E_z - E$	0	t	$\pm\frac{1}{2}\delta[z(2-z)]^{\frac{1}{2}}$
0	0	0	0	$\pm\frac{1}{2}\delta[y(2-y)]^{\frac{1}{2}}$	t	0	$E_y - E$	0	t
0	0	0	0	0	0	t	0	—	0
0	0	0	0	0	0	$\pm\frac{1}{2}\delta[z(2-z)]^{\frac{1}{2}}$	t	0	$E_z - E$

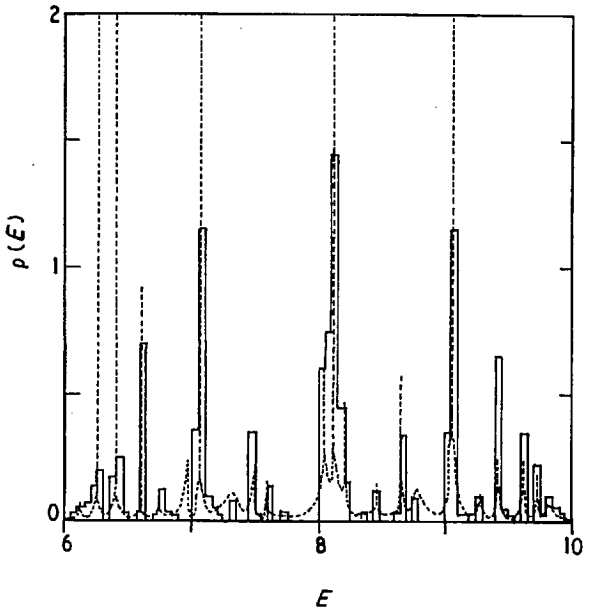

Figure 1. The density of states for alloy with $c = 0{\cdot}5$, $\delta = 16$ and $t = 1$. The peaks are very sharp and their heights are not accurately presented. The exact heights could be found by going to a finer mesh in energy scale.

Discussion of results

In figure 1 we compare our density of states (broken line) with the exact results (histogram) obtained by Butler (1973) using the method of Schmidt (1957).

It is seen that our result is very close to the exact density of states and shows the predicted sharp structure of Economou and Papatriantafillou (1972).

This verifies the convergence and accuracy of the method of Jacobs (1974) in the one case where it may be tested easily. This one-dimensional situation also poses the most severe test to any theory (a two- or three-dimensional situation is treated more accurately by a 'mean-field' method such as the CPA) and it can be seen that the present method meets the challenge and provides an excellent density of states curve. Our nine-site theory is comparable to or of greater accuracy than Butler's seven-site theory.

References

Butler W H 1973 *Phys. Rev.* B **8** 4499–510
Economou E N and Papatriantafillou C 1972 *Solid St. Commun.* **11** 197–9
Haydock R, Heine V and Kelly M J 1972 *J. Phys.* C: *Solid St. Phys.* **5** 2845–58
Jacobs R L 1974 *J. Phys.* F: *Metal Phys.* **4** 1351–8
Schmidt H 1957 *Phys. Rev.* **105** 425–35